ROLE OF THE TIGIT IMMUNE CHECKPOINT PATHWAY IN

THE ERADICATION OF HIV INFECTION

A DISSERTATION SUBMITTED TO THE GRADUATE DIVISION OF THE
UNIVERSITY OF HAWAI'I AT MĀNOA IN PARTIAL FULFILLMENT
OF THE REQUIREMENTS FOR THE DEGREE OF

DOCTOR OF PHILOSOPHY

IN

BIOMEDICAL SCIENCES
(TROPICAL MEDICINE)

JUNE 2017

By

Glen Michael Chew

Dissertation Committee:

Lishomwa Ndhlovu, Chairperson
Bruce Shiramizu
F. DeWolfe Miller
Peter Hoffmann
Maarit Tiirikainen

ACKNOWLEDGMENTS

ABSTRACT

HIV infection contributes substantially to global morbidity and mortality, with no immediate promise of an effective vaccine or cure. One major obstacle to vaccine development and therapy is to understand why HIV replication persists in a person despite the presence of viral specific immune responses. The emerging consensus has been that these immune cells are functionally 'exhausted' or anergic, and thus, although they can recognize HIV infected cells, they are unable to effectively keep up with rapid and dynamic viral replication in an individual. Negative checkpoint receptors (NCRs) are associated with immune dysfunction during chronic HIV infection. The goal of this study is to characterize an emerging NCR, TIGIT, in the context of HIV infection. The overall hypothesis is that TIGIT will be increased during HIV infection and limit anti-HIV responses, targeting the TIGIT pathway will reinvigorate existing anti-HIV T cell effector functions. Thus, these studies were conducted to elucidate the role of TIGIT in progressive HIV infection.

We have identified a combination of NCR pathways that can be targeted, TIGIT and PD-1 that may be responsible, at least in part, for making these immune cells dysfunctional and exhausted and thus unable to control the virus. We show that by blocking the TIGIT and PD-1 pathway, we can reverse the defects of these viral-specific CD8 T cells. Furthermore, we extend our findings to the clinically relevant nonhnuman primate model of HIV/AIDS. In addition, we identify potential predictors of immune reinvigoration from clinically obtainable samples. Our findings will give new directions to vaccines and therapies that will potentially reverse these dysfunctional cells and allow them to control HIV replication, but also serve in enhanced "shock and kill" HIV curative strategies.

DISSERTATION HIGHLIGHTS

- HIV infection leads to an expansion of TIGIT+ CD8 and CD4 T cells in the blood and gut
- TIGIT+ CD4 T cells are associated with HIV persistence
- TIGIT+ CD8 T cells correlate with disease progression and are regulated by common gamma chain cytokines
- TIGIT selectively dampens HIV-specific CD8 T cell responses
- Blockade of TIGIT reinvigorates pre-existing anti-HIV CD8 T cell responses
- Co-blockade of TIGIT and PD-L1 synergize to reinvigorate anti-HIV CD8 T cell responses than a single blockade alone
- As a preclinical model we identified similarities and differences between huTIGIT and rhTIGIT in a nonhuman primate SIV model of HIV/AIDS
- cART suppressed HIV infection results in an increase of *Fusobacteria* abundance in the gut
- Increased abundance of *Fusobacteria* in the gut is associated with a decreased magnitude of anti-HIV CD8 T cell reinvigoration by TIGIT blockade

TABLE OF CONTENTS

LIST OF TABLES

LIST OF FIGURES

LIST OF SCIENTIFIC PUBLICATIONS INCLUDED IN THIS DISSERTATION

1. **Chew GM**, Fujita T, Webb GM, Burwitz BJ, Wu HL, Reed JS, Hammond KB, Clayton KL, Ishii N, Abdel-Mohsen M, Liegler T, Hecht FM, Ostrowski MA, Shikuma CM, Hansen SG, Maurer M, Korman AJ, Deeks SG, Sacha JB, Ndhlovu LC. "TIGIT marks exhausted T cells, Correlates with disease progression and serves as a target for immune restoration in HIV and SIV infection" *PLoS Pathogens. 2016 Jan 7;12(1):e1005349. PMCID: PMC4704737. doi: 10.1371/journal.ppat.1005349. eCollection 2016 Jan*

LIST OF SCIENTIFIC PUBLICATIONS IN PREPARATION

1. **Chew GM** et al. "Gut Tissue-Specific Differences in TIGIT and TIGIT ligands During Chronic cART HIV Infection: Implications for Immunotherapy Efficacy" *Manuscript in preparation. 2017*

LIST OF SCIENTIFIC PAPERS NOT INCLUDED IN THIS DISSERTATION

1. Ginwala R, Caruso B, Khan ZK, **Chew GM**, Pattekar A, Corley MJ, Loonawat R, Jacobson S, Sreedhar S, Ndhlovu LC, Jain P. "HTLV-1 infection and neuropathogenesis in the context of Rag1$^{-/-}$γc$^{-/-}$ (RAG1-hu) and BLT mice" J Neuroimmune Pharmacology. *2017 Apr 4.* doi*: 10.1007/s11481-017-9740-y*

2. Abdel-Mohsen M, Chavez L, Tandon R, **Chew GM**, Deng X, Danesh A, Keating S, Lanteri M, Samules ML, Hoh R, Sacha JB, Norris PJ, Niki T, Shikuma CM, Hirashima M, Deeks SG, Ndhlovu LC, Pillai SK. "Human Galectin-9 is a Potent Mediator of HIV Transcription and Reactivation" PLoS Pathogens. *2016 Jun 2;12(6):e1005677. PMCID: PMC4890776. doi: 10.1371/journal.ppat.1005677. eCollection 2016 Jun*

3. Clayton KL, Douglas-Vail MB, Nur-ur Rahman AK. Medcalf KE, Xie IY, **Chew GM**, Tandon R, Lanteri MC, Norris PJ, Deeks SG, Ndhlovu LC, Ostrowski MA. "Soluble Tim-3 is shed from CD8+ T cells by the sheddase ADAM10, is increased in plasma during untreated HIV infection, and correlates with HIV disease progression" *J Virology. 2015 Apr;89(7):3723-36. PMCID: PMC4403393. doi: 10.1128/JVI.00006-15. Epub 2015 Jan 21*

4. Fujita T, Burwitz BJ, **Chew GM**, Reed JS, Pathak R, Seger E, Clayton KL, Rini JM, Ostrowski MA, Ishii N, Kuroda MJ, Hansen SG, Sacha JB, Ndhlovu LC. "Expansion of Dysfunctional Tim-3 Expressing Effector Memory CD8+ T cells During Simian Immunodeficiency Virus Infection in Rhesus Macaques" *J Immunology. 2014 Dec 1;193(11):5576-83. PCMID: PMC4239185. doi: 10.4049/jimmunol.1400961. Epub 2014 Oct 27*

5. Ndhlovu LC, Umaki T, **Chew GM**, Chow DC, Agsalda M, Kallianpur KJ, Paul R, Zhang G, Ho E, Hanks N, Nakamoto B, Shiramizu BT, Shikuma CM. "Treatment Intensification with Maraviroc (CCR5 antagonist) Leads to Declines in CD16-Expressing Monocytes in cART-Suppressed Chronic HIV-infected Subjects and is Associated with Improvements in Neurocognitive Test Performance: Implications for HIV-Associated Neurocognitive Disease (HAND)" *J NeuroVirology. 2014 Dec;20(6):571-82. PMCID: PMC4268390. doi: 10.1007/s13365-014-0279-x. Epub 2014 Sep 17*

6. Tandon R, **Chew GM**, Byron MM, Borrow P, Niki T, Hirashima M, Barbour JD, Norris PJ, Lanteri MC, Martin JN, Deeks SG, Ndhlovu LC. "Galectin-9 Is Rapidly Released During Acute HIV-1 Infection and Remains Sustained at High Levels Despite Viral Suppression Even in Elite Controllers" *AIDS Research and Human Retroviruses. 2014 Jul;30(7):654-64. PCMID: PMC4077009. doi: 10.1089/AID.2014.0004. Epub 2014 May 28*

7. Lanteri MC, Diamond MS, Law JP, **Chew GM**, Wu S, Inglis HC, Wong D, Busch MP, Norris PJ, Ndhlovu LC. "Increased Frequency of TIM-3 Expressing T cells is Associated with Symptomatic West Nile Virus Infection" *PLoS One. 2014 Mar 18;9(3):e92134. PMCID: PMC3958446. doi: 10.1371/journal.pone.0092134. eCollection 2014*

8. Clayton KL, Haaland MS, Douglas-Vail MB, Mujib S, **Chew GM**, Ndhlovu LC, Ostrowski MA. "T cell Ig and Mucin Domain-Containing Protein 3 is Recruited to the Immune Synapse, Disrupts Stable Synapse Formation, and Associates with Receptor Phosphastases" *J Immunology*. 2014 Jan 15; 192(2):782–791. PMCID: PMC4214929. *doi: 10.4049/jimmunol.1302663. Epub 2013 Dec 13*

9. Chagan-Yasutan H, Ndhlovu LC, Lacuesta TL, Kubo T, Leano PS, Niki T, Oguma S, Morita K, **Chew GM**, Barbour JD, Telan EF, Hirashima M, Hattori T, Dimaano EM. "Galectin-9 Plasma Levels Reflect Adverse Hematological and Immunological Features in Acute Dengue Virus Infection" *J Clinical Virology*. *2013 Dec;58(4):635-40. PMCID: PMC3880569. doi: 10.1016/j.jcv.2013.10.022. Epub 2013 Oct 27*

10. Ndhlovu LC, Leal FE, Hasenkrug AM, Jha AR, Carvalho KI, Eccles-James IG, Bruno FR, Vieira RG, York VA, **Chew GM**, Jones RB, Tanaka Y, Neto WK, Sanabani SS, Ostrowski MA, Segurado AC, Nixon DF, Kallas EG. "HTLV-1 TAX Specific CD8+ T Cells Express Low Levels of TIM-3 in HTLV-1 Infection: Implications for Progression to Neurological Complications". *PLoS Neglected Tropical Diseases. 2011 Apr 26;5(4):e1030. PMCID: PMC3082508. doi: 10.1371/journal.pntd.0001030*

CHAPTER 1

INTRODUCTION

Epidemiology

Human immunodeficiency virus (HIV) was introduced to the human population between 1915-1941 through multiple zoonotic infections from simian immunodeficiency virus (SIV) infected nonhuman primates [3, 4]. A recent study suggests that HIV subtype B has been circulating throughout the United States of America as a widespread epidemic since 1970 [5]. However, it wasn't until 1981 when the Centers for Disease Control (CDC) first reported several cases of young, homosexual men presenting with *Pneumocystis carinii* pneumonia and Kaposi's Sarcoma, which is not normally seen in young immunocompetent adults [6]. A few weeks later, the CDC reported 26 homosexual men from New York and San Francisco with similar symptoms [7]. All individuals showed signs of a compromised immune system with a hallmark depletion of cluster of differentiation (CD) 4 T cells. Several years later, two independent groups identified a blood-borne T cell lymphotropic retrovirus, that was later named HIV, as the etiological agent that causes the destruction of the immune system leading to acquired immunodeficiency syndrome (AIDS) and the onset of opportunistic infections resulting in death [8-10]. 35 years later, HIV has become a worldwide pandemic and currently remains a global health concern. In 2015, the CDC estimates there were 2.1 million new cases, 36.7 million individuals currently living with HIV and 39 million AIDS-related deaths. A majority of the infection is focused in Sub-Saharan Africa, which accounts for about 65% of all new HIV infections. Cutting edge research along with better treatment implementation approaches, increased awareness, and improved prevention has slowed worldwide HIV infection rates by 6% since 2010 and AIDS-related deaths by 45% since the peak in 2005 [11].

HIV is a blood-borne retrovirus that is predominantly transmitted through sexual contact, via percutaneous and prenatal routes [12-16]. The risk of HIV infection is dependent on the type of exposure or behavior and can range from a

CDC estimated Per-Act Probability of 9,250/10,000 for blood transfusions, 63/10,000 for needle sharing injection drug use, 138/10,000 for receptive anal intercourse, and 8/10,000 receptive penile-vaginal intercourse [17]. HIV infection disproportionally affects men who have sex with men (MSM), transgender individuals, sex workers, and injection drug users. In the United States of America, homosexual and bisexual men account for an estimated 83% while heterosexual contact accounts for an estimated 24% HIV diagnosis in 2014.

HIV Phylogeny

Two types of HIV can lead to a productive infection in humans: human immunodeficiency virus type 1 (HIV-1) and human immunodeficiency virus type 2 (HIV-2). Although, both strains share similarities in the genome arrangement, routes of transmission, replication life cycle, and clinical disease, HIV-2 has a lower transmissibility, pathogenicity and is mainly confined to West Africa [18, 19].

Several factors that contribute to the high genetic variability of HIV-1 include the error-prone reverse transcriptase and lack of nucleic acid proofreading [20], high viral turnover rate *in vivo* [21], host selective immune pressures [22], and viral recombination [23]. HIV-1 is categorized into three major phylogenetic groups based on viral sequence homology, Major (M), Outlier (O), and Non-M/Non-O (N) [24, 25]. HIV-1 Group N infection has only been identified in Cameroon and Group O is endemic to West Africa [26, 27]. HIV-1 Group M represents the main global circulating virus and is subdivided into subtype clades (A, B, C, D, E, F, G, H, J, K, and circulating recombinant forms (CRF)) that are geographically distributed. Subtype C is responsible for the majority of HIV-1 infection in parts of Africa, while Subtype B dominates infection in the Americas and Europe [28]. CRF arise from a recombination of multiple subtypes in a single infected person [29]. There has been a surge of CRF_AE infections due to an

3

increase in globalization and transportation seen in Thailand, Hong Kong, Malaysia and the Philippines [30]. The vast genetic diversity of HIV quasispecies has important implications in understanding host-viral evolution leading to better diagnostic testing, control of disease progression and therapeutic designs.

*HIV-1 will be referred to as "HIV" unless noted otherwise.

HIV Genome

HIV is a lentivirus that belongs to the Retroviridae family and is characterized to have a reverse transcription of its viral genome and subsequent integration into the host genome. The HIV viral genome consists of two copies of positive-sense, single-stranded RNA that is ~9kb in length, flanked by 5' and 3' long terminal repeats and encodes for structural (*Gag, Env*), enzyme (*Pol*), essential regulatory (*Tat, Rev*), and accessory (*Nef, Vpu, Vpr, Vif*) proteins required for host cell infection, immune evasion, and propagation of infectious virons [31].

The group-specific antigen gene (*Gag)* encodes Gag p55 protein that is cleaved to make up structural components of the matrix (p17), capsid (p24) and nucleocapsid (p7), and spacer (p6) [32]. The envelope (*Env*) gene encodes the transmembrane glycoproteins gp120 and gp41 that make up viral spikes on the surface of the mature viron and are required for host cell recognition, binding and fusion [32]. The polymerase (*Pol*) gene encodes enzymes protease (PR) required for cleavage of polyproteins during virus maturation, reverse transcriptase (RT) required for transcribing single-stranded viral RNA to double-stranded viral DNA, and integrase (IN) that mediates HIV proviral insertion into the host genomic DNA [33-35]. Essential regulatory proteins are encoded by the transcriptional transactivator (*Tat*) gene, which initiates transcription of viral RNA while *Rev* increases nuclear export of viral mRNAs [36, 37]. The accessory

proteins Nef, Vpu and Vif encoded increase pathogenicity and immune evasion. Nef is one of the first viral proteins produced and has the ability to downregulate the expression of cluster of differentiation (CD) 4 and Human Leukocyte Antigen (HLA) Class I [38, 39]. The Vpu protein increases viral progeny release and is responsible for degrading CD4 in the cytoplasm [40]. The Vpr protein plays a role in forming the pre-integration complex (PIC) and facilitating nuclear import of the double stranded HIV DNA template in the absence of mitosis [41]. The Vif protein has co-evolved to overcome the antiviral host restriction factor APOBEC3G [42]. All together, the HIV genome encodes proteins required to produce infectious virons and maintain a persistent infection.

HIV Structure

The HIV virion is approximately 120nm in diameter [43]. The viral RNA and enzymes (IN, RT) are enclosed by the viral capsid (p24) and matrix protein (p17) [44]. The core of the virus is surrounded by the matrix protein and is integrated into the external lipid bilayer envelope derived from the host cell [45]. The surface of the viron is covered in trimetric glycoprotein spikes, made of gp120 and gp41 that mediate viral tropisms and membrane fusion [46].

HIV Life Cycle

HIV replication can be divided into several steps that include entry, uncoating, reverse transcription, integration, transcription, translation, assembly, budding and maturation. HIV primarily targets host cells expressing the CD4 and CC-chemokine receptor 5 (CCR5) or CXC-chemokine receptor 4 (CXCR4) receptors namely CD4 T lymphocyte cells (CD4 T cell), macrophages and microglial cells [47]. Entry begins with the binding of gp120 to the CD4 receptor along with one co-receptor (CCR5 or CXCR4) resulting in a gp41 mediated

membrane fusion [43, 48]. The viral capsid is uncoated in the cytoplasm to release HIV RNA, enzymes and proteins [44]. HIV RNA is reverse transcribed by RT to produce a double-stranded HIV DNA template [34]. The lack of proofreading and the error-prone HIV RT promotes mutations (1/1700 error rate of incorporated nucleotide) resulting in the extremely high genetic variability of HIV [20, 49]. Vpr forms a nucleoprotein PIC that transports the pre-integrated HIV DNA into the nucleus [50]. The viral protein IN facilitates the integration of HIV DNA into the host chromosome [51]. This integrated HIV DNA, or provirus, can be transcribed as a cellular gene. The viral proteins Tat and Rev control the host transcriptional machinery to produce and export mRNA from the HIV provirus in an infected cell nucleus. Tat stimulates the transcription of the proviral 5'LTR promoter region by directing cellular transcription elongation factor (P-TEFb) to RNA polymerases [52]. HIV mRNA transcripts undergo splicing to produce a full range of mRNAs required to encode viral proteins [53]. Rev is responsible for exporting intron-containing viral mRNA out of the nucleus [54]. Translation of the HIV mRNA and protein synthesis occurs in the cytoplasm. Viral assembly happens near the plasma membrane to include all of the components required for infecting a new cell. Two copies of viral RNA and viral enzymes (PR, RT and IN) are packaged into the viral envelope and bud off of the host plasma membrane [55]. The Gag-Pol polyprotein is cleaved by the viral protease to produce a mature viron capable of infecting a new host cell [56].

HIV Infection and Disease Progression

HIV can be transmitted during sexual contact, from sharing intravenous needles, from blood transfusions, and mother-to-child [57]. Infectious virus is present in the plasma of blood, female genital secretions, and male seminal fluid [58, 59]. HIV acquisition through mucosal tissues is one of the leading causes of infection. At the site of infection, through micro-abrasions in the mucosa

epithelium, the virus gains access to tissue resident CD4 T cells and antigen presenting cells (APCs) to create a local focus of infection [60]. Tissue resident dendritic cells (DCs) are able to capture whole virus and facilitate trans-infection of CD4 T cells [61]. Infected CD4 T cells and APCs migrate to draining lymph nodes and eventually distal lymph nodes along with other tissues within two weeks of infection. The follicular dendritic network is able to retain infectious virus within immune privileged B cell follicles contributing to lymph node fibrosis and improper reconstitution of CD4 T cells [62]. Furthermore, follicular CD4 T cells (Tfh) are the main source of virus during disease progression [63].

HIV disease progression can be divided into an acute phase, chronic phase, and AIDS. The acute clinical manifestations include fever, generalized lymphadenopathy, nonspecific rash and malaise [64]. In the absence of combined antiretroviral therapy (cART), viral replication continues with a peak in plasma viremia to about 10^6 copies/mL at about 4 weeks after initial infection and slowly declines to a viral set point as the individual immune system begins to control the virus [65]. Concurrently, the CD4 T cells, which become infected with HIV, decline quickly from ~1000 cells/mL to ~500 cells/mL due to viral cytopathic effects (CPE), chronic inflammation, and adaptive immune killing [65]. The CD4 T cell nadir, the lowest ever CD4 Count, will establish an immunological set point that will determine how well CD4 T cell counts recover after acute infection [66]. The dynamics of acute HIV viremia and antibody seroconversion are categorized into Fiebig stages I-VI that are based on sequential gain in positive HIV clinical diagnostic tests starting with Fiebig I viral RNA by polymerase chain reaction (PCR), Fiebig II p24 and p31 enzyme-linked immunosorbent assay (ELISA), and Fiebig III-VI HIV-specific antibodies by ELISA and western blot [67, 68]. Currently, fourth generation immunoassays are redefining Fiebig stage I acute HIV infection into two groups with depending on the levels of HIV RNA and DNA [69]. Three-to-nine weeks after infection the CD8 T cell responses and anti-HIV antibody titers begin to rise and partially control virus replication [70, 71].

Although, HIV-specific CD8 T cell responses are more effective than anti-HIV antibodies at controlling virally infected cells [72], both arms of the adaptive immune response contribute to the overall control of virus.

The chronic infection phase can last from one to twenty years with individuals experiencing little-to-no clinical symptoms, termed "clinical latency". The virus slowly replicates throughout the body with a gradual loss of both circulating and tissue based CD4 T cells. The high density of CD4 T cells in gut associated lymphoid tissues (GALT) is most impacted. Depletion of GALT CD4 T cells leads to intestinal permeability and microbial translocation resulting in persistent peripheral immune activation [73]. HIV infection within the thymus contributes to CD4 T cell decline and regenerative failure [74]. Furthermore, HIV infection within secondary lymph nodes causes fibrosis and severely affects CD4 T cells' ability to survive and reconstitute the peripheral CD4 T cell population [62].

The AIDS phase is defined by the depletion of CD4 T cells to less than 200 cells/ml in blood, increased plasma viremia and exhibitions of opportunistic infections or cancers that include pneumocystis, pneumonia, candidiasis, Kaposi sarcoma, and wasting syndrome. During the final phase, without treatment, individuals only survive for about 3 years [75].

Disease progression rates vary depending on the infected individual. There is some evidence that host human leukocyte antigen (HLA) genetics, immune function, viral genetic variability, and co-infections may affect the progression rate to AIDS [76]. HIV infected individuals can be grouped based on their progression to AIDS. "Rapid progressors" have a fast decline in CD4 T cells and progress to AIDS within four years of primary HIV infection [76]. The majority of infected individuals are "intermediate progressors", which have persistent detectable plasma viremia and slow decline in CD4 T cells and progress to AIDS within 6-10 years [75]. "Long-term non-progressors (LTNP)" are individuals that maintain a normal CD4 count (>500 cells/μl) with low detectable plasma viremia

(<10,000 viral copies/ml) for up to 10 years in the absence cART [77]. A small subset of individuals, "elite controllers", are able to sustain spontaneous control of virus (<50 viral copies/ml) while maintaining normal CD4 counts in the absence of cART [78]. "Immunological non-responders (INR)" make up 30% of individuals on therapy, which fail to recover CD4 T cells (<500 cells/µl) despite achieving complete suppression of plasma viremia [79]. Each unique group of infected individuals has contributed to studies revealing novel and differential immune mechanisms driving HIV disease progression.

HIV Diagnosis

Blood tests for HIV are the most common definitive way to diagnose HIV infection. These test include viral RNA (PCR), p24 (ELISA), HIV specific antibody (ELISA), and HIV specific antibody (western blot). The CDC recommends using a fourth generation antigen-antibody assay followed by an antibody assay that can differentiate between HIV-1 and HIV-2 as conformation [80].

Rapid antibody tests can screen for HIV infection from a finger stick of blood or oral fluid within thirty minutes and is extremely useful in public testing bars, drop in clinics, or health fairs. However, the current rapid HIV tests have limited sensitivity in detecting HIV during an acute infection [81]. All rapid test results should be confirmed with an antigen-antibody assay.

The U.S. Preventative Services Task Force recommends that clinicians screen adolescents and adults (15-65 years) for HIV infection at least once, and every 3-6 months for individuals at risk [82]. Individuals at risk include male-to-male sexual contact, injection drug use, anal or vaginal sex without condom use, and individuals who exchange drugs or money for sex.

Non-human primate model of HIV/AIDS

Animal models provide invaluable information in the search for an HIV cure. Non-human primates are the most physiologically relevant model to study HIV/AIDS and allows for invasive interrogation of the disease in cellular and anatomical compartments, study of host-viral interaction, analytical treatment interruption and pre-clinical drug or vaccine testing.

Simian immunodeficiency virus (SIV) and HIV share similarities in the viral genome, gene products, and structure. Over 40 species of African green monkeys, sooty mangabeys and mandrills are natural hosts for SIV. Upon acute infection, the natural hosts have high levels of sustained plasma viremia, rapid T cell turnover and activation of innate and adaptive immunity [83]. However, the SIV infection does not result in chronic immune activation, depletion of peripheral CD4 T cells, or destruction of lymph node architecture [83]. As is observed in HIV, non-natural hosts, such as Rhesus macaques (RM) (*Macaca mulatta*), more closely resemble HIV pathogenesis. The commonly used strains of macaque-adapted SIV (SIVmac239, SIVmac251, or chimeric simian/human immunodeficiency virus (SHIV)) have been used to experimentally challenge RMs [84]. A single dose challenge, through intravenous or intrarectal route, is sufficient to establish a robust infection [85]. Similar to HIV infection, SIV-infected RMs experience ongoing plasma viral replication and depletion of peripheral and GALT CD4 T cells [85]. SIV disease progression is more rapid compared to HIV infection with SIV infected RMs showing AIDS-related illnesses within 2-3 years without therapeutic intervention. Similar to cART treatment for HIV-infected individuals, combinational antiretroviral therapy regimens consisting of four/five-drugs can be administered orally or subcutaneously to persistently suppress plasma viral replication in SIV infected RMs, providing robust *in vivo* models for HIV persistence and innovative therapeutic curative strategies [86].

HIV Pathogenesis

HIV infects a small portion of cells that make up the immune system, specifically cells that express CD4 cell surface receptor molecule and co-receptor C-C chemokine receptor type 5 (CCR5) or C-X-C chemokine receptor type 4 (CXCR4), this includes activated memory CD4 T cells [87], follicular helper CD4 T cells [63], and cells of myeloid lineage [88]. During untreated pathogenic infection, direct and indirect effects, such as viral cytopathic effect and systemic chronic immune activation, drive CD4 T cell depletion in the peripheral blood and secondary lymphoid tissues leading to immune dysfunction and increased susceptibility to opportunistic infections and the onset of AIDS and death.

HIV-infected individuals classified by their disease progression provide insights into pathogenic HIV-associated immune activation. For instance, CD8 T cells from cART suppressed, chronically HIV-infected individuals express high levels of immune activation markers such as CD38 and HLA-DR as well as increased levels of proliferating T cells compared to HIV-uninfected individuals [89]. The activation of CD8 T cells shows a stronger correlation with decreased survival time than viral loads or CD4 counts [90]. Residual immune activation, in the absence of replicating virus in the plasma, correlates with increased morbidity and mortality [91]. HIV-infected individuals that are able to spontaneously control viral replication, "elite controllers", show higher levels of immune activation compared to HIV-uninfected and cART suppressed individuals, and have a higher rate of developing HIV-related comorbidities [92]. HIV-infected "long-term non-progressors" display reduced levels of immune activation while maintaining CD4 T cell counts despite having high plasma viremia [93]. Finally, as previously mentioned, the non-human primate natural hosts to SIV have sustained plasma viremia and massive acute CD4 depletion, however they do not experience chronic immune activation and do not progress to AIDS. Reducing immune activation is an important component to HIV cure strategies.

Secondary lymphoid tissues, such as the gut mucosa, are largely affected by HIV infection and contribute to chronic HIV-associated immune activation. During acute HIV infection there is a massive depletion of CCR5 expressing CD4 T cells in the gut [94], including the CD4 T helper cells 17 (Th17), a subset which is crucial for maintenance of the mucosal intestinal barrier [95]. Compromised mucosal integrity along with the loss of intestinal epithelial cells and disruption of tight junctions result in microbial translocation and systemic bacteremia leading to persistent peripheral immune activation and inflammation [96]. A deeper understanding of immune function in the gut will be required to restore gut integrity and reduce immune activation during chronic HIV infection.

Lymph nodes are anatomical compartments that are responsible for generating effective immune responses [97], crucial for T cell homeostasis [98] and the main site for HIV replication and persistence [99-102]. Several functional and structural changes occur during pathogenic HIV infection. Follicular dendritic cells trap live virus and facilitate follicular helper CD4 T cell (Tfh) infection in germinal centers of lymph nodes [63, 103, 104]. Activated T regulatory cells (Tregs) produce TGF-β1 leading to collagen deposition [105] that damages the fibroblastic reticular cell (FRC) network [106]. This leads to decreased IL-7, an important cytokine in promoting naïve T cell survival, resulting in improper T cell hemostasis and impaired CD4 T cell reconstitution [106]. Additionally, the FRC remains damaged despite viral suppression during cART [106]. This vicious cycle of HIV replication and immune activation impacts cellular immune function and promotes viral persistence. Targeting HIV persistence in lymph node will need to be considered in future HIV cure strategies.

Treatment and Prevention of HIV infection

With the advent of anti-retroviral (ARV) drugs, individuals infected with HIV are now living decades longer than before. There are currently five classes of

Food and Drug Administration (FDA)-approved ARV drugs available in the USA as follows: fusion inhibitors, nucleoside/nucleotide reverse transcriptase inhibitors (N(t)RTI), non-nucleoside reverse transcriptase inhibitors (NNRTI), protease inhibitors and integrase inhibitors. Each class of ARVs works by targeting a specific stage in the HIV life cycle that is crucial for producing replication competent viral progeny. As standard of care, cART is required to simultaneously suppress multiple steps of the HIV lifecycle to control viral replication and reduce drug resistance. cART consists of two N(t)RTIs plus (one NNRTI or protease/integrase inhibitors) [107]. Recent studies suggest that immediate initiation of cART, regardless of CD4 count, leads to better long-term immune consequences and public health benefits of reducing risk of transmission [108, 109].

Despite the remarkable success of cART in controlling viral replication and reducing AIDS-related deaths, several drawbacks are associated with the lifelong therapy. The patient and doctor must consider toxicity, cost and adherence to drug regimens. Some factors that might be responsible for an individual failing to respond to treatment are non-adherence [110], drug resistance [111, 112], host genetic polymorphisms [113] and drug malabsorption [114]. HIV infected individuals in resource limited-countries, including Sub-Saharan Africa, have limited access to healthcare where cART may not be optimal. Moreover, cART fails to eradicate the viral reservoirs of the virus [115]. If cART is interrupted from an infected individual, the virus rapidly and robustly rebounds [116]. Furthermore, cART fails to restore complete immune health [117] with survival rates significantly reduced compared to HIV-uninfected individuals [118]. Moreover, cART does not fully reduce immune activation, which contributes to non-AIDS comorbidities such as cardiovascular disease, cancer, kidney disease, liver disease, neurological impairment, and bone diseases [117]. More effective therapies and strategies will be required to manage and eliminate HIV infection.

No effective cure or vaccine exists. The recommended prevention of HIV infection is to avoid high-risk behavioral activities that include unprotected sex or sharing needles. Programs such as The Joint United Nations Program on HIV/AIDS (UNAIDS) aim to educate the community, break social stigma and increase awareness about HIV infection. The UNAIDS ambitious strategy to coordinate global action in response to the HIV/AIDS epidemic is to have 95% of all individuals know their HIV status, 95% of infected individuals on cART and 95% of infected individuals with undetectable viral loads by 2030 [119].

ARVs can be used as powerful tools to potentially prevent HIV infection. Truvada, a combination of Tenofovir and Emtricitabine (both NRTIs), is the first FDA-approved ARV to be used as a daily pre-exposure prophylaxis (PrEP) to reduce HIV acquisition in at-risk populations. PrEP has been shown to be very effective in reducing sexual transmission when combined with risk-management counseling and condom use [116]. However, poor daily adherence is associated with decreased PrEP efficacy [116]. PrEP must be taken on a daily schedule to maintain optimal plasma drug consternations to prevent HIV acquisition. The two-drug regimen combined with Lopinavir/Ritonavir can also be used as Post-Exposure Prophylaxis (PEP) within 72 hours after a single high-risk HIV exposure [120]. The same two-drug backbone plus Efavirenz are used to prevent mother-to-child transmission by virally suppressing the HIV-infected mother before giving birth and during breast-feeding [120]. The effectiveness of ARV intervention will ultimately rely on community education and engagement, access to ARVs in resource-limited setting, and high level of compliance and adherence.

HIV Vaccine Approaches

Vaccines are one of the best strategies to prime the immune system to produce durable long-lasting protection against infections. However, as of today, there are no effective vaccines that prevent HIV infection. Conventional efforts to generate an HIV vaccine have failed due to the genetic diversity of HIV, limited

correlates of vaccine protection, viral escape mutations, heavily glycosylated Env spikes and early viral integration into the host genome. An ideal HIV vaccine should elicit both humoral and cellular responses that generate sterilizing protection against HIV acquisition and establishment of the viral reservoir across multiple serotypes.

Six vaccine efficacy trials during 1987 – 2013 have all failed except one with modest efficacy. Of note, the 2007 STEP trial and 2013 HVTN trial used a replication-incompetent adenovirus type 5 (Ad5) vector containing HIV DNA Gag, Pol, and Nef to prime the immune system. Both trials were discontinued due to an increased HIV acquisition in the vaccinated arms [121, 122]. However, the first evidence that an HIV vaccine may be protective was observed in the RV144 Thailand trial. The RV144 vaccine used a prime/boost strategy, individuals were "primed" with a replication-incompetent canarypox vector containing HIV DNA Env, Gag and Pro (ALVAC) and "boosted" with recombinant Env gp120 protein (AIDSVAX) in hopes of generating both humoral and cellular responses [123]. The results of the RV144 trial showed a modest vaccine efficacy of 31.2% at 42 months [124]. Interestingly, Env mediated antibody-dependent cellular cytotoxicity (ADCC) against the gp120 variable loop 2 and T cell responses correlated with decreased HIV risk of infection suggesting that humoral and cellular components may be required for an effective HIV vaccine [124]. Building off these results, a new vaccine clinical trial (HVTN 702) is scheduled to commence in South Africa in 2017. The HVTN 702 vaccine candidate is based on the RV144 ALVAC/AIDSVAX vaccine with modified components and vaccination regimen designed to increase the magnitude and duration of protective humoral and cellular immune responses.

Several research groups have identified antibodies from HIV-infected individuals that have the ability to neutralize a diverse pool of HIV isolates. These broadly neutralizing antibodies (bnAb) have been characterized to target five different sites on the HIV Env trimer: the CD4 binding site (CD4bs), the V3 and

V1V2-glycan sites, gp120-gp41 sites and the gp41 membrane proximal external region (MPER) [125, 126]. Passive administration of the bnAb PGT121, targeting the V3 glycan-binding site, to SHIV infected RMs resulted in viral control with no antibody neutralization escape in a several infected animals [127]. In a small clinical trial, passive administration of CD4bs bnAb 3BNC117 to HIV-infected individuals was able to suppress plasma viremia for four-weeks, however an emergence of resistant viral strains were observed [128]. Comparably, administration of CD4bs bnAb VRC01 resulted in an eight-week delay in viral rebound after analytical treatment interruption [129]. These data suggest that passive bnAb therapy may be an important component to HIV eradication strategies and vaccines. The next-generation of bnAbs are being modified *in vitro* to increase breadth, potency and serum half-lives [130, 131]. Nonetheless, a deeper understanding is required to identify preferential structures, conformations and sequences of Env immunogens that can induce bnAbs as an HIV vaccine.

In recent novel non-human primate vaccination studies, rhesus macaques (RMs) vaccinated with rhesus cytomegalovirus (rhCMV) vector expressing SIV proteins (rhCMV/SIV) were protected against repeated SIVmac239 challenge in approximately 50% of RMs [132, 133]. The rhCMV/SIV vaccine was later found to induce broad, diverse MHC-E restricted SIV-specific CD8 T cell responses that were able to clear pathogenic SIV infection [134]. These data suggests that lentiviral reservoirs are susceptible to antiviral CD8 T cell mediated cellular immunity. Future studies will be required to determine if similar immune responses can be recapitulated in humans.

Novel vaccine strategies should be a two-pronged approach. The first should focus on sequential rounds of engineered Env immunogens to induce potent bnAbs that can block or reduce acquisition of HIV infection. The second should potentially use a CMV-based vector to induce broad cellular responses to control breakthrough infections. Furthermore, the immune response should be

long lasting and able to block multiple routes of infections across global HIV serotypes.

HIV Reservoirs

Despite therapeutic advances, the main obstacle to eliminating virus from cART suppressed HIV-infected individuals are HIV reservoirs that harbor replication competent virus driven by T cell survival and homeostatic proliferation [135]. There have been several cellular (CD4 T cells, macrophages, follicular dendritic cells) and anatomical (brain, gut, male urogenital tract, lymph nodes) reservoirs described [136]. RM studies suggest that SIV reservoirs, able to sustain a productive infection, are seeded as early as three days post-infection [137]. HIV can establish a reversibly nonproductive infection in CD4 T cells termed "latency" [138]. Latently infected cells contain a copy of the HIV provirus, however they do not transcribe HIV or produce any viral proteins, thus making them invisible to recognition by the immune system and resistant to cART [139]. Moreover, the half-life of the latent reservoir is estimated to be 44 months, suggesting it would take 73.4 years to eliminate one million latent cells on suppressive cART [140]. Identifying latent cells that harbor HIV provirus has been pursued with great interest with one study suggesting that CD32a marks CD4 T cells harboring replication competent provirus [141]. Several mechanisms that contribute to the transcriptional silencing of HIV include sequestration of host transcriptional factors, epigenetic silencing, transcriptional interference, and inhibition of RNA polymerase II [139]. The majority of latently infected cells reside in anatomical sanctuaries where cART concentrations may not be optimal. These sites include the lymph node [63] and gut associated lymphoid tissue (GALT) [142] and serve as the main source for HIV replication and production [143]. Future HIV cure strategies should focus on targeting latently infected cells and anatomical sites to disrupt and eliminate viral reservoirs.

17

Microbiota

There is an estimated ten trillion bacteria that live on and in the human body in symbiosis [144]. A majority of the commensal bacteria is focused in the gastrointestinal tract and play intricate roles in the development and function of the systemic immune system [145, 146]. The evidence of immune mediated diseases such as Chron's disease, asthmas, diabetes, in addition to multiple sclerosis have been implicated with an alter microbial composition [147, 148]. Furthermore, the impact of microbiota-derived factors on the immune development is observed in specific-pathogen free mice, they develop significant differences in their immune cellular composition at mucosal sites [146]. Altering the microbial composition with fecal microbiota transplantation is an established way to treat *Clostridium difficile* [149]. However, to completely change the microbiota after neonatal establishment seems to be extremely difficult [150]. A better understanding of the mechanisms driving microbiota reconstitution along with the host-microbial immunological relationship is warranted.

During HIV infection, the gut is one of the earliest targeted sites of infection, it contains a high concentration of CCR5-expressing T cells resulting in CD4 T cell depletion and impaired immune reconstitution [151, 152]. Massive viral replication in the gut leads to the destruction of the epithelial barrier, indirectly leading to microbial translocation and altered community composition [73, 153]. Moreover, the early initiation of cART only partially restores gut mucosa integrity [154]. A better understanding of the roll the gut microbial composition plays during cART-suppressed HIV infection will help to inform future HIV cure strategies.

Introduction to Adaptive Immunity

The mammalian immune system plays an essential role in defending against pathogens and cancers. The immune response can be divided into two arms: innate and adaptive immunity. The innate immune system is composed of immune cells and complement proteins that can recognize and respond rapidly to nonspecific antigens [155]. Initial inflammation is generated by tissue resident innate immune cells (macrophages, neutrophils, dendritic cells (DCs), natural killer (NK) cells etc.) to prevent the spread of infection, promote tissue regeneration and recruit additional immune cells to initiate the expansion and differentiation of the adaptive immune response [155]. The adaptive immune system responds ~7-15 days after the initial antigen stimulation. Cell-mediated and antibody responses are produced by activated T cells and B cells, respectively. Antigens are processed into peptides and presented by major histocompatibility complexes (MHC) (known as human leukocyte antigens (HLA) in humans) to activate T cells. Three signals are required for T cell activation. First, antigen presenting cells (APCs) display peptide fragments restricted by HLA class I (HLA-A, HLA-B, HLA-C) to naïve CD8 T cells or by HLA Class II (HLA-DR, HLA-DP, HLA-DQ) to naïve CD4 T cells. Second, a positive co-stimulation signal by CD28 T cell surface receptors to the B7 ligand is expressed on APCs. Third, cytokines are required to regulate the magnitude and duration of the immune response. Naïve CD8 T cells differentiate into effector cytotoxic CD8 T cells that are capable of killing infected cells presenting antigen specific to its T cell receptor. Conversely, activated helper CD4 T cells interact with B cells to promote clonal expansion and antibody production. T cell and humoral mediated immunity are responsible for clearing the antigen and providing immunological memory for a faster more efficient response to the same antigen in future encounters [155].

T cell development

T cells are a type of lymphocytes that play an essential role in adaptive cell mediated immunity. They arise from hematopoietic stem cells from the bone marrow that migrate to the thymus where they undergo maturation and become immature thymocytes. These immature thymocytes, that do not express CD4 or CD8 (double-negative), undergo T cell receptor (TCR) germline DNA V(D)J recombination which contributes to the enormous T cell diversity [155]. The double-negative thymocytes go on to simultaneously express both CD4 and CD8 (double-positive) and go through a "positive selection" process that ensures the TCR is able to recognize self-HLA molecules. Successful selection (not too strong or too weak) results in survival signals and expression of either CD4 or CD8 (single-positive) [155]. A "negative selection" process follows to remove any thymocytes that react with self-derived peptides [155]. Single positive thymocytes that have successful TCR recombination capable of recognizing peptide-HLA complexes with the correct affinity exit the thymus as naïve T cells ready to interact with cognate antigen peptides presented by APCs.

CD8 T cells in HIV infection

Cytotoxic "Killer" CD8 T cells are one of the main cellular components of the adaptive immune system. Their TCR is capable of recognizing specific antigenic peptides presented by HLA-I complexes on infected cells while minimizing nonspecific bystander tissue damage. Priming of naïve CD8 T cells in secondary lymphoid organs by APCs results in differentiation and proliferation of antigen-experienced effector CD8 T cells [156]. At the peak of the primary response, effector CD8 T cells recognize infected cells, form an immunological synapse, and produce a variety of cytokines (interferon gamma, tumor necrosis factor alpha, interlukin-2, interlukin-4) [157] in addition to releasing cytotoxic lytic granules containing perforin and granzymes [158] resulting in cell lysis or

20

apoptosis. Alternatively, CD8 T cells can induce apoptosis by engaging death-inducing receptors on infected cells [159]. During immune contraction, after the infection is cleared, a portion of antigen-induced effector CD8 T cells revert to a long-lived memory state capable of responding rapidly to similar antigens in future encounters [160].

CD8 T cells play an important role in influencing the outcome of HIV infection. Several lines of evidence suggest CD8 T cells are responsible for the control of HIV replication during the clinical latency phase of chronic HIV infection. Gag-specific CD8 T cells are able to recognize HIV infected cells before viral integration and viral protein production [161]. The emergence of HIV-specific CD8 T cells is associated with the post-peak decline of plasma viremia [162, 163]. Individuals with peptides restricted by specific HLA-I allele (HLA-B*57 and HLA-B*27) elicit a greater CD8 T cell response and have decreased disease progression to AIDS [164, 165], with similar observations reported in SIV infected RMs with Mamu-B*08 and Mamu-B*17 [166, 167]. "Elite controllers" exhibit greater CD8 T cell polyfunctionality and *in vitro* killing [168, 169]. Additionally, when CD8 T cells are depleted from SIV infected RM on suppressive cART, there is an increase of plasma viremia, which becomes controlled upon CD8 T cell reconstitution, suggesting that CD8 T cells contribute to the control of HIV/SIV replication during suppressive cART [170]. However, despite the compelling evidence, CD8 T cells fail to clear the infection in a majority of HIV infected individuals.
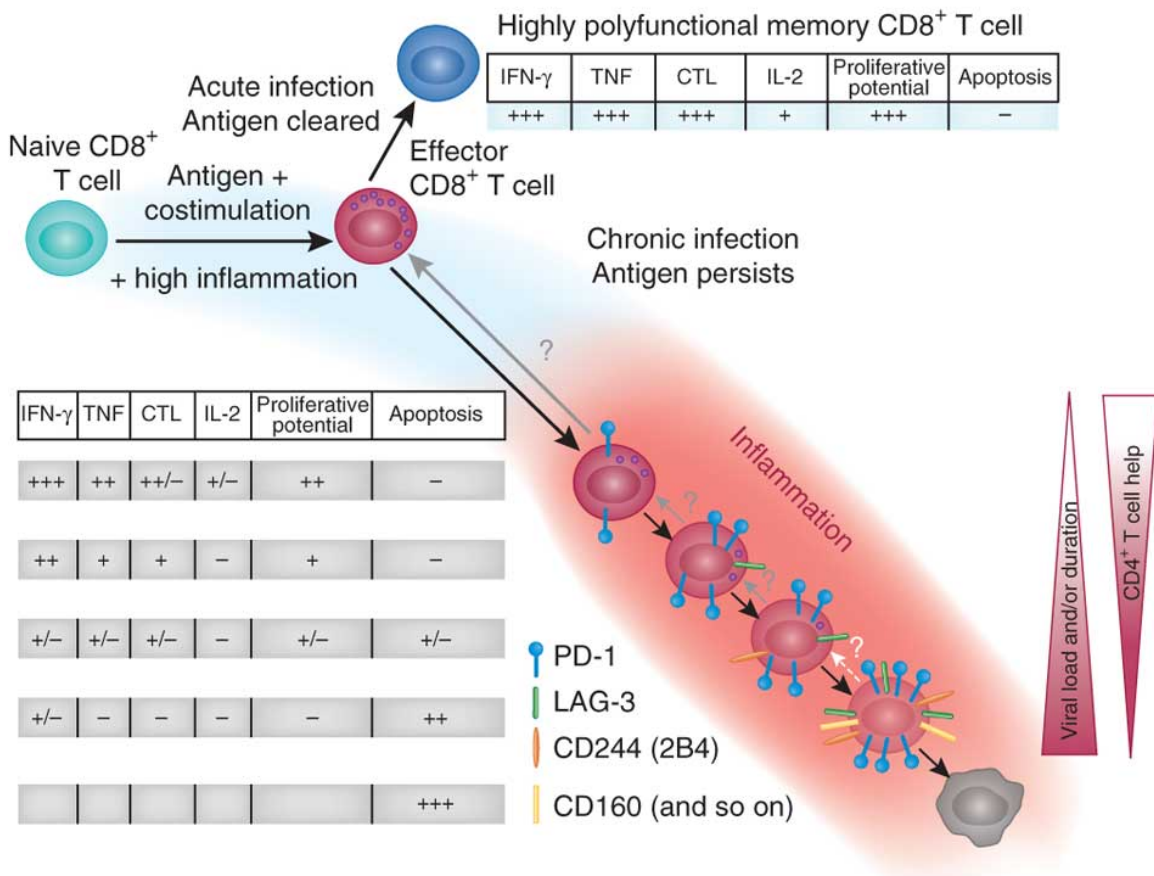
Fig.1.1 T cell exhaustion. Clearance of acute infection results in a highly polyfunctional population of memory CD8 T cells able to quickly respond to similar future antigens. However, persistent antigen and inflammation results in a loss of polyfunctional CD8 T cells associated with the simultaneous expression of negative immune checkpoint receptors. Figure adapted from [2]. Reprinted with permission.

CD8 T cell Dysfunction in HIV Infection

During unresolved chronic viral infections and cancers, low levels of persistent antigen and immune inflammation cause the impairment of antigen-specific CD8 T cells, termed "T cell exhaustion" (Figure 1.1) [2, 171]. The

concept of CD8 T cell exhaustion was originally defined in the chronic lymphocytic choriomeningitis virus (LCMV) murine model. During the course of chronic LCMV infection, virus-specific CD8 T cells were activated but failed to produce any antiviral effector functions [172]. T cell exhaustion was later defined as having a progressive loss of polyfunctionality, starting with decreased interleukin 2 (IL-2) and tumor necrosis factor alpha (TNFα) production, leading to diminished proliferative and cytotoxic capacity and ultimately lacking the ability to produce large amounts of interferon gamma (IFN-γ) [173]. Concurrently, immune regulation contributes to T cell exhaustion, where there is a stepwise upregulation of negative immune checkpoint receptors (NCRs) at the cell surface of exhausted T cells that actively inhibit immune functions [173]. NCR pathways are an important immune "check-and-balance system" for maintaining self-tolerance and prevention of autoimmunity [174]. A key feature of T cell exhaustion is the simultaneous expression of multiple NCRs on T cells, such as programmed death 1 (PD-1), T cell immunoglobulin mucin-domain 3 (TIM-3), lymphocyte activation gene 3 (Lag-3), Cytotoxic T- Lymphocyte associated protein 4 (CTLA-4), CD244, CD160 and others [171, 175]. The overexpression of these NCRs effectively dampens the T cell effector responses, ultimately resulting in the inability to control or eliminate chronic viral infections and cancers.

Increased expression of NCRs on viral-specific CD8 T cells such as PD-1, TIM-3 and LAG-3 during chronic HIV/SIV infection is associated with increased viral loads and accelerated disease progression [176-180]. Because NCR signaling is initiated by ligand-receptor interactions, they are susceptible to disruption by antibodies or recombinant forms of the ligands or receptors. Blocking these pathways with monoclonal antibodies has shown to restore viral-specific T cell effector functions *in vitro* [176, 178-180]. Targeting multiple pathways has shown to synergistically improve antiviral T cell effector functions, implying that the NCR pathways are non-redundant and functionally independent

23

[179, 181]. Blocking the PD-1 pathway has been shown to reinvigorate SIV-specific CD8 T cells and reduce plasma viremia while delaying viral rebound after cART interruption *in vivo* [182, 183]. Interestingly, targeting these pathways such as PD-1 and CTLA-4 has shown clinical benefit in cancers, generating durable responses and progression-free survival [184]. However, only a subset of individuals respond to treatment, suggesting additional mechanisms may be limiting the immune response [184]. Identifying additional NCR pathways during chronic HIV/SIV infection will inform interventions to restore T cell exhaustion and better control or clear the viral infection.

HIV Cure and Sustainable Remission Strategies

The "Berlin Patient", is the only individual who has been cured of HIV to date. He was infected with HIV for 11 years and on stable cART when he developed acute myeloid leukemia for which he received two sequential bone marrow transplants from donors with a mutant CCR5 (CCR5Δ32) gene [185]. Individuals with a homozygous CCR5Δ32 allele have been reported to be resistant to M-tropic HIV strains [186]. Remarkably, after the transplants when he stopped cART, the virus did not rebound nor could any virus be detected in his blood or tissues [185, 187]. Unfortunately, when similar hematopoietic stem cell transplantations were performed in two other HIV infected individuals, known as "The Boston Patients", the virus rebounded several months after analytical treatment interruption [188]. Ultimately, this procedure has a high risk of comorbid complications and may not feasible to scale up as a global HIV cure.

Several innovative approaches have been proposed to target the viral reservoir. Multiple groups are developing gene-editing and cell-based therapies to target the viral reservoir. Gene-editing with CRISPR/Cas9, zinc-finger nucleases or transcription activator-like effector nucleases (TALEN) systems can disrupt CCR5 or CXCR4 expression, potentially protecting cells from infection

[189-191]. Using a similar gene-editing technique, Kaminski and colleagues were able to excise the entire HIV proviral genome from latently infected T cells *in vivo* in mice [192]. Another group has engineered anti-HIV chimeric antigen receptor (CAR) T cells based on bnAbs that can recognize and kill infected cells *in vitro* [193]. It has also been suggested to transcriptionally lock the virus into a "deep latency" with gene silencing or pharmacological agents to prevent reactivation after analytical treatment interruption [194-196]. Nonetheless, further studies will be required to deliver these systems *in vivo* and translate theses approaches into clinical applications.

One HIV cure strategy of interest is the "shock and kill" approach, which involves flushing out virus and eliminating infected cells (Figure 1.2). Latency-reversing agents (LRAs) are used to reactivate cells harboring latent virus (shock), then in combination with cART, the immune system will be able to recognize and eliminate the infected cells (kill) [1].

The LRAs are classified into groups based on their mechanism of reactivation. LRAs include protein kinase C (PKC) agonists, histone deacetylase inhibitors (HDACi), histone methylation inhibitors (HMTi), DNA methyltransferase inhibitors (DNMTi), inhibitors of bromodomain and extra-terminal proteins (BET), Toll-like receptor agonist, retinoic acid-inducible gene I (RIG-I) agonist, immune checkpoint blockade and unclassified agents such as disulfiram [197-200]. Several small clinical trials have assessed the ability of these LRAs to reactivate viral production from the stable latent reservoir *in vivo*, however there was little impact on the size of the viral reservoir [201-206], suggesting additional immune mechanisms may be required for elimination of reactivated latently infected cells. A combination of attack plans will most likely be required to impact viral persistence while improving immune function to eliminate or control viral infection.

"Shock and Kill" Approach
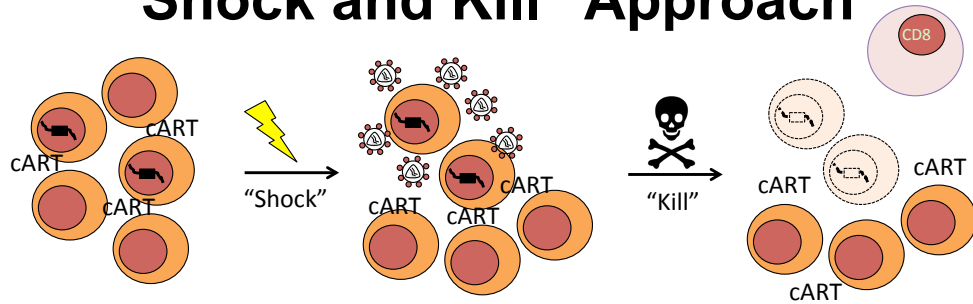
Shock: Latency Reversing Agents (LRAs)

HDACi, BET Bromodomain Inhibitors, PKC Activators, Disulfiram, TLR7 Agonist, dCas9-SAM, etc. _Without global immune activation_

Kill: Immune Mediated Mechanisms

CD8+ T cells, NK cells, B cells (bNAbs), Therapeutic Vaccines etc.

Fig.1.2 "Shock and Kill" HIV Cure strategy. Figure represents the HIV cure strategy to flush out latent HIV and eliminate infected cells while protecting new cells from being infected with cART. Figure adapted from [1].

CHAPTER 2
DISSERTATION SCOPE

Background for research questions

HIV infection remains a global health concern with an estimated 36.9 million individuals living with HIV and a total of 39 million HIV related deaths at the end of 2015. Despite therapeutic advances an effective HIV cure or vaccine does not exist. Current combinational antiretroviral therapy is able to suppress plasma viremia to undetectable levels, however it fails to target the integrated provirus and eradicate the infection. As a result, HIV infected individuals must adhere to therapy for life at a significant finical cost and potential long-term side effects.

In the absence of treatment, HIV infection is brought partially under control by the infected person's immune system, specifically by an immune system cell called a cytotoxic "killer" CD8 T cell. The response of these cells and HIV during the early stages of infection is crucial and will determine how the disease will progress. Over time, the immune damage mediated by HIV infection affects the function of the CD8 T cell even if with the addition of combination antiretroviral therapy (cART).

During unresolved chronic HIV infection, low levels of persistent antigen and immune inflammation cause viral specific CD8 T cells to become impaired and unable to eliminate virally infected cells. CD8 T cells begin to coordinately upregulate a series of negative checkpoint receptors (NCR) that increases the threshold necessary for activation. PD-1 is an early NCR associated with loss of proliferative capacity, while TIM-3 marks a more dysfunctional subset with diminished proliferative and cytokine capacity. Interfering with these NCR pathways alone or in combination has shown to restore cytoxicity and increased suppression of HIV infected CD4 T cells, however not all properties of exhausted cells are restored, implying that these pathways are non-redundant mechanisms of maintaining immune tolerance. Furthermore, adaptive resistance to PD-1 blockade has shown upregulation of alternative NCRs to compensate against

28

single blockade, identifying additional NCRs is imperative to developing novel therapies to restore immune functions.

A recently described NCR, T cell immunoreceptor with immunoglobulin and ITIM domains (TIGIT: also known as Vsig9, Vstm3 or WUCAM), has shown to be expressed on CD8 T cells and NK Cells and has indirect and direct inhibitory effects. Exploration of TIGIT and other NCRs during HIV infection is critical to identifying novel immune pathways as targets to restore immune function and control or eliminate the virus.

Long-term goal and Objectives

Our long-term goal is to understand mechanisms driving immune dysfunction that mediate the HIV disease progression and develop effective immune-based therapies for prevention or eradication of HIV infection.

To accomplish the objectives of this study, cutting edge immunophenotyping, immune pathway blockades, multiplex assays, genetic analysis and bioinformatics were employed to assess the role of TIGIT in HIV and SIV infection to identify immune pathways that can be targeted during cART suppressed HIV/SIV infection.

We hypothesize that HIV/SIV infection will result in an expansion of TIGIT+ T cells that which contributes to immune dysfunction, furthermore targeting the TIGIT pathway with novel targeted reagents will restore effector functions and contribute to the clearance of HIV infected cells.

Aims

Paper I: To investigate the role of TIGIT on CD8 and CD4 T cells in HIV and SIV infection and the relationship with disease progression and viral persistence.

Paper II in preparation: To explore the role of TIGIT and TIGIT Ligands in the blood and tissues during cART suppressed HIV infection.

Significance

The proposed research is an innovative approach to identify and characterize multiple immune pathways that can be potentially targeted to increase the immune capacity to eliminate infected cells during HIV infection. HIV infection remains a global health concern for which there is no effective cure or vaccine. Individuals on suppressive cART have increased non-AIDS comorbidities, decreased life expectancy and significant economic strain compared to HIV-uninfected population controls. The results from this study can be applied to "shock and kill" strategies currently being evaluated to eradicate HIV infection *in vivo*. This study will provide insight into immune dysfunction and HIV persistence, which will have a significant impact in the development of targeted therapeutics to enhance anti-HIV immunity.

CHAPTER 3

TIGIT MARKS EXHAUSTED T CELLS, CORRELATES WITH DISEASE PROGRESSION AND SERVES AS A TARGET FOR IMMUNE RESTORATION IN HIV AND SIV INFECTION

Chew et. al. PLoS Pathogens 2016 Jan 7;12(1):e1005349

TIGIT Marks Exhausted T cells, Correlates with Disease Progression, and Serves as a Target for Immune Restoration in HIV and SIV Infection

Glen M. Chew[1], Tsuyoshi Fujita[1,2], Gabriela M. Webb[3,4], Benjamin J. Burwitz[3,4], Helen L. Wu[3,4], Jason S. Reed[3,4], Katherine B. Hammond[3,4], Kiera L. Clayton[5], Naoto Ishii[2], Mohamed Abdel-Mohsen[6], Teri Liegler[6], Brooks I. Mitchell[1], Frederick M. Hecht[7], Mario Ostrowski[5], Cecilia M. Shikuma[1], Scott G. Hansen[3,4], Mark Maurer[8], Alan J. Korman[8], Steven G. Deeks[7], Jonah B. Sacha[3,4]* and Lishomwa C. Ndhlovu[1]*

[1]Hawaii Center for HIV/AIDS, Department of Tropical Medicine, John A. Burns School of Medicine, University of Hawaii, Honolulu, HI 96813, USA; [2]Department of Microbiology and Immunology, Tohoku University Graduate School of Medicine, Sendai 980- 8575, Japan; [3]Vaccine & Gene Therapy Institute and [4]Oregon National Primate Research Center, Oregon Health & Science University, Portland, OR 97006, USA; [5]Department of Immunology, University of Toronto, Toronto, Ontario M5S 1A8, Canada; [6]Division of Experimental Medicine and [7]HIV/AIDS Division, Department of Medicine, San Francisco General Hospital, University of California, San Francisco, CA 94110, USA; [8]Biologics Discovery California, Bristol-Myers Squibb, Redwood City, CA 94063, USA.

SHORT TITLE: Targeting TIGIT enhances HIV/SIV T cell immunity
*JBS and LCN share equal Co-senior Authorship

CORRESPONDING AUTHOR: Lishomwa C. Ndhlovu, MD, PhD, Hawaii Center for HIV/AIDS, John A. Burns School of Medicine, University of Hawaii, 651 Ilalo Street, Honolulu, HI, 96813, USA. Email: lndhlovu@hawaii.edu
Keywords: HIV, TIGIT, PD-L1, Activation, CD8 T cells, CD4 T cells, Viral Load

SPECIFIC AIMS

Specific Aim I: Determine the role of TIGIT on T cells during progressive HIV infection

A: To evaluate the expression of TIGIT on CD8 and CD4 T cells during HIV infection

Hypothesis: TIGIT expression will be elevated on T cells during chronic HIV infection.

Rationale: Chronic antigen exposure and persistent inflammation leads to an increase of other negative checkpoint receptor expressions (TIM-3, PD-1, LAG-3).

B: To determine the role of TIGIT and T cell dysfunction during HIV infection

Hypothesis: T cells expressing TIGIT will have impaired effector function.

Rationale: Engagement of TIGIT results in blunted T cell functions, such as proliferation, cytotoxicity and production of cytokines.

C: To determine the relation of CD4 T cells expressing TIGIT and the CD4 viral reservoir

Hypothesis: CD4 T cells expressing TIGIT will be enriched for HIV DNA.

Rationale: Negative checkpoint receptors inhibit T cell activation, which will prevent viral transcription and may be involved in maintaining the viral reservoir.

Aim II: Assess the role of TIGIT in the physiologically relevant non-human primate model of HIV/AIDS

A: Evaluate the expression of TIGIT in *Rhesus macaques* during SIV infection

Hypothesis: Rhesus macaques will have an increased expression of rhesus TIGIT (rhTIGIT) during SIV infection.

Rationale: Non-human primates are close genetic relatives of humans and when infected with SIV lead to AIDS-like diseases, mimicking HIV disease progression and immune exhaustion.

B: Determine the role of rhesus TIGIT and T cell dysfunction during SIV infection

Hypothesis: T cells expressing rhTIGIT will have impaired effector functions.

Rationale: Engagement of negative checkpoint receptors on T cells results in blunting T cell functions such as proliferation, cytotoxicity and production of cytokines.

Aim III: Determine the effects of blocking the TIGIT pathway on reinvigorating existing T cell effector functions during HIV/SIV infection

A: Test the activity of blocking human and rhesus TIGIT with monoclonal antibodies

Hypothesis: Blocking the TIGIT pathway will increase pre-existing T cell effector function in response to HIV/SIV antigens.

Rationale: Preventing engagement of other negative checkpoint receptors results in improved T cell functions.

B: Determine the synergistic effects of simultaneously blocking multiple NCR pathways reinvigorating existing T cell effector functions

Hypothesis: Blocking multiple negative checkpoint receptor pathways will lead to a greater increase of anti-HIV/SIV T cell functions compared to single blockade alone.

Rationale: Preventing engagement of multiple negative checkpoint receptors results in synergistic enhancement of T cell effector functions.

ABSTRACT

HIV infection induces phenotypic and functional changes to CD8 T cells defined by the coordinated upregulation of a series of negative checkpoint receptors that eventually result in T cell exhaustion and failure to control viral replication. We report that effector CD8 T cells during HIV infection in blood and SIV infection in lymphoid tissue exhibit higher levels of the negative checkpoint receptor TIGIT. Increased frequencies of TIGIT+ and TIGIT+ PD-1+ CD8 T cells correlated with parameters of HIV and SIV disease progression. TIGIT remained elevated despite viral suppression in those with either pharmacological antiretroviral control or immunologically in elite controllers. HIV and SIV-specific CD8 T cells were dysfunctional and expressed high levels of TIGIT and PD-1. *Ex-vivo* single or combinational antibody blockade of TIGIT and/or PD-L1 restored viral-specific CD8 T cell effector responses. The frequency of TIGIT+ CD4 T cells correlated with the CD4 T cell total HIV DNA. These findings identify TIGIT as a novel marker of dysfunctional HIV-specific T cells and suggest TIGIT along with other checkpoint receptors may be novel curative HIV targets to reverse T cell exhaustion.

INTRODUCTION

During chronic viral infections, high antigenic loads continually stimulate T cells leading to progressive loss of function termed "T cell exhaustion" [2]. Throughout this period, T cells increase expression of several inhibitory immune receptors that raise the threshold for activation, resulting in suppressed immune responses. While Programmed Death Receptor-1 (PD-1) was one of the earliest surface markers of immune exhaustion identified [176, 177, 180, 182, 207, 208], we have shown that the surface glycoprotein, T cell immunoglobulin- and mucin domain-containing molecule (Tim)-3, defines a state of T cell exhaustion with diminished proliferative and cytokine capacities in chronic viral infection [178, 209]. Thus, the upregulation of these and other negative checkpoints receptors may serve as potential targets for the reversal of T cell exhaustion.

Indeed, blocking the interaction of T cell negative checkpoint receptor pathways using targeted reagents against PD-1/Programmed Death-Ligand 1 (PD-L1), Tim-3, Lymphocyte-activation gene 3 (Lag-3) and CD160 has shown promise in reversing CD8 T cell exhaustion [178, 181, 182, 210, 211]. Reagents targeting many of these receptors are rapidly advancing in the clinic and are showing efficacy in the control of viral infectious disease [212] as well as anti-tumor immunity [213-218]. A single dose of an antibody against PD-1 led to sustained clearance of hepatitis C virus infection in a small subset of individuals [212]. Blockade of the PD-1/PD-L1 axis *in vivo* demonstrated efficacy in restoring simian immunodeficiency virus (SIV)-specific T cell and humoral immunity, and led to a reduction of SIV viremia and in immune activation. However, this did not completely control virus, suggesting that additional therapies are needed. Importantly, not all features of the exhausted T-cells are restored by interfering with a single pathway [177, 178, 180, 207, 219]. Synergistic simultaneous dual blockade has yielded more promising responses suggesting these co-inhibitory molecules are non-redundant [179, 181, 218, 220].

36

T cell immunoreceptor with immunoglobulin and ITIM domains (TIGIT) is a recently described immune checkpoint receptor that belongs to the CD28 family and contains an extracellular IgV domain, a transmembrane domain, and a cytoplasmic tail containing two-immunoreceptor tyrosine-based inhibitory motif (ITIM) [221]. It has been reported to be expressed on natural killer (NK) cells, CD8 and CD4 T cell subsets [221] and is induced upon activation [221-225]. TIGIT competes with DNAM-1, a co-stimulatory molecule, and TACTILE, a co-inhibitory molecule, for the poliovirus receptor (PVR) a member of the nectin family of adhesion molecules that is expressed on dendritic cells (DCs) [221, 222, 226]. Several murine and human studies strongly suggest that TIGIT is a negative modulator of T cell and NK cell function [223, 227-229]. A number of plausible mechanisms exist by which TIGIT can mediate inhibition of T and NK cell activation. Signaling through the TIGIT/PVR pathway with the standard recruitment of phosphatases via the intracellular ITIM domain of TIGIT can curtail T cell and NK cell responses [224]. This interaction has been shown to induce tolerogenic DCs to release the immunosuppressive cytokine IL-10 [223, 229]. Furthermore, disruption of DNAM-1 homodimerization by TIGIT can abrogate the positive co-stimulatory signals required for activation [217]. Recently, potent anti-viral and anti-tumor responses related to enhanced CD8 T cell effector activity were generated following synergistic dual blockade of PD-L1 and TIGIT in the mouse model of chronic lymphocytic choriomeningitis virus (LCMV) infection [217] and *ex-vivo* in patients with advanced melanoma [230].

To date, these results have not been replicated in any human viral disease, but overexpression of both TIGIT and PD-1 on virally exhausted T cells suggests that this is a promising avenue of exploration as a viable strategy to increase control or eliminate viral infections through T cell modulation. Given the potential to restore anti-HIV-specific CD8 T cell responses by synergistic modulation of negative checkpoint receptors, we investigated the expression and

37

function of TIGIT in HIV disease pathogenesis, and in the SIV non-human primate model of HIV/AIDS.

RESULTS

Expansion of TIGIT+ T cells during HIV infection and correlations with clinical parameters of HIV disease progression, T cell activation, and the CD4 cell-associated HIV DNA content.

We assessed the surface expression of TIGIT on T cells from peripheral blood mononuclear cells (PBMCs) from HIV-infected individuals that were either acutely infected (AI), non-controllers (NC), cART suppressed (AS), or elite controllers (EC), and compared these results to age-matched HIV-uninfected donors (HD) (Table 3.1; Figure 1A-D; Supplemental Figure 3.1A,B). We observed a significant expansion in the frequency of TIGIT+ CD8 T cells in HIV-infected participants (AS; 44.95%; EC 56.7%; NC, 64.5%), even among those with viral suppression, relative to HD (median: 28.05%; Figure 3.1C). We observed a non-significant trend in the expansion of TIGIT+ CD8 T cells in AI (40.4%) relative to HD (Figure 3.1C). TIGIT+ CD4 T cells were significantly elevated among NC (24.5%) compared to HD (16.05%) (Figure 3.1D).

Among the HIV-infected NC, TIGIT+ CD8 T cells inversely correlated with CD4 T cell counts, but not with CD8 T cell activation or plasma viral load (Figure 3.1E; Supplemental Figure S1E). TIGIT+ CD4 T cells did not correlate with CD4 cell counts in NC (Figure 3.1F). Among the EC, TIGIT+ CD8 T cells trended to correlate with CD8 T cell activation, while frequencies of TIGIT+ CD4 T cells correlated with CD4 T cell activation (Figure 3.1G,H). We did not observe any other significant correlations with TIGIT+ T cells (Supplemental Figure 3.1C-F,G,I). Given the high levels of TIGIT in the midst of viral suppression, we assessed the relationship between TIGIT and the cellular HIV content in highly purified CD4 T cells among HIV-infected "cART initiators" who met strict selection

criteria of well documented and long-term persistent viral suppression (L-AS; Table 3.1). We did not observe a correlation with the frequency of CD8 T cell or CD4 T cell TIGIT expression and HIV RNA from purified CD4 T cells (Supplemental Figure 3.1H,J). However, the frequency of TIGIT+ CD4 T cells positively correlated with purified CD4 T cell HIV DNA content, but not with frequency of TIGIT+ CD8 T cells (Figure 3.1I,J). These data indicate that TIGIT expression on CD4 T cells may be linked to chronic HIV disease pathogenesis, residual immune activation, and the cellular HIV DNA content among those with viral suppression.

Phenotype and function of TIGIT on CD8 T cells during HIV infection.

HIV infection leads to an expansion of intermediately differentiated memory CD8 T cells that are not fully mature effectors [231-233]. We profiled the pattern of TIGIT expression in the heterogeneous CD8 T cell subpopulations and found TIGIT was significantly expanded on the CD8 T cell intermediate/transitional and effector subsets with the highest expression of TIGIT on the effector CD8 T cell subset (Figure 3.2A; Supplemental Figure 2A-E) compared to AS. In the naïve population TIGIT expression was relatively stable with only a significant difference seen between HD and the non-controllers (Figure 3.2A). We did observe a statistically significant difference in TIGIT expression between the HD and AI group in the memory CD8 T cell population (Figure 3.2A). Thus, TIGIT is expanded on the intermediate/transitional and effector CD8 T cell subsets during chronic HIV infection, consistent with a role for TIGIT as potential regulator of intermediate/transitional and effector T cell responses.

We next profiled the expression of TIGIT on viral-specific CD8 T cells from chronically HIV-infected participants using matched HLA-I restricted pentamers for various HIV and CMV peptide epitopes. TIGIT was expressed on over half of all CD8 T cells for specific for HIV Gag (55.3%), Polymerase (54.7%), Envelope

(54.3%), Nef (52%), and also for CMV pp65 (57.8%) (Figure 3.2B,C). Comparable levels of TIGIT on HIV and CMV specific CD8 T cells were observed on a per cell basis as measured by Geometric Mean Fluorescence Intensity (GMFI) (Figure 3.2C).

We next assessed the effector phenotype and functional properties of TIGIT expressing CD8 T cells to determine whether they retain features of immune exhaustion. We found that most of the TIGIT expressing CD8 T cells co-expressed PD-1 with the frequency of TIGIT+ PD-1+ CD8 T cells significantly expanded in chronic HIV infection (AS, 18.65%; EC, 20.85%; NC, 38.15%) compared to HD (13.65%) (Figure 3.3A,B). The frequency of TIGIT+ PD-1+ CD8 T cells inversely correlated with CD4 T cell counts (Fig 3.3C) and positively correlated with plasma viral load levels (Figure 3.3D) among all chronically HIV-infected individuals. We observed significantly higher frequencies of TIGIT+PD-1+ co-expression on HIV-Gag-specific CD8 T cells compared to non-HIV-Gag-specific CD8 T cells derived from PBMCs (Figure 3.3E-G). Furthermore, the majority of the TIGIT+PD-1+ HIV-Gag-specific CD8 T cells retained a transitional/intermediate memory (CD45RA-CCR7-CD27+) phenotype (Figure 3.3H-J). These results suggest TIGIT may render a large fraction of viral specific CD8 T cells vulnerable to negative regulation.

Given the high expression of PD-1 among TIGIT+ CD8 T cells, we evaluated the functional status of the TIGIT expressing cells. We stained T cells with the nuclear antigen Ki-67, which is associated with cellular proliferation, and observed that TIGIT+ cells expressed significantly more Ki-67 than TIGIT- CD8 T cells (Figure 3.4A,B). However, in contrast, Ki-67 expression was equivalently distributed between PD-1+ and PD-1- CD8 T cells (Figure 3.4C,D). Using intracellular cytokine staining, in response to stimulation with an overlapping 15mer HIV Gag peptide pool, we observed that TIGIT+ CD8 T cells produced significantly less IFN-γ, TNF-α and IL-2 compared to TIGIT- CD8 T cells (Figure 3.4E,F). We observed phenotypically the majority of the HIV specific cytokine

responsive CD8 T cells lacked TIGIT and PD-1 dual expression and were minimally represented in the TIGIT+PD-1+ subset. However, single expressing cells retain some functional responses (Figure 3.4G).

To directly assess the functionality of the TIGIT+PD-1+ subset in HIV infected individuals, CD8 T cells expressing TIGIT and/or PD-1 on their surface were sorted to high purities (Supplemental Figure 3.3A,B), stimulated with or without anti-CD3 + anti-CD28 Dynabeads, and assessed for changes in TIGIT and PD-1 expression and their capacity to secrete 13 different cytokines. We found CD8 T cells lacking TIGIT (TIGIT-PD-1- and TIGIT-PD-1+) robustly upregulated TIGIT upon stimulation (Supplemental Figure 3.3B,C). Irrespective of PD-1 expression, the TIGIT expressing (TIGIT+PD-1- and TIGIT+PD-1+) cells only marginally increased TIGIT expression (Supplemental Figure 3.3B,C) upon stimulation. We harvested the supernatants and observed that TIGIT+PD-1+ cells had the lowest secretion of all cytokines assessed in comparison to the other three subsets (Supplemental Figure 3.3D). TIGIT+PD-1- cells produced less cytokines than TIGIT-PD-1+ cells. These data are partially in alignment with results observed in Figure 4G. However, it was notable that IL-10 production was almost exclusively produced by the TIGIT-PD-1+ cell subset. These data suggests that TIGIT+ CD8 T cells, particularly TIGIT+PD-1+ co-expressing CD8 T cells exhibit distinguishing features of exhausted T cells.

Next, we evaluated the intracellular granular content of TIGIT expressing cells. We observed that TIGIT expressing CD8 T cells contained significantly more perforin and granzyme B compared to non-TIGIT expressing CD8 T cells (Figure 3.4H,I). We observed no difference in the ability of TIGIT+ CD8 T cells to degranulate compared to TIGIT- CD8 T cells when stimulated with HIV Gag peptide pool (Figure 3.4J,K). However, upon stimulation with anti-CD3 + anti-CD28 Dynabeads, TIGIT+ cells degranulated less than TIGIT- cells (Figure 3.4J-L).

41

Induction of TIGIT on CD8 T cells during HIV infection.

To explore the regulation of TIGIT expression we stimulated HIV-specific CD8 T cells from chronically HIV-infected individuals with HIV Gag peptides. HIV Gag peptide stimulation did not significantly increase the expression of TIGIT on HIV-specific CD8 T cells, although we did observe an upregulation of TIGIT in a subset of individuals (Figure 3.5A-C). Several common gamma-chain (γ-chain) cytokines have been shown to directly upregulate negative checkpoint receptors on CD8 T cells during retroviral infections [234]. To further understand the mechanism driving TIGIT upregulation, we explored the capacity of γ-chain and non-γ-chain cytokines to regulate TIGIT expression (Figure 3.5D-F). We found that IL-2 and IL-15 prominently led to a significant increase in TIGIT expression on CD8 T cells from HIV-infected individuals unlike non-γ-chain cytokines IL-12 and IL-18 (Figure 3.5E). This effect was not evident on CD8 T cells derived from HIV-uninfected participants (Figure 3.5F). Correspondingly, TIGIT expression on CD4 T cells was upregulated primarily by IL-2 and IL-15 in HIV-infected individuals (Supplemental Figure 3.4A). IL-21 stimulation increased TIGIT expression on CD8 T cells, but not CD4 T cells (Supplemental Figure 3.4B). These data suggests that TIGIT expression may be regulated by a peripheral cytokine milieu dominated by γ-chain cytokines present during HIV infection.

Effects of anti-TIGIT and anti-PD-L1 mAb blockade on HIV-specific CD8 T cell cytokine and proliferative responses.

Since TIGIT and PD-1 are co-expressed, and dual blockade in the mouse model limits *in vivo* LCMV replication [217] and elicits anti-tumor CD8 T cell responses [230], we evaluated the effects of TIGIT and PD-L1 blockade on HIV-Gag-specific CD8 T cells using cells from chronically HIV-infected individuals at various stages of infection (Table 3.2). To evaluate the *ex vivo* HIV-specific T cell cytokine restoration, we used a modified version of our previously published *in vitro* short-term primary recall blockade assay [178]. Incubation with either anti-

TIGIT mAb alone or anti-PD-L1 mAb alone significantly increased IFN-γ production, however dual blockade of both TIGIT and PD-L1 did not enhance IFN-γ responses over anti-TIGIT or anti-PD-L1 alone (Figure 3.6A,B). We also observed that only dual blockade of TIGIT and PD-L1 significantly increased IL-2 production by CD8 T cells (Supplemental Figure 3.5A,B). Given that virus-specific IL-2 producing CD4 T cells have been associated with disease control in HIV infection we assessed the effects of TIGIT blockade on CD4 T cells [235, 236]. Similarly, only dual blockade of TIGIT and PD-L1 significantly increased IL-2 production over the single blockades alone from CD4 T cells (Supplemental Figure 3.5C,D).

Single blockade of PD-L1 significantly enhanced HIV-specific CD8 T cell proliferation while single blockade of TIGIT did not improve CD8 T cell proliferation (Figure 3.6C,D). When both anti-TIGIT and anti-PD-L1 were combined there was significant increased CD8 T cell proliferation compared to PD-L1 blockade alone (Figure 3.6C,D). Though donor OM115 had the highest baseline levels of TIGIT+ CD8 T cells among the group, no significant association was seen between the magnitude of IFN-γ production and proliferation by TIGIT blockade and baseline TIGIT+ CD8 T cell expression (r = 0.24, p = 0.257). These data suggests that HIV-specific CD8 T cell proliferation can be markedly improved with simultaneous combination blockade of TIGIT and PD-L1.

rhTIGIT is elevated on dysfunctional effector CD8 T cells in the SIV rhesus macaque model of HIV/AIDS and is associated with SIV disease progression.

To explore the role of TIGIT in the rhesus macaque model of HIV/AIDS we cloned rhesus TIGIT (rhTIGIT) (GenBank: KR534505) and observed that it shares 88.11% sequence homology with human TIGIT (Supplemental Figure 3.6A). We reasoned that rhTIGIT expression and function would mimic our

human HIV studies and be replicable in the SIV-infected rhesus macaque model of HIV/AIDS. RhTIGIT expression was significantly increased on CD8 T cells derived from the lymph node (LN) (38.6%) and splenic (60.9%) compartments when compared to SIV-uninfected macaques (LN 10.82% and spleen 25.55%), but not in PBMCs (Figure 3.7A; Supplemental 3.6B). Similar to what we observed in HIV-infected participants, the frequency of rhTIGIT+ CD8 T cells from PBMC did not correlate with plasma SIV viral load. However, we did observe a significant correlation with the frequencies of rhTIGIT+ CD8 T cells in LN and viral load (Figure 3.7B).

As observed in human HIV infection, rhTIGIT expression was more prominently expressed in SIV infection on effector memory (EM, CD28-CD95+), and central memory (CM, CD28+CD95+) CD8 T cells when compared to naïve (N, CD28+CD95-) CD8 T cells from PBMCs, LN and from the spleen (Supplemental Figure 3.6C). In the tissues, it was notable that TIGIT expression was highest on the central memory CD8 T cells when compared to PBMCs (Supplemental Figure 6C). As in HIV infection, stimulation with γ-chain cytokines such as IL-2 and IL-15 upregulated rhTIGIT on CD8 T cells from SIV-infected animals (Supplemental Figure 3.6D).

rhTIGIT was also expressed on ~40% of SIV Gag or Tat tetramer specific CD8 T cells derived from PBMCs or secondary lymphoid tissues, even in animals with full cART suppression of peripheral SIV viremia (Figure 3.7C). This was more prominently found in the tissues of SIV-infected animals where higher frequency of SIV-specific CD8 T cells co-expressed both rhTIGIT and rhesus macaque PD-1 (rhPD-1) (Supplemental Figure 3.6E-H).

While the levels of Ki-67 expression did not differ between rhTIGIT+ and rhTIGIT- CD8 T cells from SIV-infected rhesus macaques (Supplemental Figure 3.7A-D), CD8 T cells lacking rhTIGIT from PBMC produced significantly more IFN-γ compared to rhTIGIT+ CD8 T cells when stimulated with either phorbol 12-

mysistate 13-acetate (PMA) + ionomycin or SIV Gag181-189 CM9 peptide (Figure 3.7D,E).

Given the similarities of rhTIGIT and human TIGIT, we evaluated TIGIT and PD-L1 blockade on SIV peptide stimulated CD8 T cell responses. We found that dual blockade of rhPD-L1 and rhTIGIT enhanced SIV-specific CD8 T cell proliferation in PBMCs and spleen while single blockade of rhPD-L1 enhanced SIV-specific proliferation in the spleen (Figure 3.7F,G). Taken together, rhTIGIT pathway is active in the rhesus macaque model of HIV/AIDS and partially mimics human TIGIT expression and function during HIV infection.

DISCUSSION

In this report we profiled TIGIT expression on T cells in HIV-infected participants with various degrees of viral control and in SIV-infected rhesus macaques. We (1) unveil a role for TIGIT+ CD8 T cells in HIV disease progression and demonstrate its relation to T cell exhaustion, (2) observe that TIGIT appears to associate with the cellular viral reservoir in CD4 T cells, (3) we found that co-blockade of TIGIT and PD-L1 lead to a greater restoration of T cell function compared with a single blockade, and (4) by successfully cloning rhTIGIT (GenBank: KR534505) we reveal the similarities in expression and function of rhTIGIT on T cells in the non-human primate model of HIV/AIDS. Our findings reveal a novel inhibitory pathway involved in the suppression of T cell responses during chronic viral infection, the blockade of which may contribute to the reversal of T cell dysfunction in the control or elimination of HIV infection.

While TIGIT levels on CD8 T cells tracked disease progression (depletion of CD4 T cells and T cell activation), this was not evident across the various HIV-infected groups. There was a significant difference in TIGIT+ memory CD8 T cells in acute infection compared to the uninfected group, but not in the global CD8 T cell population. This suggests there may be a gradient, with an increase in

global TIGIT+ CD8 T cells in acute infection that becomes greater over time, which is distributed among the differentiated CD8 T cell populations and may differ when compared to other negative checkpoint receptors which are found elevated during the early stages of HIV infection [177, 237, 238].

TIGIT induction appears to be driven by polyclonal TCR stimulation and this is a common feature among immune checkpoint receptors [237, 239]. We observed HIV-Gag-SL9-specific CD8 T cells did not increase TIGIT expression after HIV Gag peptide stimulation as a group, however a subset of individuals with moderate levels of TIGIT increased expression after stimulation, and individuals that expressed high levels of TIGIT retained expression after stimulation. TIGIT remained elevated despite antigen in cART-suppressed individuals, previous studies have also shown that common γ-chain cytokines maintain the ability to regulate immune checkpoint receptor expression in the absence of antigenic stimulation [234, 240]. Our studies align with these previous observations and suggest that a cytokine milieu conducive for the maintenance of an exhausted T cell profile persists in HIV and SIV infection even during viral suppression.

TIGIT expression was found to be associated with T cell activation principally among ECs who represent a small population of HIV-infected individuals able to spontaneously suppress their viral load (<50 copies/ml) in the absence of cART for prolonged periods of time [241]. However, over time a subset of EC loses virologic control and develops viremia and CD4 T cell loss [242, 243]. In addition, EC maintain elevated levels of T cell activation despite viral control [92, 244]. High TIGIT expression may reflect ongoing immune activation in the EC population. The institution of cART in those EC has lead to a reduction in immune activation [245, 246]. Given our finding, in addition to cART, some EC may benefit from TIGIT blockade to alleviate the persistent T cell immune activation thereby reducing the risk of adverse non-AIDS events that have been documented to occur in this population, however such strategies need

to be considered carefully given the risk of autoimmunity as described in anti-PD-1 clinical trials in the oncology field [247, 248].

Viral clearance of the chronic strain of LCMV (clone 13) in mice by combined blockade of TIGIT and PD-L1 provided the first evidence of the advantages of targeting these two pathways [217]. In addition, targeting TIGIT and PD-L1 on CD8 tumor infiltrating lymphocytes in patients with advanced melanoma synergistically improves potent anti-tumor responses [230]. Here we extend these finding to human and simian retroviral infections. This was significant given the expansion of dual expressing TIGIT and PD-1 CD8 T cells in HIV infection despite pharmacological or immunological viral suppression. Our data shows the presence of TIGIT and PD-1 dual expressing HIV and SIV-specific CD8 T cells and co-blockade of TIGIT and PD-L1 better enhanced proliferation of HIV and SIV-specific CD8 T cell responses compared to single blockade. Although we see a significant increase among all HIV-infected individuals, it was evident that subsets of weak-responders exist and appear heterogeneous irrespective of stage of infection, viral load levels or viral suppression. Indeed, combinational blockade of CTLA-4 and PD-1 revealed a subset of weak-responders to anti-tumor activity. Different or expanded combinations of immune checkpoint blockers with anti-TIGIT may need to be considered in the arsenal to improve anti-viral T cell immunity in all individuals.

Persistence of the cellular latent HIV reservoir has been a major barrier to the eradication of HIV [249]. One proposed strategy is to "Shock" the latently infected cells to flush out virus with latency reversal agents (LRAs) [206, 250, 251]. The development of the "Shock" strategies is advancing at a rapid pace with *in vivo* studies yielding activity in reactivating of latent virus. However, the "Kill" component is less well developed. Shan and colleagues demonstrate that after reactivation of latent virus from CD4 T cells, CD8 T cells' activity had the capacity to kill latently infected CD4 T cells if appropriate pre-stimulation of HIV peptide and IL-2 was provided an *in vitro* latency assay using Bcl-2 as a survival

47

signal to prolong the longevity of the latent CD4 T cells [252]. Furthermore, recent studies show that HIV-infected individuals on cART retain broad HIV-specific cytotoxic T-lymphocyte responses that are able to target the mutated latent virus [253]. Blocking immune checkpoint pathways such as TIGIT and PD-1/PD-L1 can be harnessed to boost HIV-specific CD8 T cells responses given that these pathways persist in the setting of viral suppression. Furthermore, given our findings showing the relationship with TIGIT expression on CD4 T cells and the total cell associated HIV DNA, it remains unclear what role TIGIT may play in the establishment of the reservoir in CD4 T cells, however it is likely related to the capacity of TIGIT's ability control T cell activation or proliferation.

Our study provides a novel role for TIGIT during HIV disease pathogenesis and our demonstration of a role of rhTIGIT in the non-human primate model of HIV/AIDS provides a platform to investigate our understanding of the complex networks of co-inhibition that can be tailored to each individual or viral infection. Improving CD8 T cell functions may further aid in the "Shock and kill" approaches being considered to eliminate latent virus and improve T cell mediated vaccine responses to prevent or limit infection [1].

MATERIALS AND METHODS

Study participants

We recruited participants from the following cohorts: University of California, San Francisco (UCSF) SCOPE and OPTIONS cohorts [178] the Hawaii HIV (HHC) cohort, the Toronto-based cohort CIRC (Maple Leaf Clinic and St. Michael's Hospital, Toronto, Canada) [254] and the Duke Human Vaccine Institute (DHVI) tissue repository. SCOPE specimens (n = 80) were selected from the following groups: untreated non-controllers (n = 20) (participants who had never been treated with antiretroviral agents or who had been off therapy for at least six months), treated virologic controllers (participants who had an

48

undetectable plasma HIV RNA level for the previous six months while on cART) (*n* = 20), spontaneous "elite" virologic controllers (participants who are untreated and who have at least three documented plasma HIV RNA levels <2,000 copies/ml over at least a 12-month period) (*n* = 20), Some of these participants had persistent plasma HIV RNA levels <75 copies/ml) and HIV-infected "cART initiators" (*n* = 20) who meet strict selection criteria and well documented persistent viral suppression for over 1.5 years. Participants with acute HIV infection (*n* = 24) were obtained for the OPTIONS cohort of primary HIV infection [178] and age-matched HIV-uninfected (*n* = 20) (Table 1) and chronically infected virally suppressed leukapheresesed individuals were obtained from the HAHC cohort [255]. Additional participants with chronic infection at various stages of infection were obtained from participants with various levels of viral control from the Toronto-based cohort CIRC cohort, HHC, and DHVI.

Ethics Statement

All persons gave written informed consent to participate in the study and approval for the study was obtained from the University of Hawaii Committee of Human Subjects. Samples were obtained from Indian Rhesus macaques (*Macaca mulatta*) housed at the Oregon National Primate Research Center (ONPRC), which were SIV infected for other ongoing, unrelated studies. Oregon Health & Science University (OHSU) Institutional Animal Care and Use Committee (IACUC) Protocol #: 0989. The OHSU Institutional Animal Care and Use Committee reviewed and approved all study protocols. All macaques in this study were managed according to the ONPRC animal husbandry program, which aims at providing consistent and excellent care to nonhuman primates. This program is based on the laws, regulations, and guidelines set forth by the United States Department of Agriculture (e.g., the Animal Welfare Act and its regulations, and the Animal Care Policy Manual), Institute for Laboratory Animal Research (e.g., Guide for the Care and Use of Laboratory Animals, 8th edition),

Public Health Service, National Research Council, Centers for Disease Control, and the Association for Assessment and Accreditation of Laboratory Animal Care (AAALAC) International. The nutritional plan utilized by the ONPRC is based on National Research Council recommendations and supplemented with a variety of fruits, vegetables, and other edible objects as part of the environmental enrichment program established by the Behavioral Management Unit. Paired/grouped animals exhibiting incompatible behaviors were reported to the Behavioral Management staff and managed accordingly. All efforts were made to minimize suffering through the use of minimally invasive procedures, anesthetics, and analgesics when appropriate. Animals were painlessly euthanized with sodium pentobarbital and euthanasia was assured by exsanguination and bilateral pneumothorax, consistent with the recommendations of the American Veterinary Medical Guidelines on Euthanasia (2013).

Quantifying cellular HIV DNA and RNA

Cryopreserved PBMCs were rapidly thawed and enriched for CD4 T cells to high purities with an EasySep Human CD4 T cell enrichment kit (Stemcell Technologies, Vancouver, British Columbia, Canada). Cellular RNA and DNA from PBMC T-cell subsets cells were purified using the AllPrep DNA/RNA kit (Qiagen, Ventura CA) as specified by the manufacturer, quantified using a Nanodrop (ND-1000) spectrophotometer and normalized to cell equivalents by qPCR using human genomic TERT for DNA and GAPDH or RPLP0 expression for RNA (Life Technologies, Grand Island NY). Total cellular HIV DNA (integrated and unintegrated) and RNA (unspliced and multiply spliced) was quantified with a qPCR TaqMan assay using LTR-specific primers F522-43 (5' GCC TCA ATA AAG CTT GCC TTG A 3'; HXB2 522-543) and R626-43 (5' GGG CGC CAC TGC TAG AGA 3'; 626-643) coupled with a FAM-BQ probe (5' CCA GAG TCA CAC AAC AGA CGG GCA CA 3) [256] on a StepOne Plus Real-time PCR System (Applied Biosystems Inc, Foster City CA). Cell associated HIV DNA copy number

was determined using a reaction volume of 20 µl with 10 µl of 2x TaqMan Universal Master Mix II including UNG (Life technologies), 4 pmol of each primer, 4 pmol of probe, and 5 µl of DNA. Cycling conditions were 50 °C for 2 min, 95 °C for 10 min, then 60 cycles of 95 °C for 15s and 59 °C for 1 min. Cell associated HIV RNA copy number was determined in a reaction volume of 20 µl with 10 µl of 2x TaqMan RNA to Ct 1 Step kit (Life Technologies), 4 pmol of each primer, 4 pmol of probe, 0.5 µl reverse transcriptase, and 5 µl of RNA under identical cycling conditions. For HIV DNA measurements, external quantitation standards were prepared from pNL4-3 in a background of HIV negative human cellular DNA, calibrated to the Virology Quality Assurance (VQA, NIH Division of AIDS) cellular DNA quantitation standards. For HIV RNA measurements, external quantitation standards were prepared from full length NL4-3 virion RNA followed by copy number determination using the Abbott RealTime assay (Abbott Diagnostics, Des Plains III) and calibrated to VQA HIV RNA standards. Patient specimens were assayed with up to 800 ng total cellular RNA or DNA in replicate reaction wells and copy number determined by extrapolation against a 7-point standard curve (1 – 10,000 cps) performed in triplicate.

Antibodies and flow cytometric analysis.

Cryopreserved PBMC were rapidly thawed in warm 10% cRPMI ((RPMI 1640 medium; (Hyclone, Logan, Utah) supplemented with 10% fetal bovine serum (FBS) (Hyclone), 1% penicillin-streptomycin (Hyclone), 10 mM HEPES (Hyclone), 2 mM L-glutamine (Hyclone), and 10 µg/ml DNase I (Sigma-Aldrich, Dorset, United Kingdom)), washed with PBS + 2% FBS (Hyclone) (complete RPMI). Cells were stained for viability with an aqua amine reactive dye (AARD; Invitrogen, Carlsbad, California), then incubated with panels of conjugated anti-human monoclonal antibodies (mAbs) The following directly conjugated mAbs used in this study were obtained from BD biosciences (San Jose, California): PE-Cy5-conjugated anti-CD38 (Clone: HIT2), V450-conjugated anti-CD45RA

(HI100), FITC-conjugated anti-CD45RA (HI100), PerCP-Cy5.5-conjugated anti-CD27 (M-T271), Alexa Flour 700-conjugated anti-CD4 (RPA-T4), FITC-conjugated anti-HLA-DR (G46-6), APCH-7-conjugated anti-CD8 (SK1), FITC-conjugated anti-CD57 (NK-1), APC-conjugated CD107a (H4A3). mAb obtained from Beckman Coulter (Fullerton, California) ECD-conjugated anti-CD3 (UCHT1). mAbs obtained from eBioscience (San Diego, California) PE-Cy7-conjugated anti-CD28 (CD28.2), PerCP-eFluor 710-conjugated anti-TIGIT (MBSA43), PE-conjugated anti-TIGIT (MBSA43), Mouse IgG1 Kappa isotype control PerCP-eFluor 710 (P3.6.2.8.1), mouse IgG1 K isotype control PE (P3.6.2.8.1). mAbs obtained from Biolegend (San Diego, California) Brilliant Violet 605-conjugated anti-CCR7 (G043H7), APC-conjugated anti-PD-1 (EH12.2H7), mouse IgG1 Kappa isotype control PE (MOPC-21). Qdot 605-conjugated anti-CD8 (3B5) was obtained from Invitrogen (Carlsbad, California). In some experiments cells were fixed with 1X Lyse buffer (BD Biosciences) followed by 1X BD FACS Permeabilizing solution 2 (BD Biosciences) and stained with FITC-conjugated Ki-67 (35/Ki-67), FITC-conjugated interferon gamma (IFN-γ) (25723.11), Alexa 700-conjugated Granzyme B (GB11), PE-conjugated perforin (B-D48) (abcam, Cambridge, Massachusetts). All cells were washed with PBS + 2% FBS and then fixed in 1% paraformaldehyde (PFA, Electron Microscopy Sciences, Hatfield, Pennsylvania) before acquiring (within 18 hours) on a custom four laser LSRFortessa flow cytometer (BD Biosciences). Between 100,000 to 500,000 lymphocyte events were collected for each sample. Isotype controls or fluorescence minus one (FMO) samples were prepared to facilitate gating. Anti-mouse or anti-rat IgG-coated beads (BD Biosciences) were individually stained with each fluorochrome-conjugated antibody and used for software-based compensation. Data were analyzed using Flowjo Software version 9.5 (Treestar, Ashland, Oregon).

Cell Sorting

Cryopreserved PBMCs were rapidly thawed and enriched for CD8 T cells to high purities with an EasySep Human CD8 T cell negative selection enrichment kit (Stemcell). Cells were surface stained with the following combination of mAbs: BV711-conjugated anti-CD3, Alexa 700-conjugated anti-CD4 (BD Biosciences), PerCP-eFluor 710-conjugated anti-TIGIT (eBioscience), Qdot605-conjugated anti-CD8, APC-conjugated anti-PD-1 (Invitrogen). Cells were sorted on a BD FACS ARIA and checked for purity. Gating was facilitated by isotype controls.

Multiplex cytokine assay

The four-sorted populations (TIGT+PD-1+, TIGIT+PD-1-, TIGIT-PD-1+, TIGIT-PD-1-) were seeded at 100,000 cells per well in a 96 well culture plate with 200 µl of 10% cRPMI. Sorted cells were stimulated with anti-CD3 + anti-CD28 Dynabeads (Life Technologies) for 48 hours in an incubator at 37 °C with 5% CO_2, supernatants were harvested from the cultures and processed according to recommended manufacture procedure with a Milliplex MAP Human High Sensitivity T cell Panel (EMD Millipore, Billerica, Massachusetts) for GM-CSF, TNF-α, IL-13, IL-12 (p70), IL-10, IL-8, IL-7, IL-6, IL-5, IL-4, IL-2, IL-1b, IFN-γ. Samples were acquired on a Luminex 200 (EMD Milipore). Samples were run in duplicate. The intra-assay CV% for the conditions of each cytokines were <10%.

Peptides and polyclonal stimulation

123 Overlapping ~15mer HIV clade B gag peptides obtained from the National Institute of Health AIDS Reagent Program. Stimulations were performed with a final concentration of 10 µg/ml peptide. T cell activator (anti-CD3 + anti-CD28 mAb Dynabeads) (Life Technologies) followed recommended manufacture procedure.

Pentamer analysis

We used the following Biotin labeled pentamers: A*02:01 SLYNTVATL HIV-Gag, A*02:01 ILKEPVHGV HIV-Pol, B*07:02 IPRRIRQGL HIV-Env, B*07:02 TPGPGVRYPL HIV-Nef, and A*02:01 NLVPMVATV CMV-pp65-NV9. All pentamers were obtained from Proimmune Ltd, Oxford, UK. Using protocol outlined previously [178] and stained with antibodies against CD3, CD8, TIGIT, PD-1, TIGIT isotype control or PD-1 isotype control and acquired on the flow cytometer as above. In some experiments PBMCs were stimulated with HIV Gag Peptide pool and evaluated for pentamer phenotype.

Anti-TIGIT and anti-PD-L1 monoclonal antibodies

The TIGIT antibody clones 11G11 and 23G8 were generated in HuMab mice [257, 258] immunized with a TIGIT-Fc fusion protein and selected based on their high affinity for TIGIT and ability to block TIGIT/PVR interaction. Clone 11G11 is a fully human IgG1 antibody that was engineered to contain a well-characterized set of mutation in the Fc that eliminate FcR interaction [259]. Clone 23G8 is a fully human IgG2 antibody that cross-reacts with macaque TIGIT. The anti-human PD-L1 antibody, clone 12A4, is a fully human IgG4 (S228P) that was generated in HuMab mice immunized with PD-L1-Fc. This antibody was selected based on its ability to block the binding of PD-L1 to both PD-1 and CD80. 12A4 cross-reacts with macaque PD-L1.

Peptides and polyclonal stimulation

123 Overlapping ~15mer HIV clade B gag peptides obtained from the National Institute of Health AIDS Reagent Program. Stimulations were performed with a final concentration of 10 μg/ml peptide. T cell activator (anti-CD3 + anti-CD28 mAb Dynabeads) (Life Technologies) followed recommended manufacture procedure.

Functional assays

In the intracellular cytokine stimulation assay studies, thawed cryopreserved PBMCs were stimulated for 12 hours in an incubator at 37 °C with 5% CO_2 with 5 µg/ml brefeldin A and 5 µg/ml monensin (Sigma-Aldrich) culture media, DMSO alone, pooled HIV Gag peptides, or anti-CD3/CD28 Dynabeads (Life Technologies) in the presence or absence of purified isotype IgG control, anti-TIGIT and/or anti-PD-L1 mAbs. After stimulation, the cells were washed and stained for viability with AARD and cultured with surface phenotype panel against CD8, TIGIT or an isotype control antibody, followed by intracellular staining of CD3 and IFN-γ and acquisition on the flow cytometer as above. For the proliferation assay, thawed PMBCs were washed two times and resuspended in PBS supplemented with 0.01% BSA at a concentration of one million cells per milliliter. Cells were labeled with 1mM Carboxyfluorescein succinimidyl ester (CFSE) violet-trace (Invitrogen) using protocols previously described [178]. Cells were stimulated for seven days with DMSO alone, pooled HIV gag peptides, or anti-CD3/CD28 Dynabeads in the presence or absence of purified isotype IgG control, anti-TIGIT or anti-PD-L1 at 37 °C with 5% CO_2. At the end of the stimulation, cells were washed and stained for viability with AARD and cultured with surface phenotype panel against CD3, CD8, TIGIT or an isotype control antibody and acquired on the flow cytometer as above.

In vitro cytokine stimulation

PBMCs were thawed and one million cells were plated per stimulation condition. Stimulation conditions included media alone, 25 ng/ml IL-2 (Roche), 50 IU/ml of IL-12 (MBL international, Woburn, Massachusetts), 50 IU/ml of IL-18 (MBL international) and 25 ng/ml IL-15 (R&D Systems, Minneapolis, Minnesota). Cells were stimulated for six days in an incubator at 37 °C with 5% CO_2. After stimulation, the cells were washed and stained for viability with AARD cultured

with surface phenotype panel against CD3, CD4, CD8, TIGIT or isotype control antibody and acquired on the flow cytometer as above.

T cell function *in vitro* antibody blockade studies. HIV-infected cryopreserved PBMC from individuals identified in Table 2 were stimulated for 12 hours in an incubator at 37 °C with 5% CO2. Stimulation conditions contained culture media, DMSO alone or pooled HIV gag peptides, in the presence of brefeldin A (Sigma-Aldrich), monensin (Sigma-Aldrich), anti-TIGIT mAb anti-PD-L1 mAb or mouse IgG1 isotype control. After stimulation, cells were washed and stained for cellular viability with AARD and conjugated antibodies against CD8 and CD4, followed by intracellular staining of CD3 and IFN-γ and acquired on a flow cytometer as described above.

Statistical analysis

The repeated-measures, one-way ANOVA followed by Tukey's multiple comparison, Wilcoxon matched-pairs signed ranked test was used for paired tests and the Spearman's rho test was used for correlation analyses. Measures of central tendency are expressed as medians and interquartile ranges (IQRs; given in the form 25th percentile, 75th percentile). Statistical analyses were conducted using Prism Graphpad release 5.0d (Graphpad Software, San Diego, California) or SPSS 22.0 (IBM, Armonk, New York) and the statistical significance of the findings was set at a *p*-value of less than 0.05.

Accession Numbers

Indian rhesus macaque (*Macaca mulatta)* TIGIT (rhTIGIT): GenBank KR534505

ACKNOWLEDGEMENTS

AUTHOR CONTRIBUTIONS

Conceived and designed the experiments: GMC LCN JBS. Performed the experiments: GMC GMW TF BJB JSR HLW KBH BIM LCN JBS. Analyzed the data: GMC CMS KLC MO NI TL FMH MAM SGH MM AJK SGD JBS. Contributed reagents/materials/analysis tools: GMW BJB MM AJK KLC TF MAM. Wrote the paper: GMC CMS KLC MO NI TL FMH MAM SGH MM AJK SGD JBS LCN.

TABLES

TABLE 3.1: Participant Characteristics

Parameters	HIV+ Non-Controllers (NC; n = 20) Median (IQR)	HIV+ Elite Controller (EC; n = 20) Median (IQR)	HIV+ cART Suppressed (AS; n = 20) Median (IQR)	HIV+ Known Duration of cART (L-AS; n = 19) Median (IQR)	HIV+ Acute Infection (AI; n = 24) Median (IQR)	HIV-Uninfected Donors (HD; n = 20) Median (IQR)
Age (Years)	44 (38, 55.5)	51 (44.5, 55.75)	50 (46, 57)	43 (37,51)	35 (32, 43)	50 (47, 55)
HIV Viral Load (copies/ml) Log10	4.51 (4.21, 5.05)	1.60 (1.60, 1.60)	1.60 (1.60, 1.87)	1.60 (1.60,1.60)	4.66 (2.28, 6.715)	N/A
CD4+ T cell count (cells/mm3)	518.5 (460, 626.5)	780.5 (659.5, 1248)	719.5 (542.8, 898.5)	519 (399,726)	640 (482. 3,790)	N/A
CD4+ T cell nadir count (cells/mm3)	371.5 (298.5, 439.3)	624.5 (376, 825.5)	115.5 (26.75, 260.8)	208 (92,275)	N/A	N/A
CD4+ Activation (% CD38+ HLA-DR+)	9.66 (8.22, 15.7)	3.46 (1.91, 4.60)	3.33 (2.82, 5.34)	7.26 (5.71,9.94)	3.58 (2.28, 6.71)	1.9 (1.65,2.68)
CD8+ Activation (% CD38+ HLA-DR+)	33.65 (28.53, 41.80)	10.45 (6.77, 18.63)	8.71 (5.12, 17.10)	20.7 (14.30,30.30)	20.1 (12.45, 34.83)	6.5 (4.27,11.15)
CA-HIV DNA (copies/million CD4 cells) Log10	N/A	N/A	N/A	2.13 (1.42,2.25)	N/A	N/A
CA-HIV RNA (copies/million CD4 cells) Log10	N/A	N/A	N/A	3.71 (2.93,4.28)	N/A	N/A
Duration of Viral Suppression (days)	N/A	N/A	N/A	784.5 (670.8,1034)	N/A	N/A
Gender Distribution						
Male % (no.)	80 (16)	80 (16)	75 (15)	70 (14)	91.6 (22)	90 (18)
Female % (no.)	5 (1)	15 (3)	15 (3)	25 (5)	8.3 (2)	10 (2)
MTF % (no.)	10 (2)	5 (1)	10 (2)	5 (1)	0 (0)	0 (0)
Intersex % (no.)	5 (1)	0 (0)	0 (0)	0 (0)	0 (0)	0 (0)

N/A = Not Available

CA: Cell Associated

TABLE 3.2: Description of participants for *in vitro* mAb blockade

PID	CD4+ T cell Count (cells/mm3)	Viral Load (copies/ml) Log10	On Current cART
AS07-1	543	3.76	No
AS07-2	453	4.08	No
AS09-1	N/A	N/A	N/A
AS09-2	N/A	N/A	N/A
*AS03-1	849	1.79	No
AS08-1	718	1.60	No
*AS11-1	716	1.88	No
*AS12-1	590	1.60	No
*AS14-1	709	1.60	No
AS10-1	784	1.60	Yes
AS10-2	540	1.60	Yes
AS10-3	551	1.60	Yes
AS08-2	843	1.60	Yes
AS10-4	672	1.60	Yes
AS10-5	433	1.60	Yes
AS10-6	1054	4.25	No
AS05-1	475	4.81	No
AS07-3	360	3.87	No
AS08-3	793	1.73	Yes
AS08-4	527	3.72	No
DUKE 012	1819	3.20	No
DUKE 010	1269	1.83	No
OM11	802	4.70	No
OM115	570	3.34	No
OM25	555	4.10	No
OM288	690	1.69	Yes
OM5245	1070	1.60	Yes
OM727	621	5.17	No
OM9	550	1.94	No

AS = SCOPE Cohort
Duke = Duke Cohort
OM = Toronto Cohort
N/A = Not Available
* = Elite Controller

59
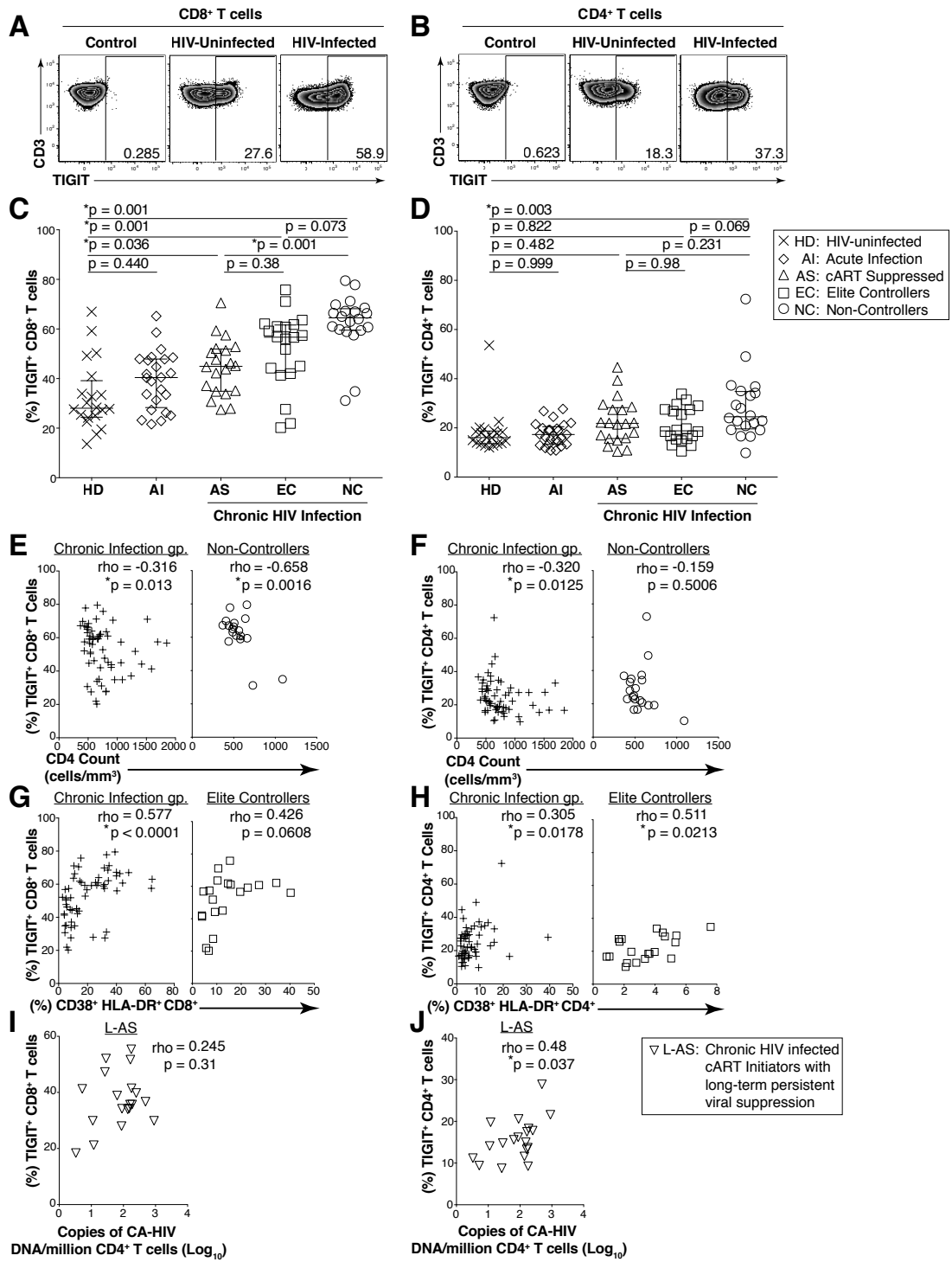
FIGURES

Figure 3.1: Expression of TIGIT on T cells during HIV infection.
Cryopreserved PBMCs were thawed and surface phenotyped for TIGIT
expression. Representative flow cytometry flow plots showing TIGIT expression
on (A) CD8 or (B) CD4 T cells compared to fluorescence minus one (FMO)
control. Graphs show compiled data of TIGIT expression on (C) CD8 and (D)
CD4 T cells stratified by disease: HIV-uninfected healthy donors (HD, X; n = 20),
acute HIV-infection (AI, open diamond; n = 24), aviremic cART suppressed (AS,
open triangles; n = 20), aviremic elite controllers (EC, open squares; n = 20), and
chronic HIV viremic non-controllers (NC, open circles; n = 20). P values were
calculated using one-way ANOVA, followed by Tukey's multiple comparisons
test. Graphs show correlation of total chronic infected (+: AS, EC, and NC; left
panel, n = 60) and non-controllers (right panel, n = 20) frequency (%) of (E)
TIGIT+ CD8+ and (F) TIGIT+ CD4 T cells against clinical CD4 Count
(cells/mm3). Graphs show correlation of total chronic infected (+: AS, EC, and
NC; left panel, n = 60) and elite controllers (right panel, n = 20) frequency (%) of
(G) TIGIT+ CD8 and (H) TIGIT+ CD4 T cells against frequency (%) of T cell
activation (CD38+HLA-DR+). Graphs show correlation of frequency (%) of (I)
TIGIT+ CD8 and (J) TIGIT+ CD4 T cell among aviremic HIV infected "ART
initiators" with known duration of long-term viral suppression from the SCOPE
cohort (L-AS, n = 19, open inverted triangles) versus copies of CD4 T cell
associated HIV DNA per million CD4 T cells (log10). Spearman's rho tests were
performed for correlations.

A

B

C
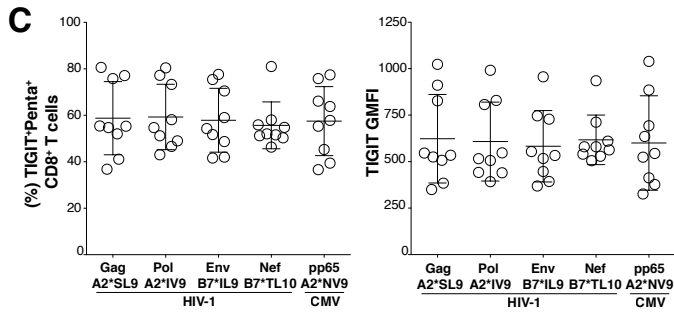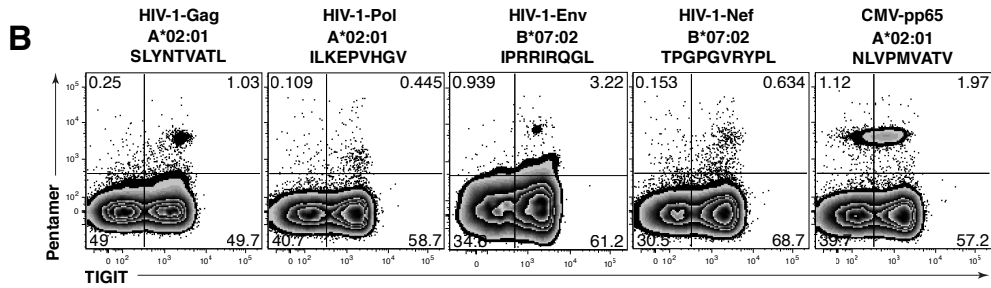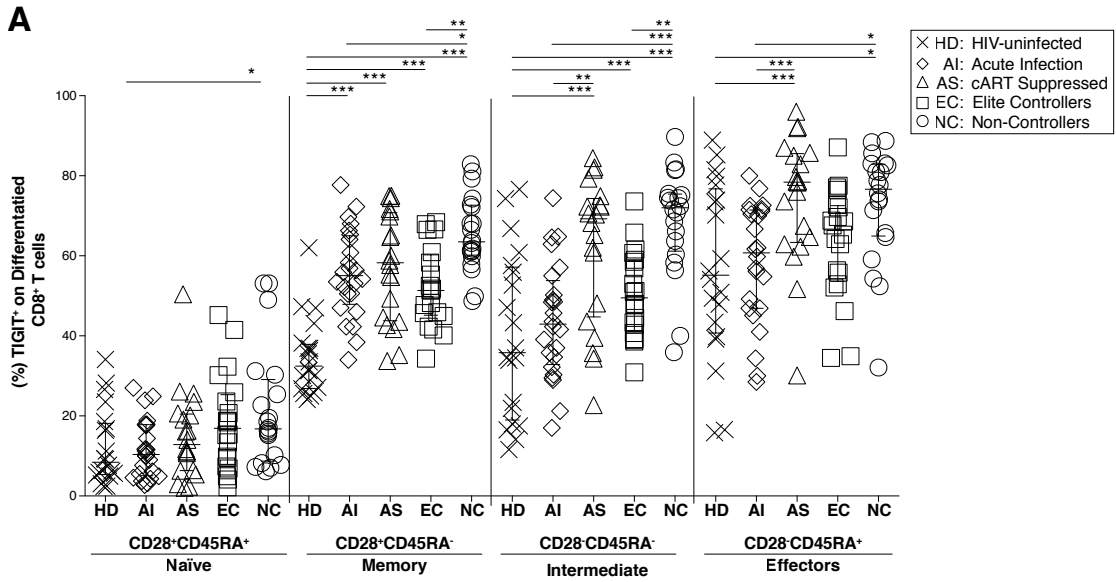
Figure 3.2: TIGIT expression on CD8 terminal effector T cells and HIV-specific CD8 T cells. Cryopreserved PBMCs were thawed and surface phenotyped for TIGIT expression on CD8 T cell compartments. (A) Graph shows compiled frequency (%) of TIGIT+ CD8 T cell expression in differentiated compartments stratified by disease status. HIV-uninfected donors (HD, X; n = 20), acute infected (AI, open diamond; n = 24), cART suppressed (AS, open triangle; n = 20), elite controller (EC, open square; n = 20), non-controllers (NC, open circle; n = 20). P values were calculated using one-way ANOVA, followed by Tukey's multiple comparisons test (*p < 0.05; **p < 0.01; ***p < 0.001). PBMCs from HLA-A*02:01 or HLA-B*07:02 HIV chronically infected individuals were stained with matched HLA pentamers presenting HIV and CMV epitopes and anti-TIGIT. (B) Representative flow cytometry plots of pentamer-specific CD8 T cells using HLA-A*02:01 HIV Gag SLYNTVATL (A2*SL9), HLA-A*02:01 HIV Pol ILKEPVHGV (A2*IV9), HLA-B*07:02 HIV-1 Env IPRRIRQGL (B7*IL9), HLA-B*07:02 HIV Nef TPGPGVRYPL (B7*TL10), and HLA-A*02:01 CMV pp65 NLVPMVATV (A2*NV9) (C) Compiled data of TIGIT expression frequency (%) on pentamer specific CD8 T cells which was recalculated to 100% (left panel, n = 9) compiled data of TIGIT geometric mean fluorescence intensity (GMFI) on pentamer specific CD8 T cells (right panel, n = 9).

A

HIV-Uninfected | HIV-Infected

TIGIT / PD-1

HIV-Uninfected: 22.6, 7.38, 66.6, 3.4
HIV-Infected: 26.5, 53.6, 14.3, 5.59

B

(%) TIGIT+PD-1+ CD8+ T cells

*p < 0.0001
*p = 0.0045
*p = 0.0130

HD | AS | EC | NC
Chronic HIV Infection

C

(%) TIGIT+PD-1+ CD8+ T cells

rho = -0.385
*p = 0.0024

CD4 Count (cells/mm³)

D

(%) TIGIT+PD-1+ CD8+ T cells

rho = 0.315
*p = 0.014

Viral Load Log₁₀ (copies/mL)

E

HIV-1 Gag A*02:01 SLYNTVATL Pentamer / CD8

Penta+ 0.382
Penta- 99.3

F

Penta+ | Penta-

TIGIT / PD-1

Penta+: 13.7, 77.3, 6.67, 2.33
Penta-: 29, 17.7, 6.52

G

Penta+ | Penta-

(%) Expression

Penta+: *
Penta-: *, ***

TIGIT + + -
PD-1 + - +

H

Penta+

TIGIT+PD-1+ | TIGIT+PD-1- | TIGIT-PD-1+ | TIGIT-PD-1-

CD45RA / CCR7

TIGIT+PD-1+: 3.45, 5.6
TIGIT+PD-1-: 29.3, 14.6
TIGIT-PD-1+: 65, 25
TIGIT-PD-1-: 28.6, 14.3

I

TIGIT+PD-1+ | TIGIT+PD-1- | TIGIT-PD-1+ | TIGIT-PD-1-

(%) of Max / CD27

J

(%) CD45RA+

(%) CCR7+

(%) CD27+

TIGIT + + - -
PD-1 + - + -

Naïve: CD45RA+CCR7+CD27+
Central Memory: CD45RA- CCR7+CD27+
Transitional Memory: CD45RA- CCR7- CD27+
Effector Memory: CD45RA- CCR7- CD27-
Terminally Differentiated: CD45RA+CCR7- CD27-

64

Figure 3.3: HIV-Gag specific CD8 T cells co-express TIGIT and PD-1 and exhibit a transitional memory phenotype. Cryopreserved PBMCs were thawed and surface phenotyped for TIGIT and PD-1 expression on CD8 T cells. (A) Representative flow cytometry plots showing TIGIT and PD-1 expression on CD8 T cells from one HIV-uninfected individual (left panel) and one HIV-infected individual (right panel). (B) Graph shows compiled frequency (%) of co-expressing TIGIT+PD-1+ CD8 T cells from HIV-uninfected (HD, n = 20), chronic HIV-infected (AS, n = 20; EC, n = 20; NC, n = 20). P values were calculated using one-way ANOVA, followed by Tukey's multiple comparisons test. (C) Graph shows correlation of TIGIT+PD-1+ CD8 T cells frequency (%) from chronic HIV-infected individuals against CD4 count (cells/mm3) or (D) viral load (copies/ml). Spearman's rho tests were performed for correlations. TIGIT and PD-1 expression on HIV-Gag-specific CD8 T cells were evaluated. (E) Representative flow cytometry plot of HIV-specific CD8+ T cells using HLA-A*02:01 HIV Gag SLYNTVATL. (F) Representative flow cytometry plots of TIGIT and PD-1 expression on HIV-Gag-specific CD8 T cells (Penta+, left panel; Penta-, right panel). (G) Graphs show compiled frequency (%) of TIGIT and PD-1 on Penta+ (left panel) and Penta- (right panel) (sample group contains; AS n = 11, EC n = 2, NC n = 2). P values were calculated using repeated-measures one-way ANOVA, followed by Tukey's multiple comparisons test (*p < 0.05; **p < 0.01; ***p < 0.001). Representative flow cytometry of (H) CD45RA and CCR7 or (I) histogram of CD27 (shaded isotype control) on Penta+ CD8 T cells expressing TIGIT+PD1+, TIGIT+PD-1-, TIGIT-PD-1+, or TIGIT-PD-1-. (J) Graphs show compiled frequency (%) of CD45RA (top panel), CCR7 (mid panel), and CD27 (bottom panel) (n = 5).

A

TIGIT | Ki-67
61 | 5.58
32.1 | 1.22

B

(%) of Ki67+ CD8+ T cells

*p < 0.0001

TIGIT+   TIGIT-

C

PD-1 | Ki-67
47.5 | 4.56
45.9 | 2.06

D

(%) of Ki67+ CD8+ T cells

p = 0.368

PD-1+   PD-1-

E

αCD3 αCD28 Dynabead

Isotope Control / IFN-γ
0.55 | 0.080
94.1 | 5.25

No Stim — TIGIT / IFN-γ
13.7 | 0.11
85.3 | 0.843

HIV-1 Gag Stim
13.9 | 0.93
83.8 | 1.41

αCD3 αCD28 Dynabeads
15.2 | 0.40
81.6 | 2.76

Isotope Control / IL-2
0.46 | 0.045
98.6 | 0.85

TIGIT / IL-2
12.7 | 0.026
87.2 | 0.069

13.6 | 0.058
86.1 | 0.26

14.5 | 0.12
84.8 | 0.64

Isotope Control / TNF-α
0.57 | 0.060
95.7 | 3.71

TIGIT / TNF-α
13.6 | 0.23
85.7 | 0.44

14.2 | 0.63
84.5 | 0.67

15.2 | 0.43
82.6 | 1.8

F

(%) IFN-γ+ HIV-1 Gag CD8+ T cells
*p = 0.002

(%) IL-2+ HIV-1 Gag CD8+ T cells
*p = 0.002

(%) TNF-α+ HIV-1 Gag CD8+ T cells
*p = 0.002

TIGIT+   TIGIT-

G

IFN-γ+ HIV-1 Gag CD8+ T cell response

(%) Phenotype
** *** ***

IL-2+ HIV-1 Gag CD8+ T cell response

(%) Phenotype
*** * *

TNF-α+ HIV-1 Gag CD8+ T cell response

(%) Phenotype
* *** ** **

TIGIT + + - -
PD-1 + - + -

H

CD8 / TIGIT
69.2 | 30.8

TIGIT+ Perforin / Granzyme B
5.42 | 79
7.7 | 8.34

TIGIT-
29.3 | 39.9
26 | 4.86

I

(%) Perforin+ Granzyme B+ CD8+ T Cells

*p=0.0226

TIGIT+   TIGIT-

J

αCD3 αCD28 Dynabead

Isotope Control / CD107a
0.112 | 0.542
65.7 | 33.6

No Stim — TIGIT / CD107a
37.9 | 6.37
48.8 | 6.88

HIV-1 Gag Stim
35.7 | 7.08
49.5 | 7.76

αCD3 αCD28 Dynabeads
33.4 | 21.3
29.3 | 16

K

HIV-1Gag Stim

Background Corrected (%) CD107a+ CD8+ T Cells

p = 0.845

TIGIT+   TIGIT-

L

αCD3 + αCD28 Dynabeads

Background Corrected (%) CD107a+ CD8+ T Cells

p = 0.084

TIGIT+   TIGIT-

66

Figure 3.4: TIGIT expressing CD8 T cells have impaired cytokine responses. Representative flow cytometry plots gated on CD8 T cells showing (A) TIGIT or (C) PD-1 expression against Ki-67 from a chronically HIV-infected individual. Compiled data of Ki-67+ CD8 T cell frequency (%) separated into (B) TIGIT+ and TIGIT- or (D) PD-1+ and PD-1- (*n* = 20). P values were calculated by Wilcoxon matched-pairs signed ranked test. *Ex vivo* PBMCs from chronically HIV-infected individuals were stimulated with HIV Gag peptide pool and assessed for cytokine production. (E) Representative flow cytometry plots gated on CD8 T cells showing TIGIT expression and either IFN-γ, IL-2, or TNF-α content after no stimulation, stimulation with an HIV Gag peptide pool, or a positive control stimulation with anti-CD3 + anti-CD28 Dynabeads. (F) Compiled data of IFN-γ, IL-2, or TNF-α CD8 T cell frequency (%) from TIGIT+ or TIGIT-CD8 T cell compartments after HIV Gag peptide pool stimulation (sample group includes; AS *n* = 4, EC *n* = 3, NC *n* = 3). P values were calculated by Wilcoxon matched-pairs signed ranked test. (G) Compiled data of TIGIT and PD-1 expression on HIV Gag responding cells (sample group includes; AS *n* = 4, EC *n* = 3, NC *n* = 3). P values were calculated with repeated-measures one-way ANOVA, followed by Tukey's multiple comparisons test (*p < 0.05; **p < 0.01; ***p < 0.001). (H) Representative flow cytometry plots of intracellular perforin and granzyme B from CD8 T cells expressing or not expressing TIGIT. (I) Compiled frequency (%) of intracellular perforin+granzyme B+ content from TIGIT+ or TIGIT- CD8 T cell compartments (AS; *n* = 12). P values were calculated by Wilcoxon matched-pairs signed ranked test. (J) Representative flow cytometry plots gated on CD8 T cells showing TIGIT and CD107a expression from TIGIT isotype control, no stimulation, HIV Gag peptide pool, positive control stimulation with anti-CD3 + anti-CD28 Dynabeads. Compiled data of background corrected CD107a after (K) HIV Gag peptide pool (L) anti-CD3 + anti-CD28 Dynabead stimulation in TIGIT+ or TIGIT- CD8 T cell compartments (AS; *n* = 10). P values were calculated by Wilcoxon matched-pairs signed ranked test.
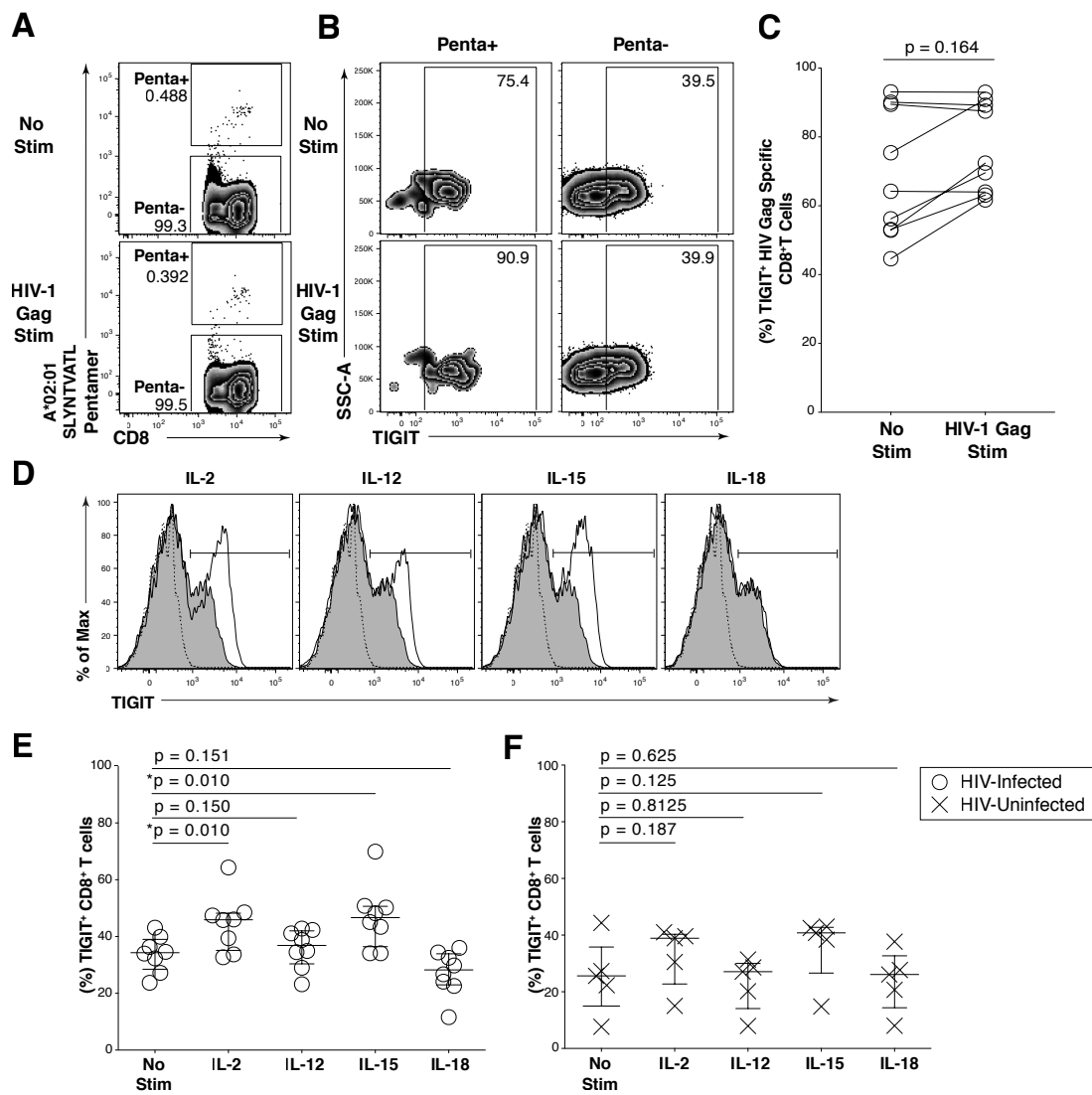
Figure 3.5: Common gamma chain cytokines regulate TIGIT expression on CD8 T cells.

Ex vivo PBMCs from chronically HIV infected individuals were stimulated with HIV Gag peptide pool for 12 hours. (A) Representative flow cytometry plot gated on CD8 T cells showing HIV Gag pentamer with no stimulation (top panel) or HIV Gag stimulation (bottom panel). (B) Representative flow cytometry plot of TIGIT expression on Penta+ and Penta- cells with no stimulation or HIV Gag stimulation. (C) Graph shows compiled frequency (%) of TIGIT on Penta+ cells with no stimulation and HIV Gag stimulation (n = 9). P values calculated with Wilcoxon matched-pairs signed-rank test. (D) Representative flow cytometry histograms gated on CD8 T cells overlaid with TIGIT expression frequency before and after cytokine stimulation. Dashed line indicates TIGIT isotype control, shaded histogram indicates TIGIT expression with no stimulation, and the solid line indicates TIGIT expression with cytokine stimulation after six days. Compiled data of TIGIT frequency (%) on CD8 T cells (E) HIV-infected participant (open circle; n = 8) (F) HIV-uninfected participant (X; n = 5). P values were calculated with repeated-measures one-way ANOVA, followed by Tukey's multiple comparisons test.

A

HIV-1 Gag Peptide Pool Stim

Isotype No Stim	Isotype	αTIGIT	αPD-L1	αTIGIT αPD-L1	αCD3 αCD28 Dynabeads

OM727

CD3 / IFN-γ

0.0427   1.73   2.02   1.79   1.93   16.3

B

(%) IFN-γ⁺ CD8⁺ T cells in response to HIV-1 Gag

*p = 0.016   *p = 0.0082   p = 0.220

Isotype	+	−	+	−	+	−
αTIGIT	−	+	−	−	−	+
αPD-L1	−	−	−	+	−	+

C

HIV-1 Gag Peptide Pool Stim

Isotype No Stim	Isotype	αTIGIT	αPD-L1	αTIGIT αPD-L1	αCD3 αCD28 Dynabeads

OM25

4.31   5.06   10.6   5.61   18.3   75.7

OM11

CD3 / CFSE

12.7   16   15   22.4   40.7   49.7

D

(%) CFSE^dim CD8⁺ T cells in response to HIV-1 Gag

p = 0.325   *p < 0.0001   *p < 0.0001

Isotype	+	−	+	−	+	−
αTIGIT	−	+	−	−	−	+
αPD-L1	−	−	−	+	−	+

70

Figure 3.6: Effect of *in vitro* blockade with anti-TIGIT and anti-PD-L1 mAbs on HIV-specific CD8 T cell responses. *Ex vivo* PBMCs from chronically HIV-infected individuals were stimulated with HIV Gag peptide pool in the presence of mAb blocking antibodies. (A) Representative flow cytometry plots gated on CD8 T cells, showing IFN-γ responses from an HIV-infected individual. No HIV Gag stimulation with an isotype control, HIV Gag stimulation with an isotype control, HIV Gag stimulation with anti-TIGIT, HIV Gag stimulation with anti-PD-L1, HIV Gag stimulation with dual blockade (anti-TIGIT + anti-PD-L1) and a positive control (anti-CD3 + anti-CD28 Dynabeads). (B) Compiled data showing variation in the frequency (%) of IFN-γ in responses to HIV Gag peptide pool with isotype control or mAb blockade; TIGIT blockade (left panel), PD-L1 blockade (middle panel), and dual blockade (right panel) (*n* = 25). P values were calculated by Wilcoxon matched-pairs signed ranked test. (C) Representative flow cytometry plots gated on 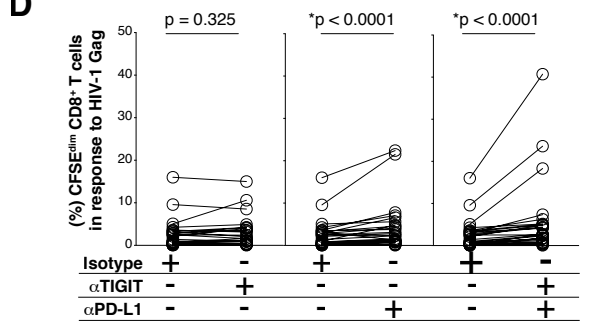CD8 T cells from HIV-infected individuals, showing intermediate and high CFSE dilution in response to HIV Gag peptide pool stimulation in the presence of either an isotype control, anti-TIGIT mAb, anti-PD-L1 mAb, a combination of both anti-TIGIT and anti-PD-L1 mAbs or anti-CD3 + anti-CD28 Dynabeads as a positive control. (D) Graphs show compiled data showing variation in the frequency (%) of CFSEdim in responses to HIV Gag peptide pool with either an isotype control or mAb blockade; TIGIT blockade (left panel), PD-L1 blockade (middle panel), and dual blockade (right panel) (*n* = 24). P values were calculated by Wilcoxon matched-pairs signed ranked test.
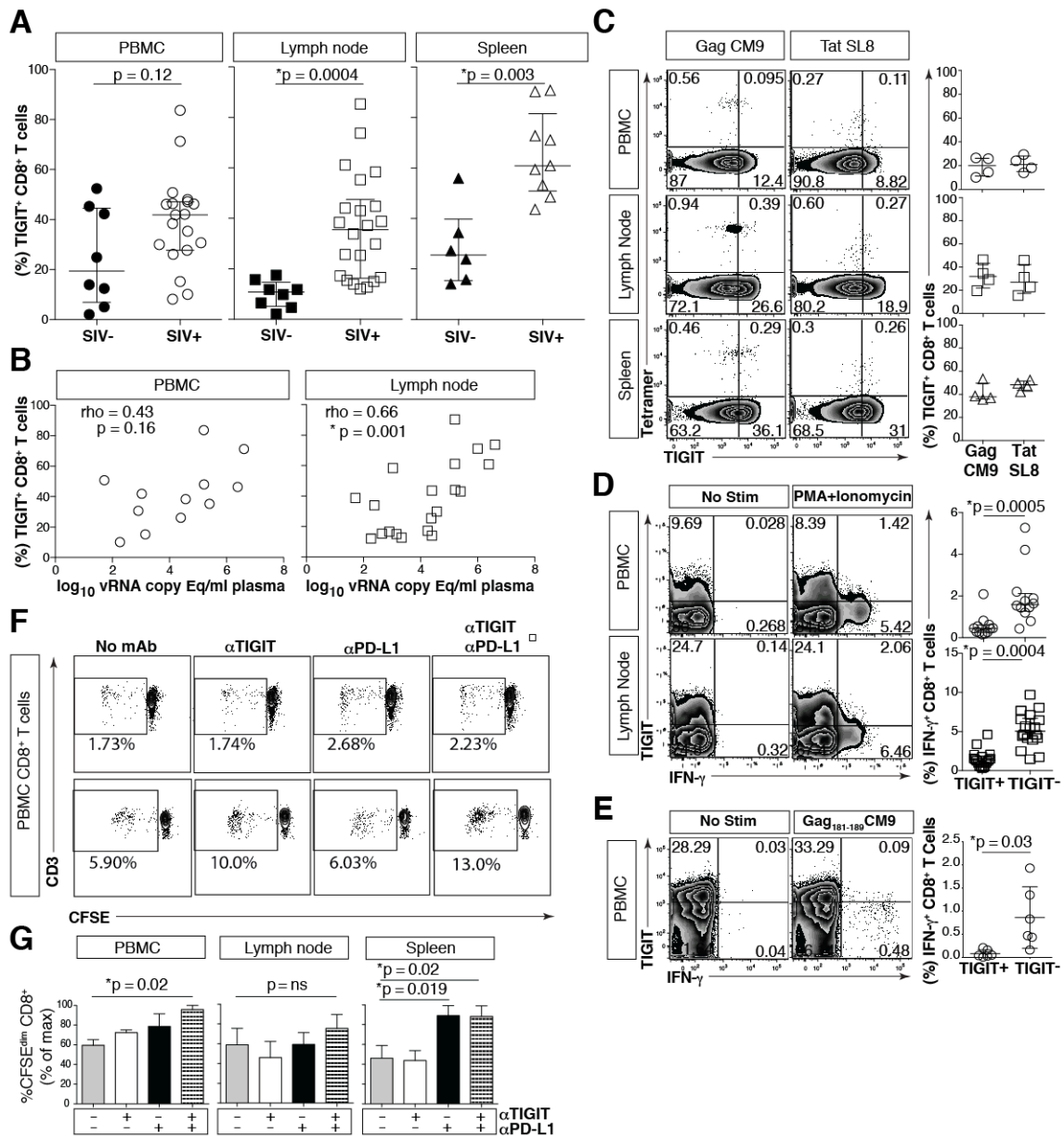
Figure 3.7: Phenotypic and functional assessment of rhTIGIT CD8 T cells.
Cryopreserved *Rhesus macaque* PBMCs were thawed, phenotyped and
assessed for function. (A) Graphs show frequency (%) of rhTIGIT+CD8 T cells
from PBMCs (circle), Lymph nodes (square; LNs), and Spleen (triangle) in SIV-
uninfected (filled) and SIV-infected (open) animals (SIV-uninfected PBMCs, n =
8; SIV-infected PBMCs, n = 19; SIV-uninfected LNs, n = 8; SIV-infected LNs, n =
22; SIV-uninfected spleen, n = 6; SIV infected spleen, n = 9). P values were
calculated with Mann-Whitney U tests. (B) Graphs show correlation of frequency
(%) of rhTIGIT+ CD8 T cells in PBMCs (circle) and lymph nodes (square) from
SIV-infected animal against plasma SIV viral load log10 vRNA copy Eq/ml
(PBMCs, n = 12; LNs, n = 20). vRNA copy Eq, viral RNA copy equivalents.
Spearman's rho tests were performed for correlations. (C) Representative flow
cytometry plots of tetramer stains for Mamu-A*01 restricted SIV-Gag CM9 and
SIV-Tat SL8 specific CD8 T cells from PBMC, LNs, and spleen, in a
representative Mamu-A*01 animal with full cART suppression. Compiled data of
rhTIGIT expression frequency (%) on tetramer specific CD8 T cells (n = 4) from
PBMCs (circle), LNs (square), and spleen (triangle) from Mamu-A*01+ macaques
with full cART suppression. (D) Representative flow cytometry plots of PBMCs (n
= 12) or lymph nodes (n = 18) stimulated without or with PMA + Ionomycin.
Graphs show frequency (%) of IFN-γ from CD8 T cells expressing TIGIT or not
expressing TIGIT. P values were calculated by Wilcoxon matched-pairs signed
ranked test. (E) Representative flow cytometry plots of PBMCs from a Mamu-
A*01+ macaque stimulated without or with SIV-Gag181-189 CM9 peptide. Graph
shows frequency (%) of IFN-γ from SIV-Gag181-189 CM9-specific CD8+ T cells
expressing TIGIT or not expressing TIGIT from Mamu-A*01+ macaques (n = 6).
P values were calculated by Wilcoxon matched-pairs signed ranked test. (F)
Representative flow cytometry plots of CD8 T cells from two separate SIV-
infected macaques showing CD8 T cell CFSE dilution in response to AT2-
inactivated SIV with either no antibody, anti-TIGIT, anti-PD-L1 or dual blockade

(anti-TIGIT + anti-PD-L1). (G) Graphs show compiled data of CD8 T cell CFSE dilution from PBMC (left panel), Lymph node (middle panel), or Spleen (right panel) as percent of max (n = 4). P values were calculated by Wilcoxon matched-pairs signed ranked test.

SUPPLEMENTAL MATERIAL AND METHODS (NONHUMAN PRIMATES)

Animals

Indian Rhesus macaques (*Macaca mulatta*), housed at the Oregon National Primate Research Center and used in this study, were cared for according to the laws, regulations, and guidelines set forth by the U.S. Department of Agriculture (e.g., the Animal Welfare Act and its regulations, and the Animal Care Policy Manual), Institute for Laboratory Animal Research (e.g., Guide for the Care and Use of Laboratory Animals, 8th edition), Public Health Service, National Research Council, Centers for Disease Control and Infection, and the Association for Assessment and Accreditation of Laboratory Animal Care International. The Oregon Health and Science University Institutional Animal Care and Use Committee approved the research involving animals reported in this study. Animals were infected with SIVsmE660, SIVmac239, or SIVmac251 for other, unrelated projects.

Antibodies and flow cytometric analysis

The following directly conjugated Abs were obtained from BD Biosciences: Alexa Fluor 700–conjugated anti-CD3 (SP34-2), PE-CF594–conjugated anti-CD4 (L200), allophycocyanin- or allophycocyanin-H7–conjugated anti-CD8 (SK1), PE-Cy5–conjugated anti-CD95 (DX2), allophycocyanin-conjugated anti–IFN-γ (B27), and PE-conjugated anti–Ki-67 (B56). PE-conjugated anti–PD-1 (EH12.2H7), and PE-Cy7–conjugated CD28 (CD28.2) were obtained from Biolegend. PE-conjugated anti-TIGIT (MBSA43) was obtained from eBioscience. Allophycocyanin-conjugated Mamu-A*01 SIV Gag181–189 CM9 (CTPYDINQM) tetramer and allophycocyanin-conjugated Mamu-A*01 SIV Tat28–35 SL8 (STPESANL) tetramer were produced as described previously [260]. An aqua amine reactive dye (Invitrogen) was used to exclude dead cells. In some experiments, cells were fixed in 2% paraformaldehyde (PFA), permeabilized with

BD FACS permeabilizing solution 2 (BD Biosciences), and stained for Ki-67 and IFN-γ (BD Biosciences).

Cloning and sequencing of rhesus macaque TIGIT

Total RNA was purified from fresh rhesus PBMC using the AllPrep DNA/RNA kit (QIAGEN, Venlo, Limburg, The Netherlands). TIGIT was reverse transcribed with Superscript III One-Step RT-PCR System with Platinum Taq High Fidelity (Invitrogen) using primers 5'-ATGCGGTGGTGTCTCTTCC-3' and 5'-CTACCCAGTCTCTGTGAAGAAGC-3'. The amplicon was purified from a 1% agarose gel and sequenced using the same primers, in addition to internal sequencing primers, 5'-ACTCAGCATTACGAATGGCCAG-3' and 5'-ACTGGACAGGAAGAACAGATTCC-3' to cover the 5' and 3' ends, respectively. CodonCode Aligner (CodonCode Corporation, Centerville, Massachusetts) was used to translate the DNA sequences, which were deposited into GenBank (KR534505).

T cell stimulation and intracellular cytokine staining

T cell stimulation and intracellular cytokine staining were performed similarly to a previous detailed description [260, 261]. Briefly, 5×10^5 cryopreserved PBMCs or LN cells were incubated for one hour at 37 °C in 200 µl RPMI 1640 containing 10% bovine growth serum and antibiotics with anti-CD28, anti-CD49d, and 10 µM the synthetic peptide SIV Gag181–189CM9 (CTPYDINQM). In additional experiments, stimulated with 50 ng/mL of PMA and 1 µg/ml of ionomycin (Life Technologies). Then, 10 µg/ml brefeldin A (Sigma-Aldrich) was added, and the cells were incubated for an additional 6-8 hours at 37 °C. Cells were washed in buffer (PBS with 10% serum), stained for surface expression of CD3, CD4, and CD8 markers, and fixed in 2% PFA (Electron Microscopy Sciences) at 4 °C. Cells were then permeabilized in wash buffer containing 1% saponin and stained for the expression of cytokines IFN-γ (BD

Biosciences). Stained cells were acquired on a custom four-laser BD Fortessa flow cytometer (BD Biosciences) with FACSDiva software and analyzed with FlowJo software (TreeStar).

SUPPLEMENTAL FIGURES
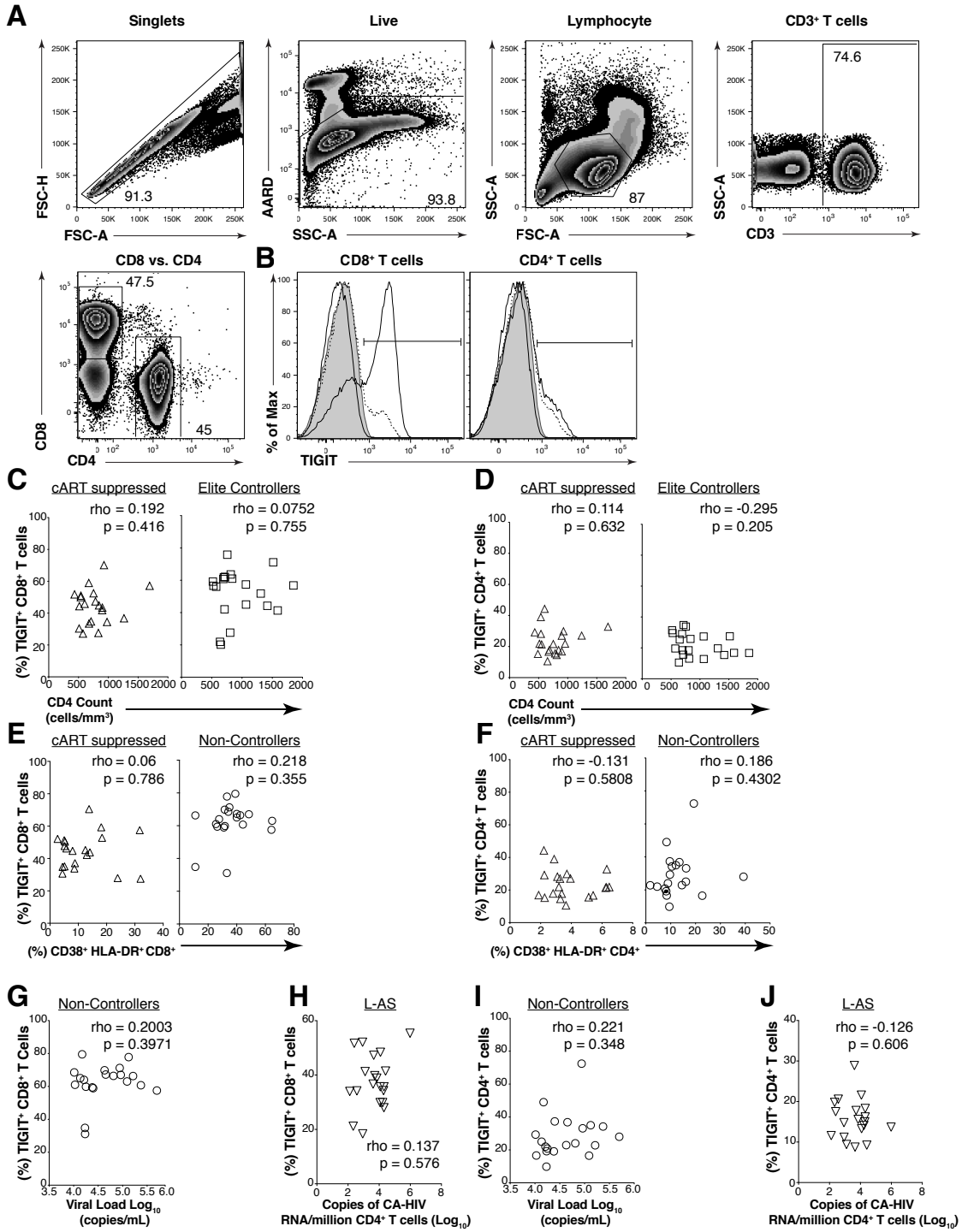
Supplemental Figure 3.1: Gating strategy of TIGIT surface expression in HIV infection and associations with HIV clinical parameters. (A) Representative flow cytometry plots showing gating scheme to isolate CD8 and CD4 T cells. Gated on singlets, excluded dead cells, gated on lymphocytes, gated on CD3 T cells, and gated on expression of CD8 or CD4. (B) Representative histograms of TIGIT Isotype, TIGIT FMO and TIGIT expression on CD8 or CD4 T cells (HIV-infected thin solid line, HIV-uninfected dashed line, TIGIT isotype control shaded, and TIGIT FMO thick solid line). Graphs show the association of the frequency (%) of (C) TIGIT+ CD8 or (D) TIGIT+ CD4 T cells against clinical CD4 count for cART suppressed (left panel, open triangle, n = 20) and elite controllers (right panel, open squares, n = 20). Graphs show the association of the frequency (%) of (E) TIGIT+ CD8 or (F) TIGIT+ CD4 T cells against T cell activation (% CD38+HLA-DR+) for cART suppressed (left panel, open triangle, n = 20) and non-controllers (right panel, open circles, n = 20). Graphs show the association of the frequency (%) of (G) TIGIT+ CD8 or (I) TIGIT+ CD4 T cells against viral load log10 (copies/ml) for non-controllers (open circles, n = 20). Graphs show the association of the frequency (%) of (H) TIGIT+ CD8 or (J) TIGIT+ CD4 T cells against copies of cell associated HIV RNA per million CD4 T cells for L-AS (inverted open triangles, n = 19). Spearman's rho tests were performed for correlations.

A

	HIV Uninfected	Acute Infection	cART Suppressed	Elite Controller	Non Controller

B

Lymphocytes → CD8⁺ T cells → CD45RA⁻ | CD45RA⁺

CD3 / CD8 — 41.6

CD27 / CD45RA — 23.6 | 75.9

CCR7 / CD27 (CD45RA⁻) — 0.568 | 13.1 (II); IV 18.8 | 67.5 (III)

CCR7 / CD27 (CD45RA⁺) — 0.448 | 50.9 (I); V 13.6 | 35.1

C

CD8 / CD28: I 98.6 | II 92.5 | III 64.2 | IV 29.2 | V 2.39

D

CD8 / TIGIT: I 4.94 | II 59.9 | III 76.7 | IV 74.5 | V 94.1

I: CD45RA⁺ CD27⁺ CCR7⁺ CD28⁺⁺ Naïve
II: CD45RA⁻ CD27⁺ CCR7⁺ CD28⁺⁺ Central Memory
III: CD45RA⁻ CD27⁺ CCR7⁻ CD28⁺/⁻ Transitional Memory
IV: CD45RA⁻ CD27⁻ CCR7⁻ CD28⁺/⁻ Effector Memory
V: CD45RA⁺ CD27⁻ CCR7⁻ CD28⁻ Terminally Differentiated

E

	I	II	III	IV	V
CD45RA	+	-	-	-	+
CD27	+	+	+	-	-
CCR7	+	+	-	-	-
CD28	++	++	+/-	+/--	-

80

Supplemental Figure 3.2: Phenotypic assessment of TIGIT expression on differentiated CD8 T cell subsets. (A) Graph shows compiled frequency (%) of TIGIT expression on CD8 T cells subsets grouped by disease category. HIV-uninfected (X; $n = 20$), acute infected (AI; open diamond; $n = 24$), cART suppressed (AS; open triangle; $n = 20$), elite controller (EC; open square; $n = 20$), and non-controllers (NC; open circle; $n = 20$). Repeated-measures one-way ANOVA, followed by Tukey's multiple comparisons test were used for comparison (*p < 0.05; **p < 0.01; ***p < 0.001). Cryopreserved PBMCs from chronically HIV-infected individuals were phenotyped for TIGIT expression on CD8 T cell subsets. (B) Representative flow cytometry plots showing gating scheme to isolate CD8 T cell subsets. Live lymphocytes gated for CD8 T cells, subset into CD45RA+ and CD45RA-, further stratified by expression of CCR7 and CD27. (C) Representative flow cytometry plots showing CD28 expression on CD8 T cell subsets. (D) Representative flow cytometry plots showing TIGIT expression on CD8 T cell subsets. (E) Graph shows compiled frequency (%) of TIGIT expression on CD8 T cell subsets ($n = 20$).
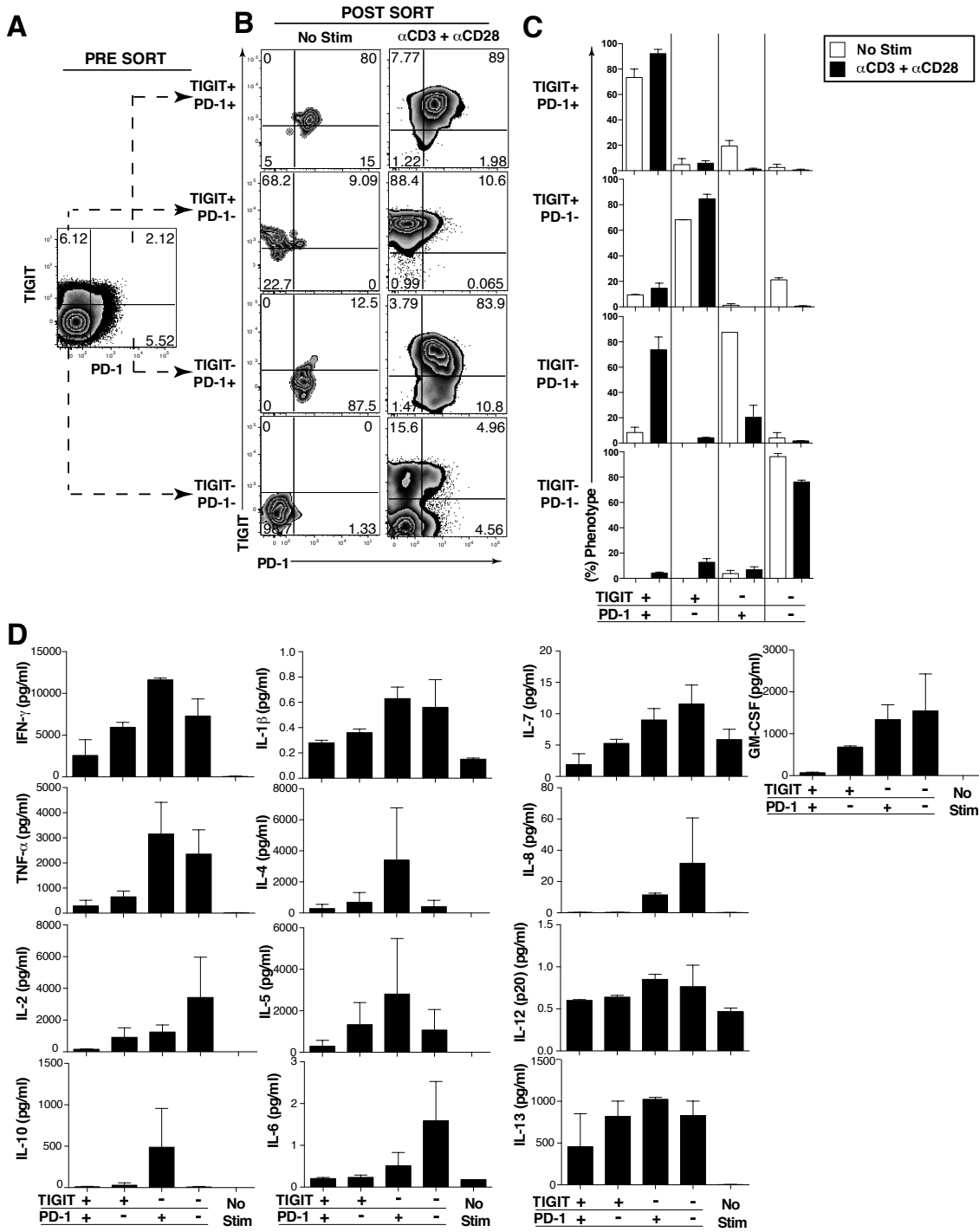
Supplemental Figure 3.3: Cytokine profile of TIGIT and PD-1 expressing CD8 T cells. *Ex vivo* CD8 T cells from chronically HIV-infected individuals were FACS sorted into populations according to their expression of TIGIT and PD-1. (A) Representative flow cytometry plot of TIGIT and PD-1 expression PRE-SORT. Gating was facilitated by isotype controls for TIGIT and PD-1. (B) Representative flow cytometry plots of CD8 T cells sorted into TIGIT+PD-1+, TIGIT+PD-1-, TIGIT-PD-1+, and TIGIT-PD-1-. No stimulation (left panel) and stimulated with anti-CD3 + anti-CD28 Dyanbeads for 48 hours (right panel). (C) Graphs show compiled data of phenotypes of sorted populations with no stimulation (open box) and anti-CD3 + anti-CD28 Dyanbeads (filled box) (*n* = 2). Supernatants were harvested and cytokine production was assessed 48 hours post anti-CD3 + anti-CD28 stimulation by high sensitivity multiplex bead array. (D) Graphs show concentrations of cytokines produced from sorted populations.
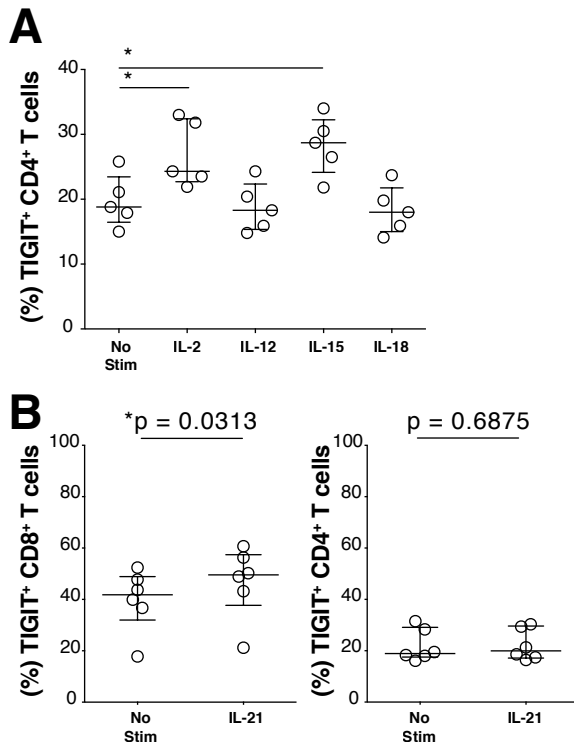
Supplemental Figure 3.4: Cytokine regulation of TIGIT expression. (A) Compiled data of HIV-infected individuals (open circle; *n* = 8) TIGIT expression frequency (%) on CD4 T cells with or without cytokine stimulation for six days. P values were calculated with repeated-measures one-way ANOVA, followed by Tukey's multiple comparisons test (*p < 0.05). (B) Compiled data of HIV-infected individuals (open circle; *n* = 6) TIGIT expression frequency (%) on CD8 T cells (right panel) and CD4 T cells (left panel) after six days of IL-21 stimulation (*n* = 6). P values were calculated by Wilcoxon matched-pairs signed ranked test.

A

No Stim Isotype | HIV-1 Gag Peptide Pool | αCD3 αCD28 Dynabeads

Isotype — αTIGIT — αPD-L1 — αTIGIT αPD-L1

CD3 / IL-2

0.295 0.417 0.455 0.513 0.555 0.617

B

(%) IL-2⁺ CD8⁺ T cells in response to HIV-1 Gag

p = 0.456   p = 0.463   *p = 0.0027

Isotype	+	−	+	−	+	−
αTIGIT	−	+	−	−	−	+
αPD-L1	−	−	−	+	−	+

C

No Stim Isotype | HIV-1 Gag Peptide Pool | αCD3 αCD28 Dynabeads

Isotype — αTIGIT — αPD-L1 — αTIGIT αPD-L1

CD3 / IL-2

0.323 0.527 0.573 0.677 0.723 2.5

D

(%) IL-2⁺ CD4⁺ T cells in response to HIV-1 Gag

p = 0.403   p = 0.107   *p = 0.0103

Isotype	+	−	+	−	+	−
αTIGIT	−	+	−	−	−	+
αPD-L1	−	−	−	+	−	+

85
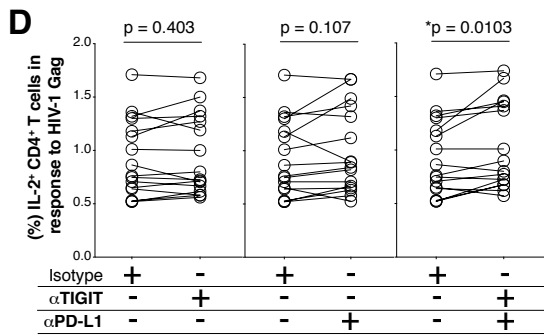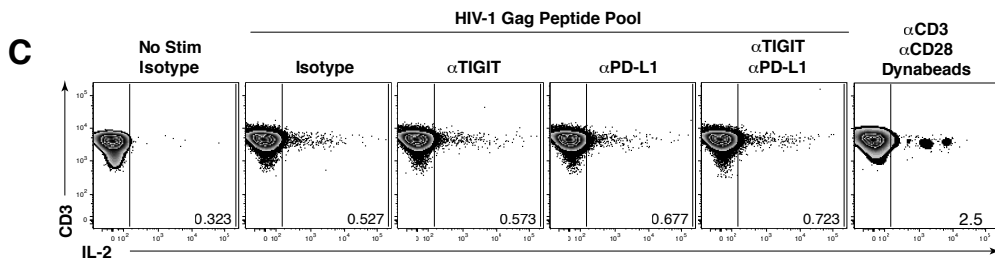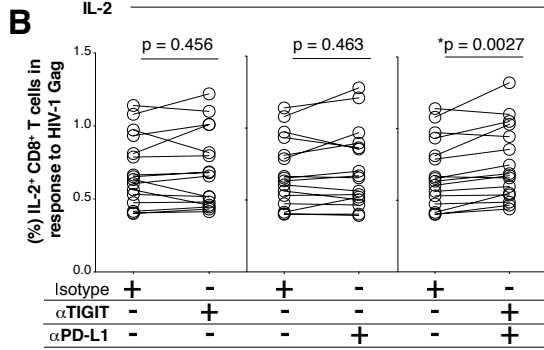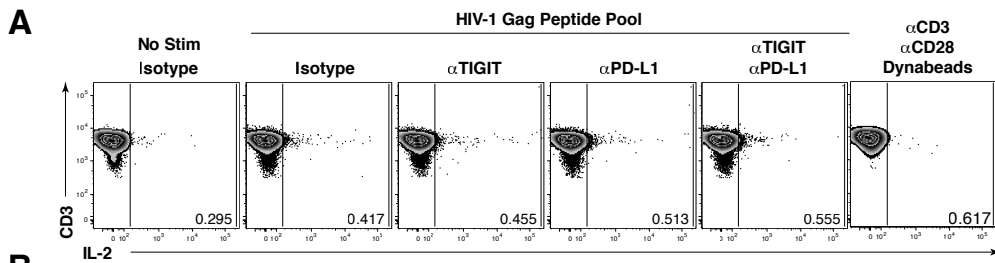
Supplemental Figure 3.5: Effect of *in vitro* blockade with anti-TIGIT and anti-PD-L1 mAbs on HIV-specific CD8 T cell IL-2 responses. *Ex vivo* PBMCs from chronically HIV-infected individuals were stimulated with HIV Gag peptide pool in the presence of mAb blocking antibodies. Representative flow cytometry plots gated on (A) CD8 or (C) CD4 T cells, showing IL-2 responses from an HIV-infected individual. No HIV Gag stimulation with an isotype control, HIV Gag stimulation with an isotype control, HIV Gag stimulation with anti-TIGIT, HIV Gag stimulation with anti-PD-L1, HIV Gag stimulation with dual blockade (anti-TIGIT + anti-PD-L1) and a positive control (anti-CD3 + anti-CD28 Dynabeads). Graphs show compiled data showing variation in the frequency (%) of (B) CD8 or (D) CD4 T cell IL-2 in responses to HIV Gag peptide pool with isotype control or mAb blockade; TIGIT blockade (left panel), PD-L1 blockade (middle panel), and dual blockade (right panel) (n = 16).
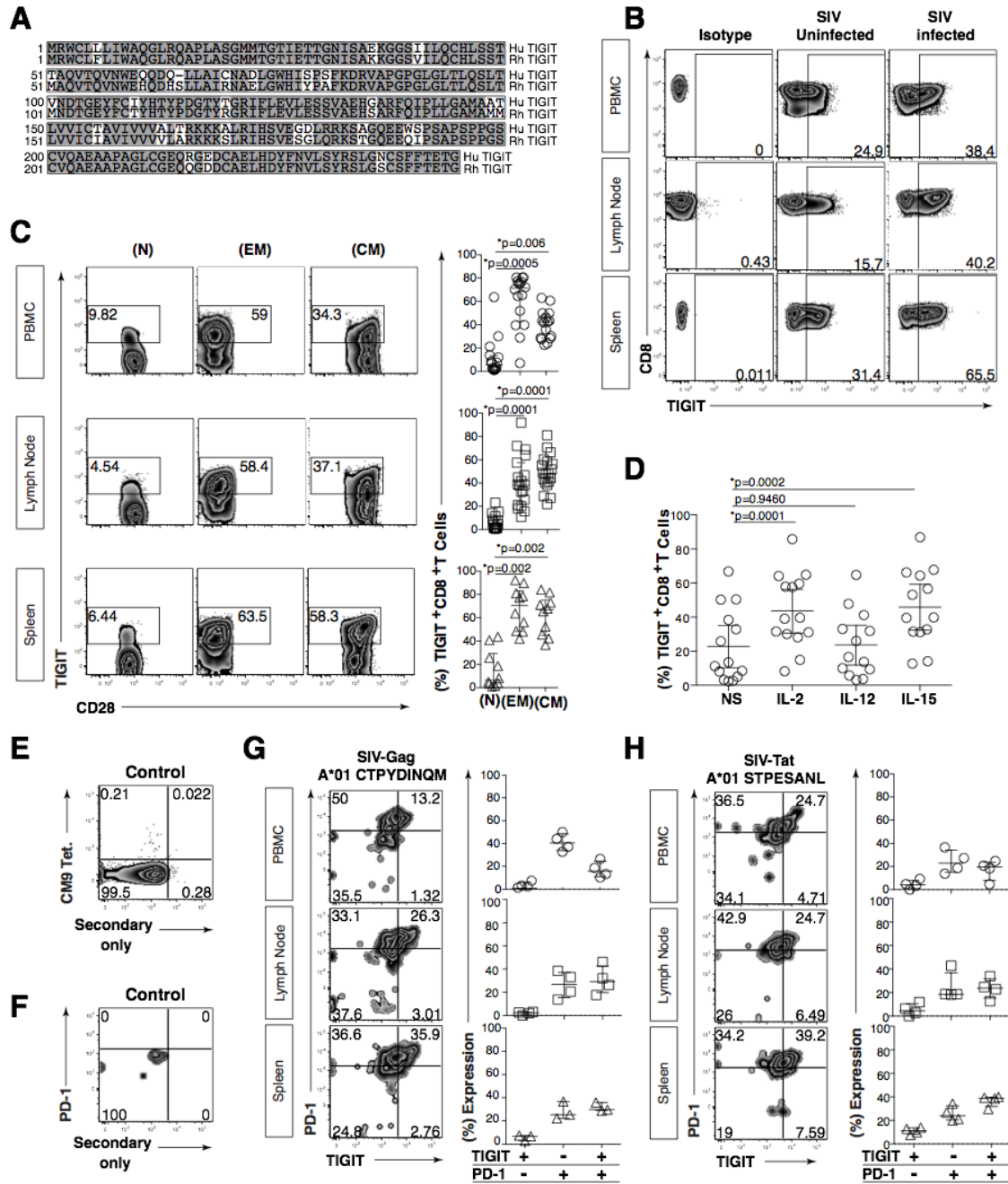
Supplemental Figure 3.6: rhTIGIT amino acid sequence alignment, surface expression, common gamma chain cytokine regulation and SIV-specific CD8 T cell expression. (A) Alignment shows amino acid sequences of human TIGIT (Hu TIGIT) and Rhesus TIGIT (Rh TIGIT). Highlighted sequences indicate homology between human and rhesus TIGIT. Dashes indicate gaps in alignment. (B) Representative flow cytometry plots depict rhTIGIT expression frequency (%) on CD8 T cells from PBMCs, Lymph nodes (LNs) and Spleen in representative non-infected and SIV-infected animals. (C) Representative flow cytometry plots depict rhTIGIT expression frequency (%) on naïve (N) (CD28+CD95-), effector memory (EM) (CD28-CD95+), and central memory (CM) (CD28+CD95+) cells from PBMCs, LNs and spleens in representative SIV-infected animals. Graphs show frequency (%) of rhTIGIT+ N, EM and CM CD8 T cells from SIV-infected RMs (open circle; n = 16), LNs (open square; n = 19), and spleens (open triangle; n = 10). P values were calculated with repeated-measures one-way ANOVA, followed by Tukey's multiple comparisons test. (D) Graph shows compiled frequency (%) of rhTIGIT+ CD8 T cells after stimulation with IL-2, IL-12 or IL-15 for six days. NS, no stimulation. P values were calculated with repeated-measures one-way ANOVA, followed by Tukey's multiple comparisons test. (E) Representative flow cytometry plot showing secondary antibody only against CM9 tetramer staining to facilitate rhTIGIT gating. (F) Representative flow cytometry plot showing PD-1 FMO and secondary antibody only to facilitate rhTIGIT and PD-1 gating. (G) Representative flow cytometry plots of rhTIGIT and

PD-1 expression on Mamu-A*01 SIV-Gag CM9 tetramer specific CD8 T cells.

Graphs show compiled data of rhTIGIT and PD-1 expression frequency (%) on

Mamu-A*01 SIV-Gag CM9 tetramer specific CD8 T cells ($n = 4$) from PBMC

(open circle), LNs (open square), and spleen (open triangle). (H) Representative

flow cytometry plots of rhTIGIT and PD-1 expression on Mamu-A*01 SIV-Tat SL8

tetramer specific CD8 T cells. Graphs show rhTIGIT and PD-1 expression

frequency (%) on Mamu-A*01 SIV-Tat SL8 tetramer specific CD8 T cells ($n = 4$)

from PBMC (open circle), LNs (open square), and spleen (open triangle).
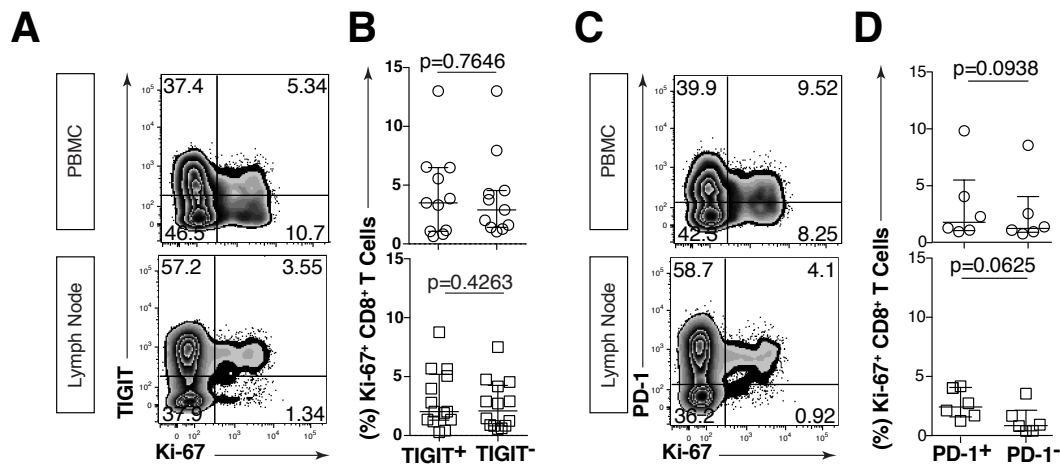
Supplemental Figure 3.7: Proliferative status of rhTIGIT expressing CD8 T cells in SIV infection. (A) Representative flow cytometry plots depict Ki-67 and rhTIGIT expression in PBMCs and Lymph nodes (LNs) from SIV-infected animals. (B) Graphs show frequency (%) of rhTIGIT+ Ki-67+ and rhTIGIT- Ki-67+ CD8 T cells in PBMCs (open circle; n = 11) and LNs (open square; n = 14) from SIV-infected animals. Wilcoxon matched-pairs signed- rank test was performed for statistical analysis (C) Representative flow cytometry plots depict Ki-67 and PD-1 expression in PBMCs and LNs from SIV-infected animals. (D) Graphs show frequency (%) of PD-1+ Ki-67+ and PD-1- Ki-67+ CD8 T cells in PBMCs (open circle; n = 6) and LNs (open square; n = 6) from SIV-infected animals. Wilcoxon matched-pairs signed- rank test was performed for statistical analysis.
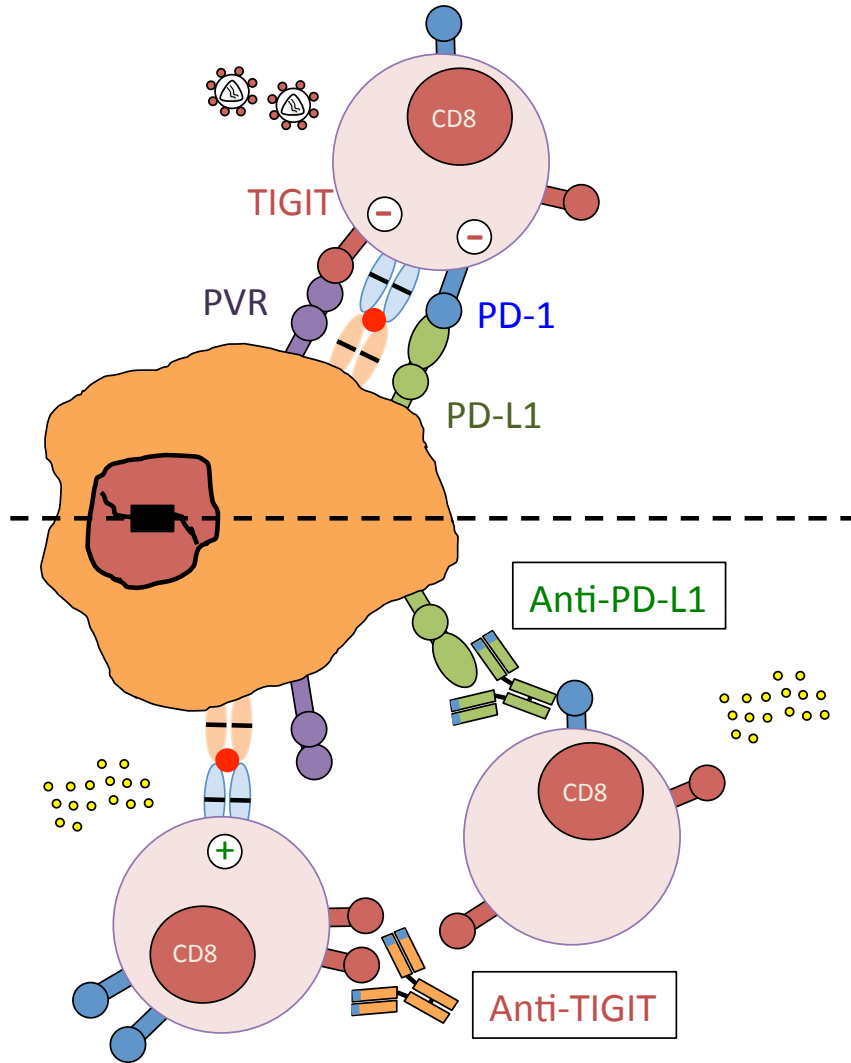
Graphical Abstract Figure 3.1: TIGIT and PD-L1 blockade. Figure represents blocking the TIGIT and PD-L1 pathways with mAbs to increase HIV/SIV-specific CD8 T cell effector functions.

Enhanced "Shock and Kill" Approach
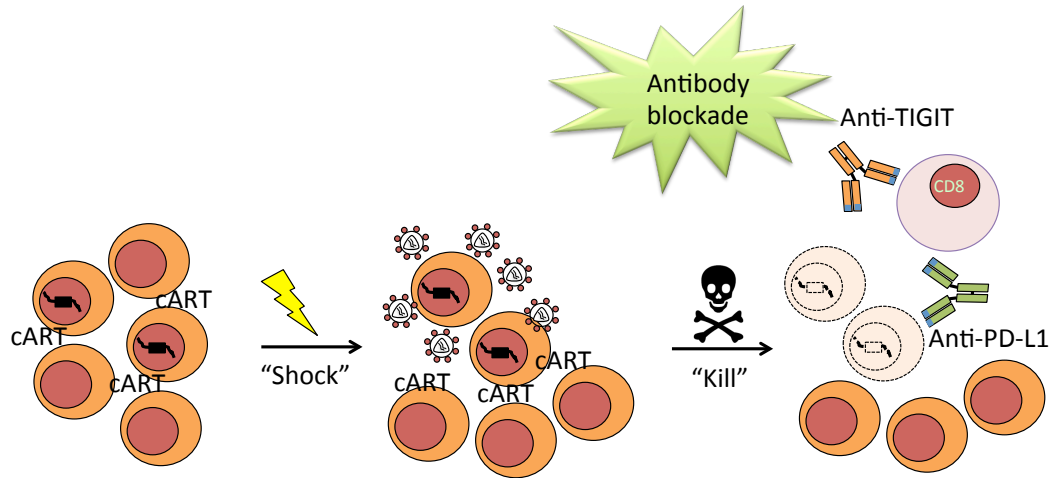
Graphical Abstract Figure 3.2: Enhanced "Shock and Kill" HIV cure strategy. Figure represents the HIV cure strategy to flush out latent HIV and eliminate infected cells while protecting new cells from being infected with cART. CD8 T cell reinvigoration with anti-TIGIT and anti-PD-L1 may be required to enhance CD8 T cell effector functions to eliminate infected cells after latency reversal.

CHAPTER 4

GUT TISSUE-SPECIFIC DIFFERENCES IN TIGIT AND TIGIT-LIGANDS DURING CHRONIC cART HIV INFECTION: IMPLICATIONS FOR IMMUNOTHERAPY EFFICACY

SPECIFIC AIMS

Aim I: Determine the role of TIGIT and TIGIT ligands in tissues during cART HIV infection

A: To compare the expression of TIGIT on CD8 and CD4 T cells from the peripheral blood and gut in cART HIV-infected and HIV-uninfected subjects

Hypothesis: TIGIT expression will be increased on gut tissue T cells compared to the peripheral blood.

Rationale: negative checkpoint receptors exhibit unique functions in tissues and play specialized roles in regulating the immune response.

B: To compare the expression of TIGIT ligands from peripheral blood and gut in cART HIV-infected and HIV-uninfected subjects

Hypothesis I: Gut tissue antigen presenting cells will have an increase of the TIGIT ligand (Polio Virus Receptor (PVR)) compared to peripheral blood during HIV infection.

Rationale: PVR is part of the nectin family that maintains intracellular adherens junctions between epithelial cells and is found in gut tissue.

Hypothesis II: There will be an increase of *Fusobacterium* in the gut microbiome of HIV infected individuals.

Rationale: Fusobacterium in the gut contains an outer membrane protein, Fap2, which binds to TIGIT and protects colon tumors from immune clearance and may be involved in anti-HIV T cell effector functions.

C: Determine the magnitude of TIGIT blockade reinvigoration and relations to levels of TIGIT and TIGIT ligands in peripheral blood and gut tissue

Hypothesis I: The magnitude of rescued response will be associated with levels of TIGIT ligands.

Rationale: Augmented dendritic cell functions through the microbiota alters CD8 T cell priming and peripheral immune function.

ABSTRACT

Despite the success of immunotherapy blockade of TIGIT and PD-1 pathways in restoring anti-HIV responses *ex vivo*, most individuals do not exhibit a robust immune reinvigoration. Blood and tissue based profiling to understand the mechanism of TIGIT and PD-1 blockade have not widely been explored. Here we use immune profiling of PBMCs, RMMCs and gut microbiota composition from cART suppressed HIV-infected individuals to evaluate the anti-HIV CD8 T cell blockade efficacy. We observed significant differences in TIGIT, PD-1, PVR, PD-L1 expression and *Fusobacteria* abundance from RMMCs compared to PBMCs in AS. The frequency of RMMC PD-L1+ pDCs correlated with the magnitude of IFN-γ anti-TIGIT CD8 T cell reinvigoration. The RMMC TIGIT+ CD8 T cells and PVR+ mDCs inversely correlated with the magnitude of CD107a anti-PD-L1 CD8 T cell reinvigoration. The RMMC PVR+PD-L1+ pDCs inversely correlated with the magnitude of CD107a combinational anti-TIGIT/anti-PD-L1 CD8 T cell reinvigoration. There was a significant increase in the abundance of *Fusobacteria* in HIV-infected individuals. The *Fusobacteria* abundance inversely correlated with the magnitude of IFN-γ reinvigoration from anti-TIGIT blockade. Interestingly, anti-TIGIT blockade positively correlated with the beneficial gut commensal bacteria, *Firmicutes* and *Lentisphaerae*, abundance. These data support the idea that the relationship between RMMC phenotypes and microbiota abundance correlate with the magnitude of CD8 immune reinvigoration after immunotherapy *ex vivo*, we identify clinically accessible immunotherapy treatment predictors of anti-HIV CD8 T cell responses to anti-TIGIT and anti-PD-L1 blockade.

OVERVIEW

Chronic HIV infection is associated with increased expression of negative checkpoint receptors (NCRs) on HIV-specific T cells in the peripheral blood that contribute to immune dysfunction and viral persistence [176-178, 180, 207, 208, 262]. Cytotoxic CD8 T cells contribute significantly to the control of viral replication [163, 165, 169, 263-265], however, persistent viral antigens may stimulate CD8 T cells that subsequently leads to a progressive loss of function termed "T cell exhaustion" [2]. During this process, the expressions of several NCRs on the surface of T cells are increased, raising the threshold for T cell activation, and eventually results in blunted immune responses. NCR suppression is mediated by receptor-ligand interactions, therefore they are susceptible to disruption by monoclonal antibodies or recombinant proteins. We have shown that a surface glycoprotein, TIGIT, is overexpressed on peripheral CD8 T cells during chronic HIV infection and remains elevated despite effective viral suppression. Additionally, TIGIT marks impaired viral-specific CD8 T cells and *in vitro* blockade of TIGIT and PD-1 pathways synergistically enhancing virus-specific CD8 T cell effector functions [262]. In tissue, gamma chain cytokines, a cytokine family with the ability to regulate the expression of NCRs, are present at high concentrations in tissue microenvironments and may play a role in regulating the tissue immune responses [234, 240, 262]. For instance, gamma chain cytokines are enriched in the intestine and play an important role in maintaining T cell hemostasis [266]. Taken together, TIGIT and other potential NCRs that are upregulated in HIV infection may serve as potential targets for the reversal of T cell exhaustion both within the periphery and in the tissue.

Targeting NCRs is currently being evaluated as an alternative method in cancer therapies [267-270]. Cytotoxic T-Lymphocyte Associated Protein 4 (CTLA-4) and Programmed Death 1 (PD-1) were the first class of NCRs targeted in clinical studies. Blocking PD-1 led to a dramatic increase in overall survival

and progression-free survival in individuals with advanced melanoma (31-44%) [271, 272], non-small-cell lung cancer (19-20%) [273, 274], and renal cell carcinoma (22-25%) [275]. Unfortunately, therapies aimed at modulating these pathways were only successful in a subset of individuals and associated with severe immune-related adverse events (IrAEs) [276, 277]. Recently, the immunotherapeutic focus has switched to the second tier of NCRs (TIGIT, TIM-3 and Lag-3) that display less toxicity. In our study, we have observed a dynamic range of individuals who have enhanced response to HIV antigens in the presence of anti-TIGIT or anti-PD-L1 blockade with no association in the frequency of peripheral TIGIT or PD-1 T cell expressions *ex vivo*. Identifying pretreatment predictors of anti-HIV responses to anti-TIGIT and anti-PD-L1 are essential to future clinical application of immunotherapy in HIV cure strategies.

Studies characterizing immune function in the periphery have provided insight into HIV pathogenesis, however circulating lymphocytes only represent about 25% of the body's total lymphocyte [278]. The retention of infected cells in tissues remains a major barrier to the eradication of HIV. Low-level viral replication despite cART and viral rebound as a result of treatment interruption suggests that tissue reservoirs harbor stable, replication-competent virus [279, 280]. Mucosal tissues in the gastrointestinal tract are thought to play an important role in the acquisition and persistence of HIV. The gut contains about 85% of the body's lymphoid tissue in organized lymphoid follicles (Peyer's patches) and up to 90% of the body's lymphocytes [281, 282]. During acute infection, there is a large abundance of highly susceptible activated CCR5-expressing CD4 T cells that are targeted by HIV in gut associated lymphoid tissues (GALT) [96, 281]. Furthermore, rectal biopsies from infected individuals on combination antiretroviral therapy (cART) show stable HIV RNA and DNA levels up to two-fold higher than in the blood [283]. Characterizing gut lymphocytes during chronic HIV infection is critical to understanding the pathogenesis of HIV and developing curative strategies.

In addition to lymphocytes, antigen-presenting cells such as dendritic cells (DCs) also play a fundamental role in inducing immunity and maintaining immune tolerance [284]. DCs can be divided into different subsets: myeloid-derived dendritic cells (mDCs), which express CD11c, and plasmacytoid dendritic cells (pDCs), which express CD123 [285]. Receptor-ligand interactions during direct cell-to-cell contact and cytokines secreted from DCs ultimately determine the fate of T cells. TIGIT and PD-1 on T cells interact with their respective ligands on DCs, Poliovirus receptor (PVR) [224] and programmed death-1 ligand (PD-L1) [286] respectively, to prevent T cell activation and promote tolerance. DCs can be found in the lamina propria, small and large intestine are known to control specialized aspects of tissue immunity [287]. Characterizing the role of TIGIT-ligand expressing DCs in the intestine will help increase our understanding of intestinal immunity during chronic HIV infection.

The human intestinal microbiota plays an intricate role in the development and function of the systemic immune system [145, 146]. Recent studies have showed the role of intestinal microbiota and its ability to promote cancer therapies through the targeting of NCR pathways. *Bacteroidetes* was reported to enhance the efficacy of CTLA-4 blockade and elimination of metastatic melanoma in mice and humans [288]. In a similar study, anti-tumor immune effects by CD8 T cell was restored upon the blockade of PD-L1 and the resulting tumor clearance relied on gut *Bifidobacterium* colonization [289]. Another bacterium, *Fusobacteria,* was shown to associate with T cell responses in malignancy. *Fusobacteria* is a core member of the human anaerobic oral microbiota and is non-native to the human gut. However, overabundance of *Fusobacteria* in the gut has been associated with the promotion of colonic tumor formation and shown to inhibit immune function through Fap2, a membrane protein, through its interaction with TIGIT [290, 291]. Identifying microbiome composition during chronic HIV infection may inform anti-viral immunity and responsiveness to anti-TIGIT and anti-PD-L1 immunotherapy.

In the present study, we aim to explore the correlation between rectosigmoid mucosal mononuclear cells (RMMCs) phenotypes with their peripheral blood mononuclear cell (PBMC) counterparts. Additionally, we characterized the microbiome communities of cART suppressed HIV-infected individuals and compared them to matched HIV-uninfected individuals and explored if the change in HIV-associated gut microbial abundance was associated with the changes in CD8 T cell phenotype and function. By profiling matched peripheral immune responses of CD8 T cells to immunotherapeutic blockade, we found motivating correlates of efficacy. The magnitude of reinvigoration correlated with ligand phenotypes from RMMC APCs and abundance of *Fusobacteria*. These data suggest a potential approach to HIV eradication through CD8 T cell functional modulation with gut microbial manipulation.

MATERIALS AND METHODS

Human subjects

Patients and specimens: For this study, fresh rectosigmoid biopsies from the Gut Biopsy Assessment Study (PI: Ndhlovu) were conducted at HICFA. Twelve gut biopsies and peripheral blood were obtained from each participant as outlined below. The Queen's Medical Center Research and Institutional Review Committee have approved this study.

Inclusion Criteria: HIV-infected participants: HIV infection as documented by ELISA and/or confirmed by other standard assay at any time prior to study entry, received continuous antiretroviral (ARV) medication for >6 months with HIV RNA viral loads <48 copies/ml, and CD4 count within past 6 months >200 cells/ml. HIV-uninfected participants: Negative HIV ELISA test. All subjects for the study must be >50 years of age and plan to undergo a screening colonoscopy as standard of care, are able and willing to provide informed consent, and have the following laboratory parameters documented prior to study

99

entry: hemoglobin >12.0; absolute neutrophil count >500/µL; platelet count >40,000/µL; PT/PTT within normal limits.

Exclusion Criteria: All subjects with history of cardiac condition, current or history of past malignancies excluding basal cell carcinoma and Kaposi's sarcoma restricted to the skin, history of bleeding tendency and use of anticoagulants, use of any immunomodulators, investigational therapies and any vaccination within 30 days of study entry, requirement of acute therapy for other AIDS-defining or other serious illnesses within fourteen days prior to study entry, history of other chronic illnesses except subjects on stable physiologic replacement therapy for low testosterone or thyroid levels, current active substance or alcohol abuse, pregnancy, breast-feeding, intention to become pregnant during the course of the study, any condition that places subject at increased risk of complications from colonoscopy or biopsies, and acute or chronic diarrhea or history of enteropathies.

Peripheral Blood Mononuclear Cells Isolation

Venous whole blood was collected in plastic whole blood tubes with spray-coated K2EDTA (BD Biosciences, San Jose California) separated within 30 minutes of the blood draw. PBMCs were isolated using Ficoll-Hypaque (Sigma-Aldrich, Dorset, United Kingdom) density gradient centrifugation. Separated PBMCs were cryopreserved or directly used for phenotypic and polyfunctional analysis.

Isolation of rectosigmoid mucosal mononuclear cells from fresh gut biopsy

To generate a single cell suspension of rectosigmoid mucosal mononuclear cells (RMMCs), nine to twelve endoscope-obtained tissue fragments were washed thoroughly with cRPMI (RPMI 1640 medium; (Hyclone, Logan, Utah) supplemented with 10% fetal bovine serum (FBS) (Hyclone), 1% penicillin-streptomycin (Hyclone), 10 mM HEPES (Hyclone), 2 mM L-glutamine

(Hyclone) and digested with collagenase II (Sigma-Aldrich, Dorset, United Kingdom) solution, and filtered through a 70 μm nylon mesh. Leftover undigested tissue was re-digested with collagenase II solution. RMMCs were washed PBS + 2% FBS (Hyclone) and re-suspended for flow cytometry analysis.

Antibodies and flow cytometric analysis

Freshly obtained or frozen PBMCs and isolated RMMCs were washed with PBS + 2% FBS (Hyclone). Cells were stained for viability with a Live/Dead aqua amine reactive dye (AARD; Invitrogen, Carlsbad, California), then incubated with panels of fluorochrome conjugated anti-human monoclonal antibodies (mAbs). The following directly conjugated mAbs used in this study were obtained from BD biosciences (San Jose, California): Alexa700-conjugated CD4 (clone: RPA-4T), mAb obtained from Beckman Coulter (Fullerton, California) ECD-conjugated anti-CD3 (UCHT1). mAbs obtained from eBioscience (San Diego, California) PE-Cy7-conjugated anti-CD28 (CD28.2), PerCP-eFluor 710-conjugated anti-TIGIT (MBSA43), PE-conjugated anti-TIGIT (MBSA43), Mouse IgG1 Kappa isotype control PerCP-eFluor 710 (P3.6.2.8.1), mouse IgG1 K isotype control PE (P3.6.2.8.1). Qdot 605-conjugated anti-CD8 (3B5) was obtained from Invitrogen (Carlsbad, California). Flow analyses were performed on a custom 4-laser BD LSRFortessa. Between 100,000 to 500,000 lymphocyte events were collected for each sample. Isotype controls or fluorescence minus one (FMO) samples were prepared to facilitate gating. Anti-mouse or anti-rat IgG-coated beads (BD Biosciences) were individually stained with each fluorochrome-conjugated antibody and used for software-based compensation. Data were analyzed using Flowjo Software version 9.5 (Treestar, Ashland, Oregon).

Anti-TIGIT and anti PD-L1 monoclonal antibodies

The TIGIT antibody clones 11G11 were generated in HuMab mice [257, 258] immunized with a TIGIT-Fc fusion protein and selected based on their high affinity for TIGIT and ability to block TIGIT/PVR interaction. Clone 11G11 is a fully human IgG1 antibody that was engineered to contain a well-characterized set of mutation in the Fc that eliminate FcR interaction [259]. The anti-human PD-L1 antibody, clone 12A4, is a fully human IgG4 (S228P) that was generated in HuMab mice immunized with PD-L1-Fc. This antibody was selected based on its ability to block the binding of PD-L1 to both PD-1 and CD80.

Ex vivo antigen stimulation with antibody blockade assay

Cryopreserved PBMCs were rapidly thawed and seeded at one million cells per stimulation condition with isotype control antibody (IgG1), single or combination of purified anti-TIGIT and/or anti-PD-L1 and stimulated with/without pooled HIV Gag peptides. The HIV clade B Gag peptide pool consists of 123 overlapping ~15mer peptides designed to elicit broad T cell responses (NIH). After a three-day incubation at 37°C with 5% CO_2, cells were washed and supplemented with media plus IL-2 for 2 days. On day five, cells were re-stimulated overnight with pooled HIV Gag peptides and the same blockade conditions along with APC-conjugated CD107a (BD Biosciences, Clone H4A3), 5 µg/ml brefeldin A and 5 µg/ml monensin (Sigma-Aldrich) culture media. After stimulation, the cells were washed and stained for viability with AARD, cultured with surface phenotype panel against Qdot605-conjugated CD8 (Invitrogen), PerCP-eFluor 710-conjugated TIGIT (eBioscience) or an isotype control antibody, followed by intracellular staining of ECD-conjugated CD3 (Beckman Coulter), FITC-conjugated IFN-γ (BD Bioscience, Clone 25723.11), and Alexa700-conjugated TNF-α (eBioscience, Clone MAb11), acquired on the flow cytometer then analyzed as above.

Bacterial 16S rRNA sequencing

One to two tissue fragments (50-100mg) were collected from rectosigmoid biopsies in cRPMI 10% without 1% penicillin-streptomycin and re-suspended and lysed in beta mercaptoethanol-added lysis buffer. Total DNA and RNA was isolated using AllPrep DNA/RNA/miRNA Universal kit (Qiagen), followed by DNA/RNA yield analysis using NanoDrop 2000 UV-Vis Spectrophotometer. We amplified 7 of 9 hypervariable regions in the bacterial 16S rRNA gene with PCR primers designed to target more than 805 sequences in the Greengenes database [292, 293] using Ion 16S Metagenomics Kit (Ion Torrent, Life Technologies). Amplified DNA were subsequently purified, ligated with sequencing adapters, and quantified. 16S libraries were templated using the Ion PGM™ Template Kit (Ion Torrent, Life Technologies) and sequenced on the Ion Torrent PGM instrument (Ion Torrent, Life Technologies). The sequence reads were analyzed using the Metagenomics workflow in the Ion Reporter™ software and plotted against the Greengenes database.

Statistical analysis

The repeated-measures, one-way ANOVA followed by Tukey's multiple comparison, Mann-Whitney U Tests, Wilcoxon matched-pairs signed ranked and the Spearman's rho test were performed using Graphpad release 5.0d (Graphpad Software, San Diego, California) or SPSS 22.0 (IBM, Armonk, New York) with the statistical significance of the findings set at a p value of less than 0.05. Measures of central tendency are expressed as medians and interquartile ranges (IQRs; given in the form 25th percentile, 75th percentile).

RESULTS

Differential expression pattern of TIGIT and PD-1 from matched rectal mucosal mononuclear cells and peripheral blood mononuclear cells.

Chronic HIV infection leads to NCRs-mediated T cell exhaustion that actively inhibits antigen-specific T cell responses both in the periphery and tissues [178, 262]. In this study, we profiled the expression of TIGIT and PD-1 on T cells from rectal mucosal mononuclear cells (RMMCs) and peripheral blood mononuclear cells (PBMCs) from cART suppressed HIV-infected (AS) and compared these results with age-matched HIV-uninfected (HD) individuals (Table 4.1, Figure 4.1A-G). We observed significantly higher TIGIT+PD-1+ CD8 T cells from RMMCs compared to PBMCs (Median: 33% vs. 14.2% respectively, p = 0.046) from the AS individuals (Figure 4.1B right panel). When comparing RMMCs and PBMCs from AS individuals, we observed significantly higher TIGIT+ CD4 T cells (39.7% vs18% respectively, p = 0.015), PD-1+ CD4 T cells (71.8% vs. 36.9% respectively, p = 0.015) and TIGIT+PD-1+ CD4 T cells (35.3% vs. 6.8% respectively, p = 0.015) (Figure 4.1C). We did not observe any significant differences in T cell expression of TIGIT or PD-1 from RMMCs compared to PBMCs from HD individuals (Figure 4.1E-F). Between AS and HD RMMCs, we observed significantly lower PD-1+ CD8 T cells (AS 46% vs. HD 61.6%, p = 0.048) and significantly higher TIGIT+ CD4 T cells (AS 39.7% vs. HD 28.8%, p = 0.048) (Figure 4.1G). These data suggest that despite viral suppression, TIGIT expression remains higher on RMMC-resident T cells compared to those found in the periphery and may have a dominant role in regulating T cell immune response while maintaining CD4 T cell viral persistence in the gut.

PVR and PD-L1 expression profile varies on antigen presenting cells by anatomical location.

Effective adaptive immune responses depend on the efficient presentation of antigen by professional antigen-presenting cells (APCs). Dendritic cells (DCs) are sentinel APCs that capture antigen, migrate through tissues and produce cytokines that impact T cell maturation and activation [294]. We next assessed the expression of poliovirus receptor (PVR) and programmed death 1 ligand (PD-L1), ligands to TIGIT and PD-1, respectively, on dendritic cell subsets from RMMCs and PBMCs from AS individuals and compared these results with HD individuals (Table 4.1, Figure 4.2A-G). When comparing RMMCs to PBMCs from AS individuals, we observed significantly lower PVR+ mDCs (78.6% vs. 93.4% respectively, p = 0.015), significantly higher PD-L1+ mDCs (80.3% vs. 28.9% respectively, p = 0.015) and significantly higher PVR+PD-L1+ mDCs (87.5% vs. 28.7% respectively, p = 0.015) (Figure 4.2B). When comparing RMMCs to PBMCs from AS individuals, we observed significantly higher PVR+ pDCs (93.5% vs. 54.6% respectively, p = 0.015), PDL1+ pDCs (66.4% vs. 24.2% respectively, p = 0.015), and PVR+PD-L1+ pDCs (50.3% vs. 20.8% respectively, p = 0.031) (Figure 4.2C). We did not observe any significant differences in dendritic cell expression of PVR or PD-L1 in RMMCs compared to PBMCs from HD individuals (Figure 4.E-F). When comparing AS to HD RMMCs, we observed significantly higher PD-L1+ mDCs (80.3% vs. 62.75% respectively, p = 0.0101) and significant increase of PVR+PD-L1+ mDCs (87.5%vs 64.1% respectively, p = 0.025) (Figure 4.2G). Taken together, these data suggest that antigen-presenting cells in the gut may be interacting with T cells to suppress immune function through ligand-receptor NCR interactions.

Group differences in the microbiome distribution among cART-suppressed HIV-infected and HIV-uninfected individuals.

The intricate balance between the host immune system, eliminating pathogens while maintain self-tolerance is essential to overall immune health. Intestinal microbiota has been considered an important modulator of immune

responses, specifically T cell immune activation in malignancies [294]. We assessed the microbiome profiles from rectosigmoid biopsies collected from AS and compared these results with HD individuals. Microbiome comprehensive identification of 16s ribosomal RNA sequencing was determined by pipeline using the Greengenes database [292, 293]. We observed significantly higher levels of *Fusobacteria* in AS compared to HD individuals (0.15% vs. 0.0024% respectively, p = 0.03) (Table 4.2; Figure 4.3-B). Although not statistically significant, during the comparative phyla analysis between AS and HD individuals, we observed a lower abundance of *Firmicutes* (33.36% vs. 44.95% respectively) and *Bacteroidetes* (28.75% vs. 20.21%) and a higher abundance of *Actinobacteria* (0.23% vs. 0.015%) (Table 4.2; Figure 4.3A). The enrichment of the pathogenic *Fusobacteria* and alterations to the intestinal microbial community during chronic cART-suppressed HIV infection may drive the systemic immune dysfunction in AS individuals.

Magnitude of TIGIT and PD-L1 monoclonal antibody blockade reinvigoration and periphery/tissue parameters.

In chronic HIV infection there is an increase in the active inhibition of the CD8 T cell effector functions that induces a progressive loss of CD8 T cell effector activity. PD-1 blockade leads to a dramatic increase in overall survival and progression-free survival in individuals with various malignancies [271-275]. However, subsets of individuals remain unresponsive to this method of immunotherapy. In the current study, we assessed the anti-HIV immune reinvigoration of peripheral CD8 T cells in the presence of anti-TIGIT and anti-PD-L1 blocking antibodies to matched rectosigmoid biopsy immune cell phenotypes and microbiome composition. We observed an increased in the fold change of interferon gamma (IFN-γ) RMMC responses to single anti-TIGIT and anti-PD-L1 blockade. We observed an increased fold change of interferon gamma (IFN-γ) CD8 T cell HIV Gag responses to single anti-TIGIT and anti-PD-

L1 blockade, and a higher fold change increase was observed in the combined anti-TIGIT plus anti-PD-L1 monoclonal antibodies (mAb) blockade (Figure 4.4A, 4.4B left panel, Combo). Similar trend was also observed in CD107a, lysosomal-associated membrane protein-1 marker of cellular degeneration, CD8 T cell Gag responses (Figure 4.4A, 4.4B right panel).

Next, we explored the correlation between RMMC T cells and antigen presenting DCs phenotypes and fold change in the cell restoration marker after antibody blockade. We observed a significant correlation between higher RMMC PD-L1+ pDCs and increased fold change of IFN-γ+ CD8 T cell Gag responses in the presence of anti-TIGIT blockade (p = 0.012, rho = 0.89) (Figure 4.4C). We also observed a significant inverse correlation between higher RMMC TIGIT+ CD8 T cells and PVR+ mDCs and decreased fold change of CD107a+ CD8 T cells HIV Gag responses in the presence of anti-PD-L1 blockade (p = 0.023, rho = -0.85; p = 0.034, rho = -0.79 respectively) (Figure 4.4D). A significant inverse correlation was also observed between higher RMMC PVR+PD-L1+ pDCs with decreased fold change of CD107a+ CD8 T cell Gag responses in the presence of the combination of anti-TIGIT plus anti-PD-L1 blockade (p = 0.048, rho = -0.78) (Figure 4.4E).

Finally, we evaluated the magnitude of anti-HIV T cell reinvigoration by mAb blockade relative to gut microbial abundance. Our study showed that decreased IFN-γ+ CD8 T cell HIV Gag responses by TIGIT blockade was negatively correlated with higher *Fusobacteria* abundance (p = 0.034, rho = -0.821) and with lower abundance of two non-pathogenic commensals, *Lentisphaerae* and *Firmicutes* (p=0.014, rho= 0.85 and p=0.04, rho= 0.78, respectively) (Figure 4.4F). Taken together, these data imply that the peripheral TIGIT and PD-L1 blockade efficacy may be affected by gut tissue immune cells and gut dysbiosis in cART-suppressed HIV-infected individuals.

DISCUSSION

Here we report several findings relevant to the understanding of the peripheral anti-HIV CD8 T cell responses to anti-TIGIT and anti-PD-L1 blockade in cART-suppressed individuals chronically infected with HIV. We (1) unveiled the expression of TIGIT in the context of PD-1 in the rectosigmoid mucosa and demonstrate compartmental differences within HIV-infected and HIV-uninfected individuals, (2) evaluated the expression of TIGIT and PD-1 ligands, PVR and PD-L1 respectively, from rectosigmoid mucosal DC subsets and demonstrate differences in HIV-uninfected individuals, (3) explored the microbiome composition and show differences in the bacterial abundance with the colonization of pathogenic *Fusobacteria* in HIV-infected individuals, and (4) demonstrate the magnitude of peripheral anti-HIV CD8 T cell immune reinvigoration by anti-TIGIT and anti-PD-L1 blockade correlates with bacterial abundance and immunological tissue parameters.

Preventing the establishment of viral reservoirs in the gut has been shown to result in sustained simian immunodeficiency virus (SIV) control and immune reconstitution after cART is withdrawn [295]. Blocking α4β7, an integrin involved in lymphocyte homing and retention, prevents the establishment of virus in the gut during acute infection and leads to decreased viral loads in a rhesus macaque model of HIV/AIDS [296]. The exact mechanism of control is unknown and whether it translates to humans that are chronically infected has yet to be determined. However, these data suggest that targeting the gut to improve immune function may prove to be an effective means of eliminating virus and bringing us closer to a functional or sterilizing cure. The higher frequency of RMMC TIGIT+PD-1+ CD8 T cells may be contributing to T cell dysfunction and viral persistence in the gut of HIV-infected individuals. Unfortunately, due to limited number of RMMCs derived from the rectosigmoid biopsies, we were unable to perform additional functional studies to evaluate the effects of TIGIT

and PD-L1 blockade on HIV-specific CD8 T cells in the gut. Future studies will be aimed at evaluating the functional capacity of exhausted T cells in the gut.

Interestingly, we observed a higher frequency of RMMC PD-1+ CD8 T cells from HIV-uninfected compared to HIV-infected individuals. PD-1 has been suggested to play a key role in intestinal tolerance. One study evaluated the effects of intestinal epithelium-specific antigen in PD-1-/- transgenic mice and observed a fatal CD8 T cell-mediated inflammatory response as well as the destruction of epithelial barriers only in the intestine [297]. Furthermore, *Rhesus macaques* display a decrease in RMMC PD-1+ CD8 T cells after SIV infection [298]. Our data suggests that HIV-infected individuals have increase in proinflammatory RMMC PD-1- CD8 T cells that may contribute to the persistence of HIV-induced gut damage.

TIGIT has been described to mark a subset of highly suppressive regulatory CD4 T cell (Tregs) [228, 299, 300]. Additionally, TIGIT+ Tregs have been reported to selectively inhibit proinflammatory T helper type 1 (Th1) and T helper type 17 (Th17), which is an important CD4 T cell subsets in maintaining gut immunity and integrity [228]. Moreover, Tregs also express PD-1 on the surface of activated Tregs in lymph nodes in the blood [301, 302]. Furthermore, memory CD4 T cells expressing multiple NCRs are enriched in inducible HIV DNA [303]. We observed an enrichment of TIGIT+, PD-1+ and TIGIT+PD-1+ CD4 T cells in RMMCs compared to PBMCs with a significantly higher RMMC TIGIT+ CD4 T cells in HIV-infected compared to HIV-uninfected individuals. Our data indicates that the TIGIT+ CD4 T cells may be further contributing to the HIV-induced gut damage in addition to viral persistence. Our future panels will be modified to include the transcription factor forkhead box P3 (FOXP3), Helios and surface receptor CD25, CD27, and CD45RA to better characterize Treg and memory CD4 T cell subsets.

Dendritic cells bridge the innate and adaptive immune systems and have the potent ability to induce immune tolerance through receptor-ligand interactions

and secreted cytokines to prevent immune activation and autoimmunity while maintaining immune hemostasis [285]. PD-1:PD-L1 interactions can directly inhibit T cell proliferation and survival [304]. While PD-L1+ antigen presenting cells have been implicated in several histolytic and dendritic cell disorders [305], during HIV infection there is an increase of peripheral PD-L1+ DCs and correlate directly with viral load [306, 307]. Furthermore, TIGIT:PVR interact bidirectionally to induce T cell dysfunction while promoting mature immunoregulatory DCs [221]. Our observations of the expansion of RMMC PD-L1+ and PVR+PD-L1+ mDCs during HIV infection indicate that DCs could be selectively supporting the persistence of dysfunctional TIGIT+ and PD-1+ T cells in the gut and periphery.

From analysis of the gut microbiome, we detected *Fusobacteria* presence in all HIV-infected individuals and HIV-uninfected controls, however the relative abundance was significantly higher in HIV-infected subjects compared to their matched controls. *Fusobacterium*, the main member of *Fusobacteria* phyla, is an anaerobic gram-negative species frequently isolated from the oral cavity of both healthy and diseased individuals, and is associated with periodontal disease [308, 309].

While the *Fusobacteria* are non-native to the human gut, their presence are detected and associated with colorectal cancer and promotes colonic tumor formation [291], suggesting that despite the distance from their natural oral niche, *Fusobacteria* possess the ability to translocate and colonize other organs, including the gut. The route in which *Fusobacteria* might translocate from the oral cavity to gut includes transient bacteremia that occurs following tooth brushing [310]. Normally, bacterial clearance is conducted by the liver, however in individuals with impaired liver function due to side effects of cART treatment, the liver's ability to clear peripheral bacteremia can be impaired [310].

In HIV infection, greater prevalence of *Fusobacteria* was identified from subgingival plaque from HIV-infected patients compared to HIV-uninfected individuals with chronic periodontitis [309]. HIV-infected individuals also possess

a higher risk of periodontal attachment loss that can lead to chronic periodontal disease, which is reported to be higher in these individuals compared to the general population [311, 312]. The combination of higher oral *Fusobacteria* colonization with increased risk of periodontal disease put HIV-infected subjects at higher risk for *Fusobacteria* bacteremia and *Fusobacteria* colonization in different organs that may be followed by systemic and local immune reaction to the bacterial colonization.

The higher gut *Fusobacteria* abundance in HIV-infected individuals in our study suggests a special HIV-related condition that can drive the bacterial translocation from its original habitat to the gut mucosa. In HIV infection, the high concentration of CCR5-expressing T-cells causes gut tissue to be the earliest mucosal target and a site for CD4 T-cell depletion causing epithelial injury that leads to microbial translocation and gut dysbiosis [152, 313]. Early introduction to cART only partially restores gut integrity, causing persistent disturbance in intestinal homeostasis and driving the microbial translocation immune activation in chronic HIV patients. [314, 315]. Our current study supports the hypothesis that gut microbial abundance in HIV-infected individuals differs from HIV-uninfected controls with a significantly higher abundance of *Fusobacteria*. The presence of *Fusobacteria* may trigger local and systemic immune activation in these patients suggesting a creation of mechanistic pathological cycle between gut dysbiosis, disrupted gut hemostasis and immune activation/dysfunction that persists despite viral suppression.

T cells depend on environmental nutrient composition and dynamic metabolic reprogramming to perform essential effector and memory functions [316]. In mice, chronic lymphocytic choriomeningitis virus (LCMV) infection results in a PD-1 mediated repression of glycolytic and mitochondrial metabolism in CD8 T cells [317]. *Fusobacteria* Fap2 engagement of TIGIT in the gut may induce metabolic reprograming that is not restored by peripheral anti-TIGIT blockade. Normal non-diabetic glucose concentrations in the periphery are 100

fold lower than in the gut, implying altered immunometabolism requirements in different anatomical sites throughout the body [318, 319]. As a result, the anti-TIGIT blockade may require nutrient composition similar to the tissues where the T cell is primed and TIGIT is engaged. In the future, it would be interesting to evaluate the metabolic demands in the presence of *Fusobacteria* Fap2 in mitochondrial stress assays.

Lymphocytes are constantly circulating throughout our bodies and traffic from the periphery through secondary lymphoid organs and tissues in search of cognate peptide-MHC complexes [320]. Priming of T cells depends on interactions between DCs in the lymph node and tissue microenvironments which ultimately influence peripheral immune tolerance [321]. Ligation of TIGIT has been shown to inhibit the priming of CD4 and CD8 T cells [223]. Studies using specific-pathogen-free mice have been conducted to understand the role of the microbiome in influencing the priming and activation of the systemic host immune system [322]. Our data suggests that gut microbiota and tissue immune parameters can predict peripheral immune response to immunotherapy..

The identification and treatment of *Fusobacteria* from rectal biopsies may be required as an anti-TIGIT pre-treatment predictors. Moreover, dietary supplements with probiotics [323] or fecal microbiota transplants [324] maybe be useful as adjunctive therapy to "reboot" the gut microbial ecosystem before anti-TIGIT therapy. Furthermore, it would be clinically relevant to extend our findings to oncologic therapies targeting TIGIT and PD-1 pathways.

In summary, these data provide a comprehensive analysis of TIGIT and TIGIT ligands in the gut of HIV-infected and HIV-uninfected individuals and identifies potential novel predictive biomarkers for identifying anti-HIV CD8 T cell reinvigoration by TIGIT and PD-L1 blockade. Results from this study will help characterize gut T cells during chronic aviremic HIV infection and allow for a better understanding of the specialized role of TIGIT plays in regulating distinct aspects of peripheral immunity. A better understanding of these facets of HIV

immunity will aid in the development of more effective immune-based therapies for the eradication of HIV.

TABLES

Table 4.1: Participant Characteristics

	HIV+ cART Suppressed (AS; n = 7)	HIV-Uninfected Donors (HD; n = 5)	p value
Parameters	**Median (IQR)**	**Median (IQR)**	
Age (Years)	57 (52, 62)	53 (51, 58)	0.4533
CD4 T cell Count (cells/mm3)	560 (387, 922)	N/A	
HIV Viral Load (copies/ml)	<20	N/A	
cART Therapy	Yes	N/A	
Gender Distribution			
Male % (no.)	85 (6)	80 (4)	0.998

N/A= Not Applicable

cART: Combinational Antiretroviral Therapy

Table 4.2:
Microbiota Abundance
(percent mapped reads)

Microbiota	HIV-Infected (n = 7)	HIV-Uninfected (n = 5)	p value
	Median (IQR)	Median (IQR)	
Firmicutes	33.36 (20.70, 40.27)	44.95 (20.15, 55.28)	0.52
Proteobacteria	30.84 (15.74, 51.61)	17.18 (15.27, 59.26)	0.82
Actinobacteria	3.56 (1.51, 7.14)	2.71 (0.39, 7.22)	0.502
Bacteroidetes	28.75 (8.56, 41.68)	20.21 (11.24, 36.05)	0.82
Acidobacteria	0.233 (0.021, 0.67)	0.015 (0.000826, 1.286)	0.601
Other phylla	0.209 (0.43, 0.32)	0.043 (0.019, 0.27)	0.41
Fusobacteria	0.15 (0.021, 1.041)	0.0024 (0.0016, 0.039)	*0.03
Unclassified	0.122 (0.23, 0.24)	0.021 (0.011, 0.27)	0.601
Cyanobacteria	0.101 (0.038, 0.27)	0.014 (0.0061, 0.22)	0.26
Tenericutes	0.0016 (0.00079, 0.0027)	0.00098 (0.00024, 0.38)	0.82
Verrucomicrobia	0.0016 (0.00079, 0.0027)	0.00098 (0.0024, 0.38)	0.63
Lentisphaerae	0.00027 (0, 0.0018)	0.00029 (0.00012, 0.26)	0.65
Spirochaetes	0.00027 (0, 0.0015)	0.00058 (0, 0.018)	0.097

115
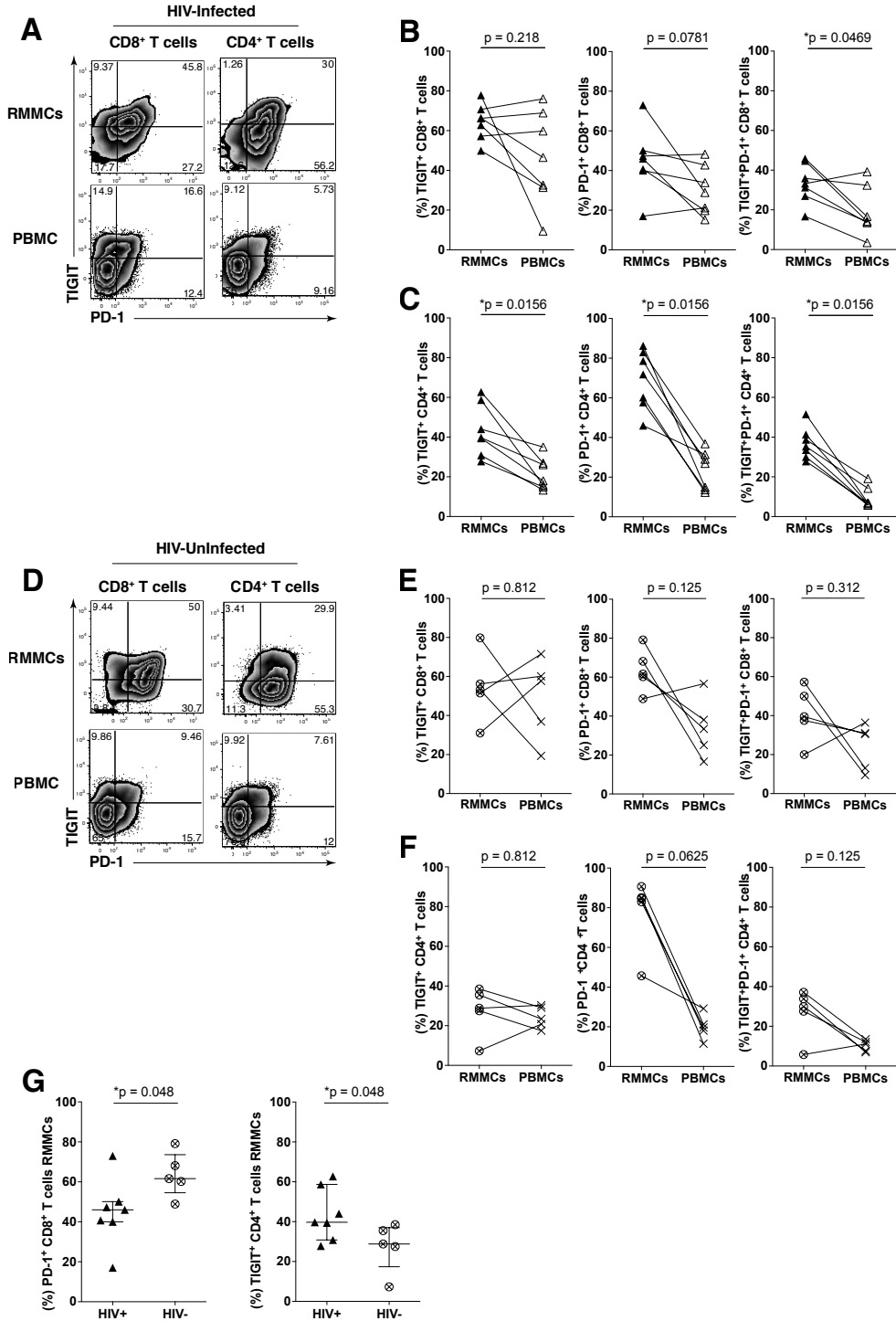
FIGURES

Figure 4.1: TIGIT and PD-1 are upregulated on mucosal mononuclear T cells derived from rectosigmoid biopsies. RMMCs and PBMCs from cART suppressed HIV-infected and HIV-uninfected individuals were stained for viability and antibodies against CD3, CD4, CD8, TIGIT and PD-1. Representative flow cytometry plots of matched RMMCs and PBMCs gated on live CD3+ lymphocytes, from representative (A) HIV-infected and (D) HIV-uninfected individuals. Compiled data comparing the differences of TIGIT and PD-1 expression on CD8 T cells from RMMCs and matched PBMCs of (B) HIV-infected (n = 7) and (E) HIV-uninfected (n = 5). Compiled data comparing the differences of TIGIT and PD-1 expression on CD4 T cells from RMMCs and matched PBMCs of (C) HIV-infected (n = 7) and (F) HIV-uninfected (n = 5). (I) Compiled data of PD-1+ CD8 T cells and TIGIT+CD4 T cells from RMMCs from HIV-infected (n = 7) and HIV-uninfected individuals (n = 5). The p-values were calculated using Wilcoxon matched-pairs signed ranked test for matched pairs and Mann-Whitney U test for cohort comparison.
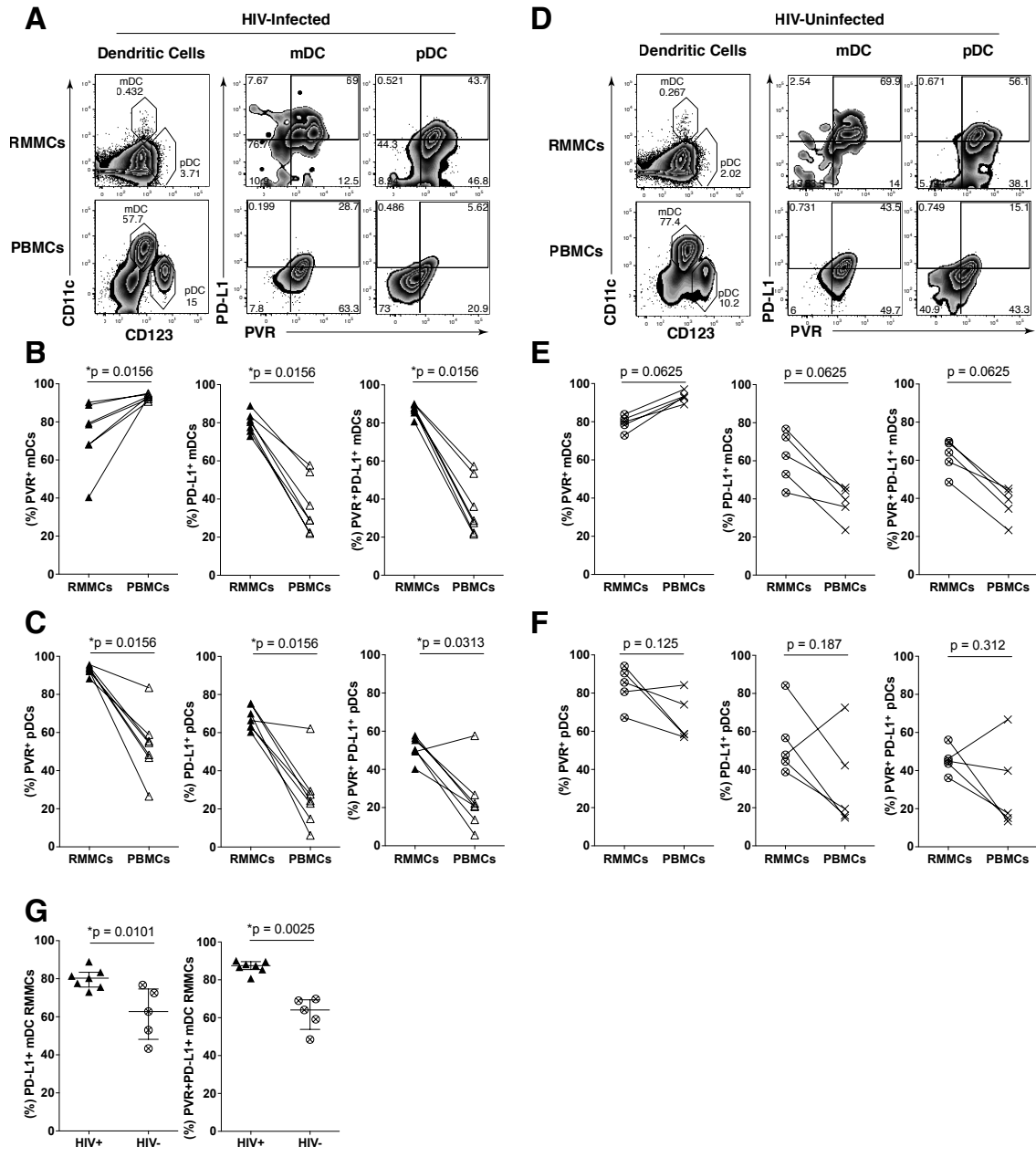
Figure 4.2: PVR and PD-L1 were differentially expressed on dendritic cell subsets from mucosal mononuclear T cells derived from rectosigmoid biopsies. RMMCs and PBMCs from cART suppressed HIV-infected and HIV-uninfected individuals were stained for viability and antibodies against CD3, CD7, CD14, CD19, CD20, CD11b, CD11c, CD123, HLA-DR, PVR, PD-L1. Representative flow cytometry plots of matched RMMCs and PBMCs gated on live CD3-, CD19-, CD7-, CD20-, CD14-, HLA-DR+ population from representative (A) HIV-infected and (D) HIV-uninfected individuals. Compiled data comparing the differences of PVR and PD-L1 expression on mDCs from RMMCs and matched PBMCs of (B) HIV-infected (n = 7) and (E) HIV-uninfected (n = 5). Compiled data comparing the differences of PVR and PD-L1 expression on pDCs from RMMCs and matched PBMCs of (C) HIV-infected (n = 7) and (F) HIV-uninfected (n = 5). (I) Compiled data of PD-L1+ mDCs and PVR+PD-L1+ mDCs from RMMCs from HIV-infected (n = 7) and HIV-uninfected (n = 5) individuals. P values were calculated using Wilcoxon matched-pairs signed ranked test for matched pairs and Mann-Whitney U test for cohort comparison
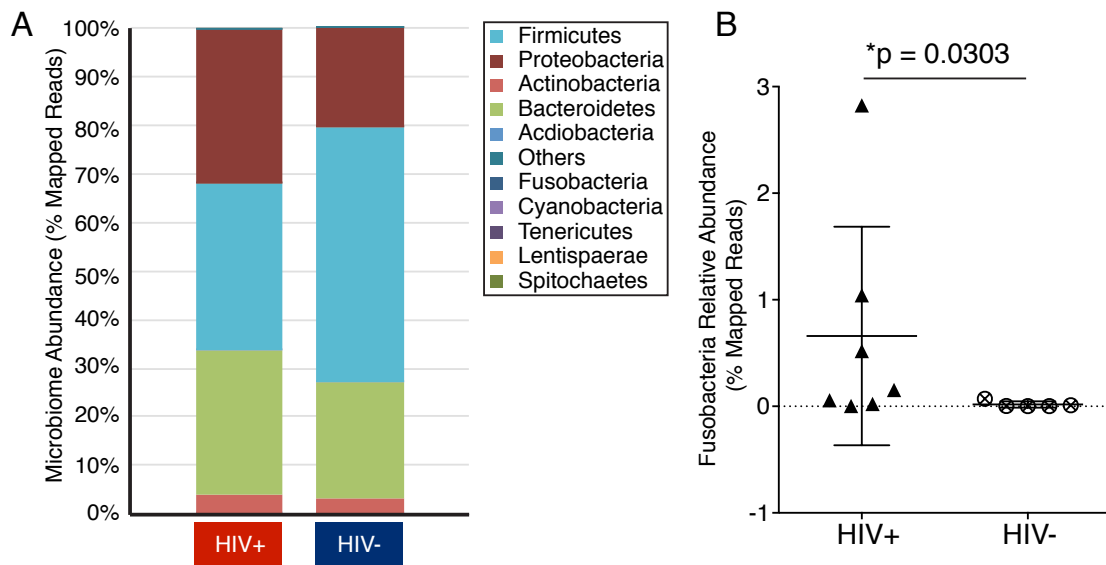
Figure 4.3: Microbiome compositions among HIV-infected and HIV-uninfected individuals. RNA was isolated from rectosigmoid biopsies and sequenced for microbial 16S rRNA from cART suppressed HIV-infected (HIV+) and HIV-uninfected (HIV-) individuals. Sequences were mapped to the Greengenes Database. (A) Compiled data of percent mapped reads of microbiome abundance at the phyla level, grouped as HIV+ (n = 7) and HIV- (n = 5). (C) Compiled data of *Fusobacteria* relative abundance as percent mapped reads, grouped as HIV+ (n = 7) and HIV- (n = 5). P values were calculated using Mann-Whitney U test.

A

No Stim | HIV Gag Peptide Pool

IgG1 | IgG1 | αTIGIT | αPD-L1 | Combo

IFN-γ

CD107a

B

Fold change of IFN-γ CD8 T cells in response to HIV Gag Peptide

*p = 0.01
p = 0.18
p = 0.18
*p = 0.01

Isotype	−	+	−	−	−
αTIGIT	−	−	+	−	+
αPD-L1	−	−	−	+	+

Fold change of CD107a CD8 T cells in response to HIV Gag Peptide

*p = 0.006
p = 0.18
p = 0.69
*p = 0.01

Isotype	−	+	−	−	−
αTIGIT	−	−	+	−	+
αPD-L1	−	−	−	+	+

C

(%) PD-L1⁺ pDC RMMCs

rho = 0.89
*p = 0.012

Fold change of anti-HIV Gag IFN-γ CD8 T cells with αTIGIT blockade

D

(%) TIGIT⁺ CD8 T cells RMMCs

rho = −0.85
*p = 0.023

Fold change of anti-HIV Gag CD107a CD8 T cells with αPD-L1 blockade

(%) PVR⁺ mDC RMMCs

rho = −0.79
*p = 0.034

Fold change of anti-HIV Gag CD107a CD8 T cells with αPD-L1 blockade

E

(%) PVR⁺PD-L1⁺ pDC RMMCs

rho = −0.78
*p = 0.048

Fold change of anti-HIV Gag CD107a CD8 T cells with Combo blockade

F

Fusobacteria Abundance (% Mapped Reads)

rho = −0.82
*p = 0.034

Fold change of anti-HIV Gag IFN-γ CD8 T cells with αTIGIT blockade

Firmicutes Abundance (% Mapped Reads)

rho = 0.78
*p = 0.048

Fold change of anti-HIV Gag IFN-γ CD8 T cells with αTIGIT blockade

Lentisphaerae Abundance (% Mapped Reads)

rho = 0.85
*p = 0.028

Fold change of anti-HIV Gag IFN-γ CD8 T cells with αTIGIT blockade

121

Figure 4.4: Peripheral CD8 T cell immune restoration is associated with RMMC phenotypes or microbiome abundance. PBMCs were stimulated with a HIV Gag peptide pool i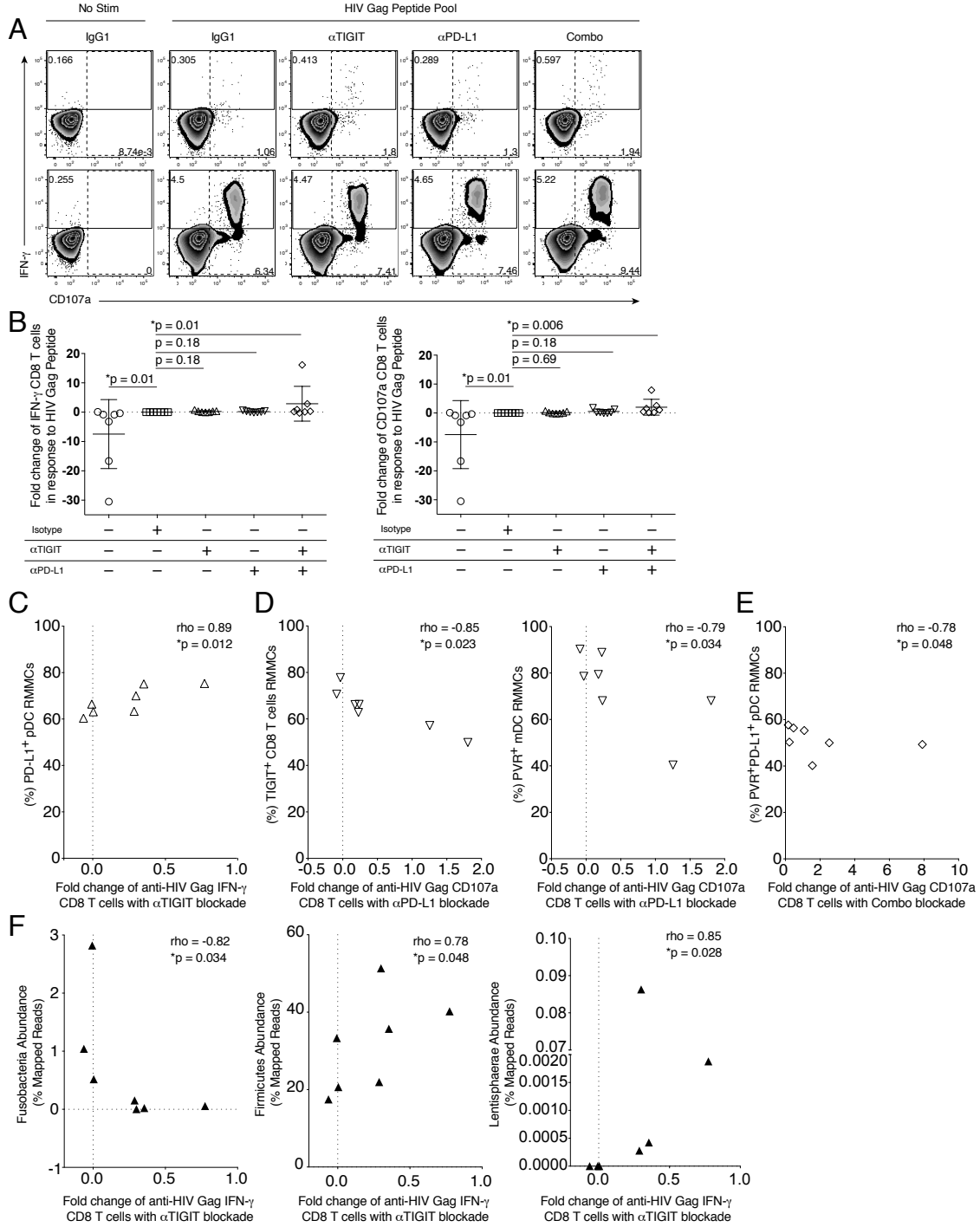n the presence, absence or combination of anti-TIGIT and/or anti-PD-L1 monoclonal blocking antibodies or IgG1 isotype and assessed for the production of interferon gamma (IFN-γ) and degranulation (CD107a). (A) Representative flow cytometry plots gated on Live CD3+ CD8 T cells, showing IFN-γ (solid gate) and CD107a (dashed gate) responses from two cART suppressed HIV-infected individuals. No HIV Gag stimulation with an isotype control, HIV Gag stimulation with an isotype control, HIV Gag stimulation with anti-TIGIT, HIV Gag stimulation with anti-PD-L1, HIV Gag stimulation with dual blockade (anti-TIGIT + anti-PD-L1) (B) Graphs show compiled data of the fold change of IFN-γ (B, right panel) and CD107a (B, left panel) in the presence of blocking mAbs normalized to HIV Gag stimulation with IgG1 isotype. Matched phenotypes from RMMCs were compared with the reinvigoration of PBMC CD8 T cells effector functions by mAb blockade. (C) Graph shows correlation of the frequency (%) of PD-L1+ pDCs from RMMCs against the fold change of anti-HIV Gag IFN-γ CD8 T cells with anti-TIGIT blockade. (D) Graph shows correlation of the frequency (%) of TIGIT+ CD8 T cells (D, left panel) PVR+ mDCs (D, right panel) from RMMCs against the fold change of anti-HIV Gag CD107a CD8 T cells with anti-PD-L1 blockade. (E) Graph shows correlation of the frequency (%) of PVR+PDL1+ pDCs from RMMCs against the fold change of anti-HIV Gag CD107a CD8 T cells with dual blockade. (F) Graph shows correlation of the relative abundance of *Fusobacteria* (F, left panel), *Firmicutes* (F, middle panel) and *Lentisphaerae* (F, right panel) from rectosigmoid biopsies against the fold change of anti-HIV Gag IFN-γ CD8 T cells with anti-TIGIT blockade. P values were calculated using values were calculated using one-way ANOVA, followed by Tukey's multiple comparisons test, Spearman's rho test was performed for correlations.
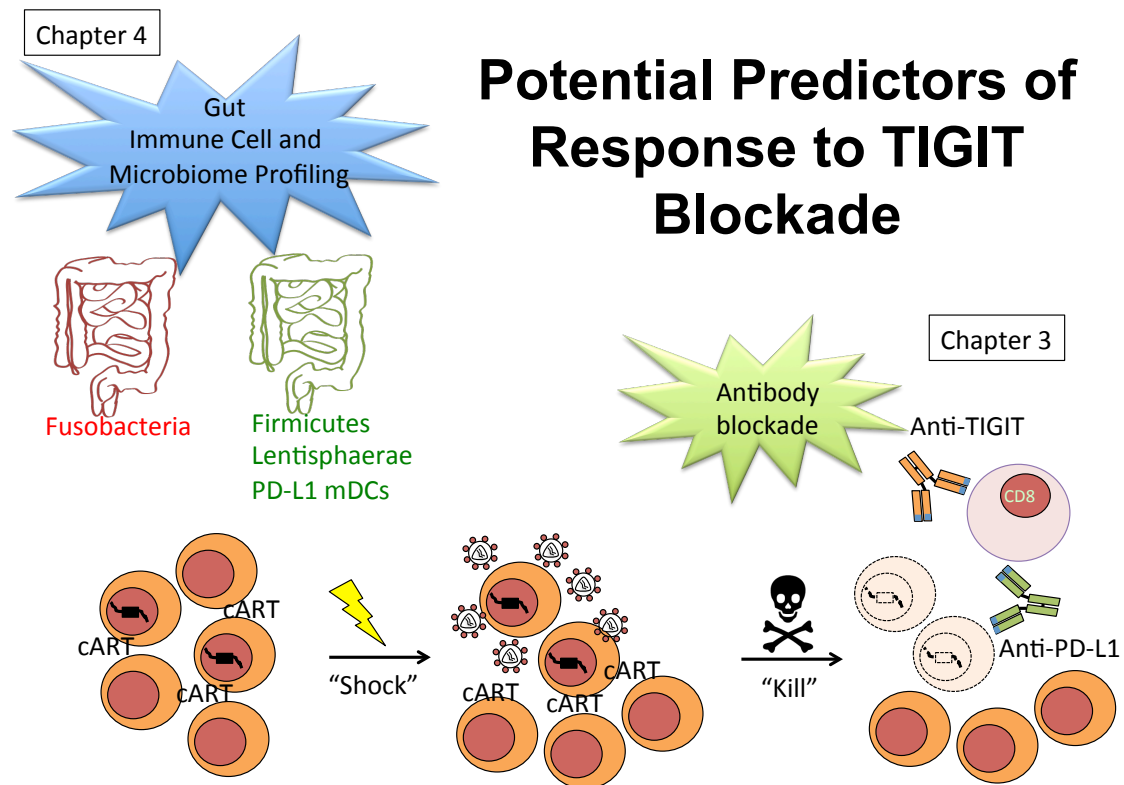
Graphical Abstract Figure 4.1: Potential pretreatment predictors of response to TIGIT blockade in enhanced "shock and kill" HIV cure strategies. Figure represents evaluating gut immune parameters and gut microbiome of individuals before enhanced "shock and kill" eradication strategies using TIGIT and PD-L1 blockade.

CHAPTER 5

DISSERTATION SUMMARY AND FUTURE PERSPECTIVES

DISSERTATION SUMMARY

An estimated 36 million individuals have died from HIV/AIDS since the first cases were reported in 1981 with roughly 36 million individuals currently living with HIV at the end of 2015 worldwide. Despite the significant advancements in antiretroviral therapy, the understanding of viral pathogenesis and immunological host interactions gained from several decades of research, an effective HIV cure or vaccine does not exist. The main obstacle to an HIV cure is that the virus is able to stably integrate into the host genome and lay latent, enabling it to avoid recognition by the immune system [138]. Combination antiretroviral therapy (cART) is able to suppress viral replication while increasing survival and the quality of life of HIV infected individuals. However, once cART is withdrawn, a rapid and aggressive rebound of plasma viremia occurs [138]. Lifelong cART regimens are associated with toxicity [325] chronic inflammation and aging related comorbidities [326, 327]. New approaches to HIV eradication are needed with the goal of achieving a functional or sterilizing cure that does not necessitate dependence of cART.

Several lines of evidence indicate that cytotoxic CD8 T cells significantly contribute to control of viral replication [163, 165, 169, 263-265]. However, chronic HIV infection is associated with an increased expression of negative checkpoint receptors (NCRs) on HIV-specific CD8 T cells in peripheral blood that leads to progressive loss of function, termed "T cell exhaustion" [2] which further contribute to immune dysfunction and viral persistence [176-178, 180, 207, 208]. Identifying additional NCRs that persist and can be targeted during chronic HIV infection is imperative to the future of HIV cure strategies.

The extremely stable reservoir of latently infected memory CD4 T cells that harbor replication competent HIV provirus [328] remains a major barrier to HIV eradication. Current HIV cure strategies focus on the "shock and kill" approach. Small pharmacological compounds are clinically being evaluated to

125

reactivate (shock) latent HIV provirus without inducing host cell activation in order to expose them to the immune system for elimination (kill) [1]. However, there is little impact on the size of the latent reservoir in small clinical trials of latency reversing agents [202, 203, 206]. This suggests that additional immune mechanisms may be required to enhance the clearance of virally infected cells.

The main purpose of this dissertation was to evaluate the expression and function of the T -cell immunoreceptor with immunoglobulin and ITIM domains (TIGIT; also known as Vsig9, Vstm3 or WUCAM) in the context of HIV infection. The goal of this study was to identify clinically targetable pathways to reinvigorate robust anti-HIV responses during enhanced "shock and kill" eradication strategies. The long-term goal of this study was to understand immune dysfunction that contributes to HIV disease progression and pathogenesis.

The first objective focused on the T cell phenotype expression of TIGIT in the context of HIV infection. Peripheral blood mononuclear cells (PBMCs) were collected from individuals with varying stages of HIV disease progression and matched to HIV-uninfected individuals. We demonstrated that an expansion of TIGIT+ CD8 T cells during chronic HIV infection despite viral suppression strongly correlated with disease progression. We also show that gamma chain cytokines have the potent ability to increase the expression of TIGIT in the context of HIV infection. Furthermore, TIGIT was co-expressed with PD-1 on HIV-specific CD8 T cells across several HLA-restricted HIV epitopes. These data suggest that TIGIT and PD-1 may play a dominant role in negatively regulating broad anti-HIV CD8 T cell responses. We next assessed the functional capacity of TIGIT expressing HIV-specific CD8 T cells and found them to be impaired in the ability to generate anti-HIV effector immune responses. Moreover, CD4 T cells expressing TIGIT strongly correlated with the CD4 HIV DNA content, suggesting TIGIT may be involved in maintaining the viral reservoir by suppressing CD4 T cell activation. The work reported here indicates that the

TIGIT pathway is involved in HIV disease progression and is responsible for immune dysfunction and viral persistence.

The second objective was to evaluate the TIGIT pathway in the physiologically relevant *Rhesus macaque* (RM) nonhuman primate model of HIV/AIDS. Lymphocytes from peripheral blood and lymphoid tissues derived from SIV infected RMs were used to evaluate the expression and function of rhesus-TIGIT (rhTIGIT). We cloned rhTIGIT and show an 88.11% amino acid homology with human TIGIT and reasoned that expression and function would mimic human TIGIT during HIV infection. We observed elevated levels of rhTIGIT+ CD8 T cells in the periphery with a significant elevation in lymphoid tissues, which correlated with plasma viremia in SIV-infected RMs compared to SIV-uninfected controls. Moreover, rhTIGIT was regulated by gamma chain cytokines, similar to human TIGIT. We also observed that TIGIT co-expressed with rhesus PD-1 on SIV-specific CD8 T cells and rhTIGIT+ CD8 T cells failed to respond to SIV peptides. These data recapitulated the observations of human TIGIT during HIV infection and characterized a preclinical model to study the *in vivo* safety and efficacy of interfering with the TIGIT pathway in enhanced "shock and kill" HIV eradication strategies.

The third objective aimed to evaluate the effects of interfering with the TIGIT and PD-1 pathways to restore existing anti-HIV/SIV T cell effector functions. Clinically validated blocking monoclonal antibodies (mAbs) against TIGIT and PD-L1 were gifted to us in order to investigate blockade strategies *in vitro*. Blocking mAbs combined with our HIV peptide stimulation assay resulted in significant reinvigoration of pre-existing anti-HIV CD8 T cell effector functions when blocking a single or combination of TIGIT and PD-1 pathways. Anti-HIV CD8 T cell interferon gamma responses were significantly increased when TIGIT or PD-1 pathways were blocked, while a combination of anti-TIGIT and PD-L1 significantly increased CD8 T cell proliferation. In parallel, these data were repeated in restoring SIV-specific CD8 effector functions by TIGIT and PD-L1

blockade in RMs. Our data indicates we can reverse T cell exhaustion and restore existing anti-HIV CD8 T cell effector functions to potentially allow them to more potently target HIV infected cells.

Our final objective was to evaluate the magnitude of peripheral CD8 T cell reinvigoration by TIGIT blockade to the expression of TIGIT with TIGIT ligands in peripheral blood and gut tissues. We observed a dynamic range in the restoration of CD8 T cell effector functions with TIGIT and PD-L1 blockade with no correlation between CD8 TIGIT or TIGIT ligand expression in the periphery. Similarly, in cancer immunotherapy, PD-L1 tumor expression as a pretreatment predictor of PD-1 blockade remains suboptimal [329, 330]. Studies characterizing immune function in the periphery have provided insight into HIV pathogenesis, however circulating lymphocytes only represent about 25% of the body's total lymphocyte with a majority of them residing in gut tissues [278]. We generated single cell suspensions from rectosigmoid biopsies and evaluated the expression of TIGIT and TIGIT ligands in the context of PD-1. We observed tissue specific differences during HIV infection in the expression of TIGIT and PD-1 in addition to their respective ligands PVR and PD-L1. Interestingly, TIGIT had previously been shown to interact with *Fusobacteria* Fap2 to inhibit immune clearance of colon adenocarcinoma [290]. We further evaluated the microbiota composition and observed a significant increase in the abundance of *Fusobacteria* compared to HIV-uninfected controls. Bivariate analysis revealed that the magnitude of peripheral CD8 T cell reinvigoration by TIGIT blockade was correlated with RMMC PD-L1 pDC expression and the *Fusobacteria* abundance. Our data indicates that RMMC tissue immune parameters and microbiota composition may predict which individuals will respond to TIGIT blockade therapy as part of the enhanced "shock and kill" eradication strategies.

In conclusion, the information gained from these studies provides additional insight into the mechanisms driving HIV-associated immune dysfunction. Efforts to understand CD8 T cell exhaustion in the clearance of HIV

128

infection remain paramount in the search for an HIV cure. In addition, this data provides the rationale for further investigation into the role that TIGIT plays in HIV immune dysfunction. It is our hope that a better understanding of this pathway will lead to the development of novel curative therapies.

FUTURE PERSPECTIVES

With data generated in this dissertation, we will be exploring the *in vitro* and *in vivo* killing of HIV infected cells with a NIH funded R21/33 (1R21AI122393-01 PI: Lishomwa Ndhlovu). In the R21 phase we propose to determine the ability of TIGIT and PD-L1 blockade to reinvigorate the antiviral efficacy *in vitro* and deplete or inactivate HIV/SIV latently activated cells by enhancing anti-HIV/SIV CD8 T cell effector functions. In the R33 phase we will test the ability of TIGIT and PD-L1 blockade to clear the latent reservoir during fully suppressive cART in the SIV-infected *Rhesus macaque* model of HIV/AIDS. These studies are the first steps towards a novel approach that may lead to a sustained or functional HIV cure.

In addition to these studies we aim to elucidate the role of T cell immunometabolism and T cell reinvigoration. T cells undergo dramatic metabolic changes to meet the energy demands of and effective antiviral responses [331]. Interestingly, engagement of PD-1 results in an altered T cell metabolic reprograming and the inhibition of glycolysis, glutaminolysis, and amino acid metabolism [332]. Understanding the bioenergetics needs of CD8 T cells during immune checkpoint blockade (ICB) might improve therapies targeting TIGIT and further explain their capacity to be reinvigorated.

Furthermore, epigenetic mechanisms such as DNA methylation regulate transcriptional expression profiles in immune cells that ultimately direct cellular differentiation and function. Recent studies have revealed that gene expression of negative checkpoint receptors PD-1 and CTLA-4 are controlled by epigenetic regulation [333, 334]. Epigenetic studies have revealed that exhausted T cells

harbor a unique epigenetic and chromatin landscape profile relative to functioning T cells [335]. Unfortunately, there is lack of knowledge about how second tier immune checkpoint receptors such as TIGIT are epigenetically regulated and sustained during HIV infection. While TIGIT is upregulated on T cells during HIV infection, little is known about the genome-wide epigenetic states of TIGIT+ and TIGIT- CD8 and CD4 T cells. Furthermore, the impact of epigenetic manipulation on the CD8 T cell reinvigoration by TIGIT blockade is poorly defined. In future directions, we seek to define genome-wide epigenetic and transcriptional profiles in TIGIT+ and TIGIT- CD8 T cells subsets in cART suppressed HIV participants to provide a roadmap for candidate sites of the genome regulating dysfunctional TIGIT+ T cells. We will use genome-wide DNA methylation profiling of TIGIT+ and TIGIT- CD8 T cells from HIV-infected individuals to define the DNA methylation landscape. These reference methylomes will reveal a distinct DNA methylation state of CD8 T cells that may be a target for epigenetic manipulation.

This dissertation has demonstrated a prominent role for ICB during chronic HIV infection. However, there is a need to better understand the mechanisms by which ICB offers benefits that are less toxic but retain optimal anti-tumor and anti-viral efficacy for all patients. In the future, we plan to use integrated cellular, transcriptional, and epigenetic profiling of HIV-specific CD8 T cells to provide a mechanistic insight into ICB in the setting of HIV infection.

REFERENCES

1.   Deeks, S.G., *HIV: Shock and kill.* Nature, 2012. **487**(7408): p. 439-40.
2.   Wherry, E.J., *T cell exhaustion.* Nat Immunol, 2011. **12**(6): p. 492-9.
3.   Korber, B., et al., *Timing the ancestor of the HIV-1 pandemic strains.* Science, 2000. **288**(5472): p. 1789-96.
4.   Hahn, B.H., et al., *AIDS as a zoonosis: scientific and public health implications.* Science, 2000. **287**(5453): p. 607-14.
5.   Worobey, M., et al., *1970s and 'Patient 0' HIV-1 genomes illuminate early HIV/AIDS history in North America.* Nature, 2016. **539**(7627): p. 98-101.
6.   Centers for Disease, C., *Pneumocystis pneumonia--Los Angeles.* MMWR Morb Mortal Wkly Rep, 1981. **30**(21): p. 250-2.
7.   Centers for Disease, C., *Kaposi's sarcoma and Pneumocystis pneumonia among homosexual men--New York City and California.* MMWR Morb Mortal Wkly Rep, 1981. **30**(25): p. 305-8.
8.   Barre-Sinoussi, F., et al., *Isolation of a T-lymphotropic retrovirus from a patient at risk for acquired immune deficiency syndrome (AIDS).* Science, 1983. **220**(4599): p. 868-71.
9.   Levy, J.A., et al., *Isolation of lymphocytopathic retroviruses from San Francisco patients with AIDS.* Science, 1984. **225**(4664): p. 840-2.
10.   Popovic, M., et al., *Detection, isolation, and continuous production of cytopathic retroviruses (HTLV-III) from patients with AIDS and pre-AIDS.* Science, 1984. **224**(4648): p. 497-500.
11.   UNAIDS, *AIDS by the numbers 2015.* http://www.unaids.org/en/resources/documents/2015/AIDS_by_the_numbers_2015., 2016
12.   Hladik, F. and M.J. McElrath, *Setting the stage: host invasion by HIV.* Nat Rev Immunol, 2008. **8**(6): p. 447-57.
13.   Baggaley, R.F., et al., *Risk of HIV-1 transmission for parenteral exposure and blood transfusion: a systematic review and meta-analysis.* AIDS, 2006. **20**(6): p. 805-12.
14.   Sperling, R.S., et al., *Maternal viral load, zidovudine treatment, and the risk of transmission of human immunodeficiency virus type 1 from mother to infant. Pediatric AIDS Clinical Trials Group Protocol 076 Study Group.* N Engl J Med, 1996. **335**(22): p. 1621-9.
15.   Boily, M.C., et al., *Heterosexual risk of HIV-1 infection per sexual act: systematic review and meta-analysis of observational studies.* Lancet Infect Dis, 2009. **9**(2): p. 118-29.
16.   Baggaley, R.F., R.G. White, and M.C. Boily, *HIV transmission risk through anal intercourse: systematic review, meta-analysis and implications for HIV prevention.* Int J Epidemiol, 2010. **39**(4): p. 1048-63.

17. Patel, P., et al., *Estimating per-act HIV transmission risk: a systematic review.* AIDS, 2014. **28**(10): p. 1509-19.

18. Nyamweya, S., et al., *Comparing HIV-1 and HIV-2 infection: Lessons for viral immunopathogenesis.* Rev Med Virol, 2013. **23**(4): p. 221-40.

19. Clavel, F., et al., *Isolation of a new human retrovirus from West African patients with AIDS.* Science, 1986. **233**(4761): p. 343-6.

20. Roberts, J.D., K. Bebenek, and T.A. Kunkel, *The accuracy of reverse transcriptase from HIV-1.* Science, 1988. **242**(4882): p. 1171-3.

21. Ho, D.D., et al., *Rapid turnover of plasma virions and CD4 lymphocytes in HIV-1 infection.* Nature, 1995. **373**(6510): p. 123-6.

22. Michael, N.L., *Host genetic influences on HIV-1 pathogenesis.* Curr Opin Immunol, 1999. **11**(4): p. 466-74.

23. Temin, H.M., *Retrovirus variation and reverse transcription: abnormal strand transfers result in retrovirus genetic variation.* Proc Natl Acad Sci U S A, 1993. **90**(15): p. 6900-3.

24. Plantier, J.C., et al., *A new human immunodeficiency virus derived from gorillas.* Nat Med, 2009. **15**(8): p. 871-2.

25. Sharp, P.M. and B.H. Hahn, *Origins of HIV and the AIDS pandemic.* Cold Spring Harb Perspect Med, 2011. **1**(1): p. a006841.

26. Yamaguchi, J., et al., *Identification of HIV type 1 group N infections in a husband and wife in Cameroon: viral genome sequences provide evidence for horizontal transmission.* AIDS Res Hum Retroviruses, 2006. **22**(1): p. 83-92.

27. Zouhair, S., et al., *Group o human immunodeficiency virus type 1 infection that escaped detection in two immmunoassays.* J Clin Microbiol, 2006. **44**(2): p. 662-5.

28. Buonaguro, L., M.L. Tornesello, and F.M. Buonaguro, *Human immunodeficiency virus type 1 subtype distribution in the worldwide epidemic: pathogenetic and therapeutic implications.* J Virol, 2007. **81**(19): p. 10209-19.

29. Korber, B., et al., *Evolutionary and immunological implications of contemporary HIV-1 variation.* Br Med Bull, 2001. **58**: p. 19-42.

30. Oyomopito, R.A., et al., *Risk group characteristics and viral transmission clusters in South-East Asian patients infected with human immunodeficiency virus-1 (HIV-1) circulating recombinant form (CRF) 01_AE and subtype B.* Kaohsiung J Med Sci, 2015. **31**(9): p. 445-53.

31. Barre-Sinoussi, F., *HIV as the cause of AIDS.* Lancet, 1996. **348**(9019): p. 31-5.

32. Freed, E.O., *HIV-1 gag proteins: diverse functions in the virus life cycle.* Virology, 1998. **251**(1): p. 1-15.

33. Ashorn, P., et al., *An inhibitor of the protease blocks maturation of human and simian immunodeficiency viruses and spread of infection.* Proc Natl Acad Sci U S A, 1990. **87**(19): p. 7472-6.

34. Hu, W.S. and S.H. Hughes, *HIV-1 reverse transcription.* Cold Spring Harb Perspect Med, 2012. **2**(10).

35. Bushman, F.D., T. Fujiwara, and R. Craigie, *Retroviral DNA integration directed by HIV integration protein in vitro.* Science, 1990. **249**(4976): p. 1555-8.
36. Ruben, S., et al., *Structural and functional characterization of human immunodeficiency virus tat protein.* J Virol, 1989. **63**(1): p. 1-8.
37. Zapp, M.L. and M.R. Green, *Sequence-specific RNA binding by the HIV-1 Rev protein.* Nature, 1989. **342**(6250): p. 714-6.
38. Kim, S.Y., et al., *Temporal aspects of DNA and RNA synthesis during human immunodeficiency virus infection: evidence for differential gene expression.* J Virol, 1989. **63**(9): p. 3708-13.
39. Garcia, J.V. and A.D. Miller, *Downregulation of cell surface CD4 by nef.* Res Virol, 1992. **143**(1): p. 52-5.
40. Bour, S. and K. Strebel, *The HIV-1 Vpu protein: a multifunctional enhancer of viral particle release.* Microbes Infect, 2003. **5**(11): p. 1029-39.
41. Heinzinger, N.K., et al., *The Vpr protein of human immunodeficiency virus type 1 influences nuclear localization of viral nucleic acids in nondividing host cells.* Proc Natl Acad Sci U S A, 1994. **91**(15): p. 7311-5.
42. Stopak, K., et al., *HIV-1 Vif blocks the antiviral activity of APOBEC3G by impairing both its translation and intracellular stability.* Mol Cell, 2003. **12**(3): p. 591-601.
43. Engelman, A. and P. Cherepanov, *The structural biology of HIV-1: mechanistic and therapeutic insights.* Nat Rev Microbiol, 2012. **10**(4): p. 279-90.
44. Campbell, E.M. and T.J. Hope, *HIV-1 capsid: the multifaceted key player in HIV-1 infection.* Nat Rev Microbiol, 2015. **13**(8): p. 471-83.
45. Fiorentini, S., et al., *Functions of the HIV-1 matrix protein p17.* New Microbiol, 2006. **29**(1): p. 1-10.
46. Chan, D.C., et al., *Core structure of gp41 from the HIV envelope glycoprotein.* Cell, 1997. **89**(2): p. 263-73.
47. Clapham, P.R. and A. McKnight, *HIV-1 receptors and cell tropism.* Br Med Bull, 2001. **58**: p. 43-59.
48. Berson, J.F., et al., *A seven-transmembrane domain receptor involved in fusion and entry of T-cell-tropic human immunodeficiency virus type 1 strains.* J Virol, 1996. **70**(9): p. 6288-95.
49. Arien, K.K., G. Vanham, and E.J. Arts, *Is HIV-1 evolving to a less virulent form in humans?* Nat Rev Microbiol, 2007. **5**(2): p. 141-51.
50. Bukrinsky, M.I., et al., *Active nuclear import of human immunodeficiency virus type 1 preintegration complexes.* Proc Natl Acad Sci U S A, 1992. **89**(14): p. 6580-4.
51. Craigie, R. and F.D. Bushman, *HIV DNA integration.* Cold Spring Harb Perspect Med, 2012. **2**(7): p. a006890.
52. Sodroski, J., et al., *Location of the trans-activating region on the genome of human T-cell lymphotropic virus type III.* Science, 1985. **229**(4708): p. 74-7.

53. Karn, J. and C.M. Stoltzfus, *Transcriptional and posttranscriptional regulation of HIV-1 gene expression.* Cold Spring Harb Perspect Med, 2012. **2**(2): p. a006916.

54. Sodroski, J., et al., *A second post-transcriptional trans-activator gene required for HTLV-III replication.* Nature, 1986. **321**(6068): p. 412-7.

55. Sundquist, W.I. and H.G. Krausslich, *HIV-1 assembly, budding, and maturation.* Cold Spring Harb Perspect Med, 2012. **2**(7): p. a006924.

56. Hill, M., G. Tachedjian, and J. Mak, *The packaging and maturation of the HIV-1 Pol proteins.* Curr HIV Res, 2005. **3**(1): p. 73-85.

57. Stewart, G.J., et al., *Transmission of human T-cell lymphotropic virus type III (HTLV-III) by artificial insemination by donor.* Lancet, 1985. **2**(8455): p. 581-5.

58. Cohen, M.S., et al., *Reduction of concentration of HIV-1 in semen after treatment of urethritis: implications for prevention of sexual transmission of HIV-1. AIDSCAP Malawi Research Group.* Lancet, 1997. **349**(9069): p. 1868-73.

59. Ghys, P.D., et al., *The associations between cervicovaginal HIV shedding, sexually transmitted diseases and immunosuppression in female sex workers in Abidjan, Cote d'Ivoire.* AIDS, 1997. **11**(12): p. F85-93.

60. Deeks, S.G., et al., *HIV infection.* Nat Rev Dis Primers, 2015. **1**: p. 15035.

61. Wu, L. and V.N. KewalRamani, *Dendritic-cell interactions with HIV: infection and viral dissemination.* Nat Rev Immunol, 2006. **6**(11): p. 859-68.

62. Zeng, M., et al., *Cumulative mechanisms of lymphoid tissue fibrosis and T cell depletion in HIV-1 and SIV infections.* J Clin Invest, 2011. **121**(3): p. 998-1008.

63. Perreau, M., et al., *Follicular helper T cells serve as the major CD4 T cell compartment for HIV-1 infection, replication, and production.* J Exp Med, 2013. **210**(1): p. 143-56.

64. Fox, R., et al., *Clinical manifestations of acute infection with human immunodeficiency virus in a cohort of gay men.* AIDS, 1987. **1**(1): p. 35-8.

65. O'Brien, S.J. and S.L. Hendrickson, *Host genomic influences on HIV/AIDS.* Genome Biol, 2013. **14**(1): p. 201.

66. Kelley, C.F., et al., *Incomplete peripheral CD4+ cell count restoration in HIV-infected patients receiving long-term antiretroviral treatment.* Clin Infect Dis, 2009. **48**(6): p. 787-94.

67. McMichael, A.J., et al., *The immune response during acute HIV-1 infection: clues for vaccine development.* Nat Rev Immunol, 2010. **10**(1): p. 11-23.

68. Fiebig, E.W., et al., *Dynamics of HIV viremia and antibody seroconversion in plasma donors: implications for diagnosis and staging of primary HIV infection.* AIDS, 2003. **17**(13): p. 1871-9.

69. Ananworanich, J., et al., *A novel acute HIV infection staging system based on 4th generation immunoassay.* Retrovirology, 2013. **10**: p. 56.

70. Moir, S. and A.S. Fauci, *B cells in HIV infection and disease.* Nat Rev Immunol, 2009. **9**(4): p. 235-45.

71.	Benito, J.M., M. Lopez, and V. Soriano, *The role of CD8+ T-cell response in HIV infection.* AIDS Rev, 2004. **6**(2): p. 79-88.

72.	Walker, C.M., et al., *CD8+ lymphocytes can control HIV infection in vitro by suppressing virus replication.* Science, 1986. **234**(4783): p. 1563-6.

73.	Brenchley, J.M., et al., *Microbial translocation is a cause of systemic immune activation in chronic HIV infection.* Nat Med, 2006. **12**(12): p. 1365-71.

74.	Bonyhadi, M.L., et al., *HIV induces thymus depletion in vivo.* Nature, 1993. **363**(6431): p. 728-32.

75.	Pantaleo, G. and A.S. Fauci, *Immunopathogenesis of HIV infection.* Annu Rev Microbiol, 1996. **50**: p. 825-54.

76.	Langford, S.E., J. Ananworanich, and D.A. Cooper, *Predictors of disease progression in HIV infection: a review.* AIDS Res Ther, 2007. **4**: p. 11.

77.	Migueles, S.A., et al., *HLA B*5701 is highly associated with restriction of virus replication in a subgroup of HIV-infected long term nonprogressors.* Proc Natl Acad Sci U S A, 2000. **97**(6): p. 2709-14.

78.	Walker, B.D., *Elite control of HIV Infection: implications for vaccines and treatment.* Top HIV Med, 2007. **15**(4): p. 134-6.

79.	Gazzola, L., et al., *The absence of CD4+ T cell count recovery despite receipt of virologically suppressive highly active antiretroviral therapy: clinical risk, immunological gaps, and therapeutic options.* Clin Infect Dis, 2009. **48**(3): p. 328-37.

80.	Prevention, C.f.D.C.a., *Laboratory testing for the diagnosis of HIV infection.* online http://dx.doi.org/10.15620/cdc.23447, 2016.

81.	Pilcher, C.D., et al., *Performance of rapid point-of-care and laboratory tests for acute and established HIV infection in San Francisco.* PLoS One, 2013. **8**(12): p. e80629.

82.	Moyer, V.A. and U.S.P.S.T. Force*, *Screening for HIV: U.S. Preventive Services Task Force Recommendation Statement.* Ann Intern Med, 2013. **159**(1): p. 51-60.

83.	Chahroudi, A., et al., *Natural SIV hosts: showing AIDS the door.* Science, 2012. **335**(6073): p. 1188-93.

84.	Letvin, N.L., et al., *Induction of AIDS-like disease in macaque monkeys with T-cell tropic retrovirus STLV-III.* Science, 1985. **230**(4721): p. 71-3.

85.	Kumar, N., A. Chahroudi, and G. Silvestri, *Animal models to achieve an HIV cure.* Curr Opin HIV AIDS, 2016. **11**(4): p. 432-41.

86.	Shytaj, I.L., et al., *A highly intensified ART regimen induces long-term viral suppression and restriction of the viral reservoir in a simian AIDS model.* PLoS Pathog, 2012. **8**(6): p. e1002774.

87.	Schnittman, S.M., et al., *Preferential infection of CD4+ memory T cells by human immunodeficiency virus type 1: evidence for a role in the selective T-cell functional defects observed in infected individuals.* Proc Natl Acad Sci U S A, 1990. **87**(16): p. 6058-62.

88.   Mehraj, V., et al., *Immune Suppression by Myeloid Cells in HIV Infection: New Targets for Immunotherapy.* Open AIDS J, 2014. **8**: p. 66-78.

89.   Giorgi, J.V., et al., *CD8+ lymphocyte activation at human immunodeficiency virus type 1 seroconversion: development of HLA-DR+ CD38- CD8+ cells is associated with subsequent stable CD4+ cell levels. The Multicenter AIDS Cohort Study Group.* J Infect Dis, 1994. **170**(4): p. 775-81.

90.   Giorgi, J.V., et al., *Shorter survival in advanced human immunodeficiency virus type 1 infection is more closely associated with T lymphocyte activation than with plasma virus burden or virus chemokine coreceptor usage.* J Infect Dis, 1999. **179**(4): p. 859-70.

91.   Sauce, D., et al., *HIV disease progression despite suppression of viral replication is associated with exhaustion of lymphopoiesis.* Blood, 2011. **117**(19): p. 5142-51.

92.   Hunt, P.W., et al., *Relationship between T cell activation and CD4+ T cell count in HIV-seropositive individuals with undetectable plasma HIV RNA levels in the absence of therapy.* J Infect Dis, 2008. **197**(1): p. 126-33.

93.   Rotger, M., et al., *Comparative transcriptomics of extreme phenotypes of human HIV-1 infection and SIV infection in sooty mangabey and rhesus macaque.* J Clin Invest, 2011. **121**(6): p. 2391-400.

94.   Veazey, R.S., et al., *Gastrointestinal tract as a major site of CD4+ T cell depletion and viral replication in SIV infection.* Science, 1998. **280**(5362): p. 427-31.

95.   Brenchley, J.M., et al., *Differential Th17 CD4 T-cell depletion in pathogenic and nonpathogenic lentiviral infections.* Blood, 2008. **112**(7): p. 2826-35.

96.   Brenchley, J.M. and D.C. Douek, *HIV infection and the gastrointestinal immune system.* Mucosal Immunol, 2008. **1**(1): p. 23-30.

97.   Allen, C.D., T. Okada, and J.G. Cyster, *Germinal-center organization and cellular dynamics.* Immunity, 2007. **27**(2): p. 190-202.

98.   Zeng, M., A.T. Haase, and T.W. Schacker, *Lymphoid tissue structure and HIV-1 infection: life or death for T cells.* Trends Immunol, 2012. **33**(6): p. 306-14.

99.   Brenchley, J.M., et al., *CD4+ T cell depletion during all stages of HIV disease occurs predominantly in the gastrointestinal tract.* J Exp Med, 2004. **200**(6): p. 749-59.

100.   Embretson, J., et al., *Massive covert infection of helper T lymphocytes and macrophages by HIV during the incubation period of AIDS.* Nature, 1993. **362**(6418): p. 359-62.

101.   Pantaleo, G., et al., *HIV infection is active and progressive in lymphoid tissue during the clinically latent stage of disease.* Nature, 1993. **362**(6418): p. 355-8.

102.   Pantaleo, G., et al., *Lymphoid organs function as major reservoirs for human immunodeficiency virus.* Proc Natl Acad Sci U S A, 1991. **88**(21): p. 9838-42.

103.   Hong, J.J., et al., *Spatial alterations between CD4(+) T follicular helper, B, and CD8(+) T cells during simian immunodeficiency virus infection: T/B cell*

homeostasis, activation, and potential mechanism for viral escape. J Immunol, 2012. **188**(7): p. 3247-56.

104.	Brenchley, J.M., et al., *Differential infection patterns of CD4+ T cells and lymphoid tissue viral burden distinguish progressive and nonprogressive lentiviral infections.* Blood, 2012. **120**(20): p. 4172-81.

105.	Estes, J.D., et al., *Simian immunodeficiency virus-induced lymphatic tissue fibrosis is mediated by transforming growth factor beta 1-positive regulatory T cells and begins in early infection.* J Infect Dis, 2007. **195**(4): p. 551-61.

106.	Schacker, T.W., et al., *Collagen deposition in HIV-1 infected lymphatic tissues and T cell homeostasis.* J Clin Invest, 2002. **110**(8): p. 1133-9.

107.	Adolescents, P.o.A.G.f.A.a., *Guidelines for the use of antiretroviral agents in HIV-1-infected adults and adolescents.* Department of Health and Human Services. Available at http://www.aidsinfo.nih.gov/ContentFiles/AdultandAdolescentGL.pdf., 2016.

108.	Grinsztejn, B., et al., *Effects of early versus delayed initiation of antiretroviral treatment on clinical outcomes of HIV-1 infection: results from the phase 3 HPTN 052 randomised controlled trial.* Lancet Infect Dis, 2014. **14**(4): p. 281-90.

109.	Group, I.S.S., et al., *Initiation of Antiretroviral Therapy in Early Asymptomatic HIV Infection.* N Engl J Med, 2015. **373**(9): p. 795-807.

110.	Schneider, J., et al., *Better physician-patient relationships are associated with higher reported adherence to antiretroviral therapy in patients with HIV infection.* J Gen Intern Med, 2004. **19**(11): p. 1096-103.

111.	Ssemwanga, D., et al., *Update on HIV-1 acquired and transmitted drug resistance in Africa.* AIDS Rev, 2015. **17**(1): p. 3-20.

112.	Oette, M., et al., *Primary HIV drug resistance and efficacy of first-line antiretroviral therapy guided by resistance testing.* J Acquir Immune Defic Syndr, 2006. **41**(5): p. 573-81.

113.	Michaud, V., et al., *The dual role of pharmacogenetics in HIV treatment: mutations and polymorphisms regulating antiretroviral drug resistance and disposition.* Pharmacol Rev, 2012. **64**(3): p. 803-33.

114.	Ullrich, R., et al., *Small intestinal structure and function in patients infected with human immunodeficiency virus (HIV): evidence for HIV-induced enteropathy.* Ann Intern Med, 1989. **111**(1): p. 15-21.

115.	Siliciano, R.F. and W.C. Greene, *HIV latency.* Cold Spring Harb Perspect Med, 2011. **1**(1): p. a007096.

116.	Katlama, C., et al., *Barriers to a cure for HIV: new ways to target and eradicate HIV-1 reservoirs.* Lancet, 2013. **381**(9883): p. 2109-17.

117.	Phillips, A.N., J. Neaton, and J.D. Lundgren, *The role of HIV in serious diseases other than AIDS.* AIDS, 2008. **22**(18): p. 2409-18.

118.	Lohse, N., et al., *Survival of persons with and without HIV infection in Denmark, 1995-2005.* Ann Intern Med, 2007. **146**(2): p. 87-95.

119.	UNAIDS, *On the Fast-Track to end AIDS.* UNAIDS 2016-2021 Strategy, 2016.

120. Baggaley, R., et al., *The Strategic Use of Antiretrovirals to Prevent HIV Infection: A Converging Agenda.* Clin Infect Dis, 2015. **60 Suppl 3**: p. S159-60.

121. Hammer, S.M., et al., *Efficacy trial of a DNA/rAd5 HIV-1 preventive vaccine.* N Engl J Med, 2013. **369**(22): p. 2083-92.

122. Buchbinder, S.P., et al., *Efficacy assessment of a cell-mediated immunity HIV-1 vaccine (the Step Study): a double-blind, randomised, placebo-controlled, test-of-concept trial.* Lancet, 2008. **372**(9653): p. 1881-93.

123. Rerks-Ngarm, S., et al., *Vaccination with ALVAC and AIDSVAX to prevent HIV-1 infection in Thailand.* N Engl J Med, 2009. **361**(23): p. 2209-20.

124. Corey, L., et al., *Immune correlates of vaccine protection against HIV-1 acquisition.* Sci Transl Med, 2015. **7**(310): p. 310rv7.

125. Mascola, J.R. and B.F. Haynes, *HIV-1 neutralizing antibodies: understanding nature's pathways.* Immunol Rev, 2013. **254**(1): p. 225-44.

126. Burton, D.R. and J.R. Mascola, *Antibody responses to envelope glycoproteins in HIV-1 infection.* Nat Immunol, 2015. **16**(6): p. 571-6.

127. Barouch, D.H., et al., *Therapeutic efficacy of potent neutralizing HIV-1-specific monoclonal antibodies in SHIV-infected rhesus monkeys.* Nature, 2013. **503**(7475): p. 224-8.

128. Caskey, M., et al., *Viraemia suppressed in HIV-1-infected humans by broadly neutralizing antibody 3BNC117.* Nature, 2015. **522**(7557): p. 487-91.

129. Bar, K.J., et al., *Effect of HIV Antibody VRC01 on Viral Rebound after Treatment Interruption.* N Engl J Med, 2016. **375**(21): p. 2037-2050.

130. Sievers, S.A., et al., *Antibody engineering for increased potency, breadth and half-life.* Curr Opin HIV AIDS, 2015. **10**(3): p. 151-9.

131. Ko, S.Y., et al., *Enhanced neonatal Fc receptor function improves protection against primate SHIV infection.* Nature, 2014. **514**(7524): p. 642-5.

132. Hansen, S.G., et al., *Profound early control of highly pathogenic SIV by an effector memory T-cell vaccine.* Nature, 2011. **473**(7348): p. 523-7.

133. Hansen, S.G., et al., *Immune clearance of highly pathogenic SIV infection.* Nature, 2013. **502**(7469): p. 100-4.

134. Hansen, S.G., et al., *Broadly targeted CD8(+) T cell responses restricted by major histocompatibility complex E.* Science, 2016. **351**(6274): p. 714-20.

135. Chomont, N., et al., *HIV reservoir size and persistence are driven by T cell survival and homeostatic proliferation.* Nat Med, 2009. **15**(8): p. 893-900.

136. Schrager, L.K. and M.P. D'Souza, *Cellular and anatomical reservoirs of HIV-1 in patients receiving potent antiretroviral combination therapy.* JAMA, 1998. **280**(1): p. 67-71.

137. Whitney, J.B., et al., *Rapid seeding of the viral reservoir prior to SIV viraemia in rhesus monkeys.* Nature, 2014. **512**(7512): p. 74-7.

138. Chun, T.W., et al., *Presence of an inducible HIV-1 latent reservoir during highly active antiretroviral therapy.* Proc Natl Acad Sci U S A, 1997. **94**(24): p. 13193-7.

139. Archin, N.M., et al., *Eradicating HIV-1 infection: seeking to clear a persistent pathogen.* Nat Rev Microbiol, 2014. **12**(11): p. 750-64.
140. Siliciano, J.D., et al., *Long-term follow-up studies confirm the stability of the latent reservoir for HIV-1 in resting CD4+ T cells.* Nat Med, 2003. **9**(6): p. 727-8.
141. Descours, B., et al., *CD32a is a marker of a CD4 T-cell HIV reservoir harbouring replication-competent proviruses.* Nature, 2017. **543**(7646): p. 564-567.
142. Yukl, S.A., et al., *The distribution of HIV DNA and RNA in cell subsets differs in gut and blood of HIV-positive patients on ART: implications for viral persistence.* J Infect Dis, 2013. **208**(8): p. 1212-20.
143. Fletcher, C.V., et al., *Persistent HIV-1 replication is associated with lower antiretroviral drug concentrations in lymphatic tissues.* Proc Natl Acad Sci U S A, 2014. **111**(6): p. 2307-12.
144. Sender, R., S. Fuchs, and R. Milo, *Revised Estimates for the Number of Human and Bacteria Cells in the Body.* PLoS Biol, 2016. **14**(8): p. e1002533.
145. McAleer, J.P. and J.K. Kolls, *Maintaining poise: commensal microbiota calibrate interferon responses.* Immunity, 2012. **37**(1): p. 10-2.
146. Hooper, L.V., D.R. Littman, and A.J. Macpherson, *Interactions between the microbiota and the immune system.* Science, 2012. **336**(6086): p. 1268-73.
147. Asher, I. and N. Pearce, *Global burden of asthma among children.* Int J Tuberc Lung Dis, 2014. **18**(11): p. 1269-78.
148. Ananthakrishnan, A.N., *Epidemiology and risk factors for IBD.* Nat Rev Gastroenterol Hepatol, 2015. **12**(4): p. 205-17.
149. Cammarota, G., G. Ianiro, and A. Gasbarrini, *Fecal microbiota transplantation for the treatment of Clostridium difficile infection: a systematic review.* J Clin Gastroenterol, 2014. **48**(8): p. 693-702.
150. Torow, N. and M.W. Hornef, *The Neonatal Window of Opportunity: Setting the Stage for Life-Long Host-Microbial Interaction and Immune Homeostasis.* J Immunol, 2017. **198**(2): p. 557-563.
151. Macal, M., et al., *Effective CD4+ T-cell restoration in gut-associated lymphoid tissue of HIV-infected patients is associated with enhanced Th17 cells and polyfunctional HIV-specific T-cell responses.* Mucosal Immunol, 2008. **1**(6): p. 475-88.
152. Guadalupe, M., et al., *Severe CD4+ T-cell depletion in gut lymphoid tissue during primary human immunodeficiency virus type 1 infection and substantial delay in restoration following highly active antiretroviral therapy.* J Virol, 2003. **77**(21): p. 11708-17.
153. Dillon, S.M., et al., *An altered intestinal mucosal microbiome in HIV-1 infection is associated with mucosal and systemic immune activation and endotoxemia.* Mucosal Immunol, 2014. **7**(4): p. 983-94.
154. Vujkovic-Cvijin, I., et al., *Dysbiosis of the gut microbiota is associated with HIV disease progression and tryptophan catabolism.* Sci Transl Med, 2013. **5**(193): p. 193ra91.

155. Charles A Janeway, J., Paul Travers, Mark Walport, and Mark J Shlomchik, *Immunobiology.* 2001. **5th edition**.

156. Zhang, N. and M.J. Bevan, *CD8(+) T cells: foot soldiers of the immune system.* Immunity, 2011. **35**(2): p. 161-8.

157. Paliard, X., et al., *Simultaneous production of IL-2, IL-4, and IFN-gamma by activated human CD4+ and CD8+ T cell clones.* J Immunol, 1988. **141**(3): p. 849-55.

158. Voskoboinik, I., J.C. Whisstock, and J.A. Trapani, *Perforin and granzymes: function, dysfunction and human pathology.* Nat Rev Immunol, 2015. **15**(6): p. 388-400.

159. Waring, P. and A. Mullbacher, *Cell death induced by the Fas/Fas ligand pathway and its role in pathology.* Immunol Cell Biol, 1999. **77**(4): p. 312-7.

160. Demkowicz, W.E., Jr., et al., *Human cytotoxic T-cell memory: long-lived responses to vaccinia virus.* J Virol, 1996. **70**(4): p. 2627-31.

161. Sacha, J.B., et al., *Gag-specific CD8+ T lymphocytes recognize infected cells before AIDS-virus integration and viral protein expression.* J Immunol, 2007. **178**(5): p. 2746-54.

162. Koup, R.A., et al., *Temporal association of cellular immune responses with the initial control of viremia in primary human immunodeficiency virus type 1 syndrome.* J Virol, 1994. **68**(7): p. 4650-5.

163. Borrow, P., et al., *Antiviral pressure exerted by HIV-1-specific cytotoxic T lymphocytes (CTLs) during primary infection demonstrated by rapid selection of CTL escape virus.* Nat Med, 1997. **3**(2): p. 205-11.

164. Altfeld, M., et al., *HLA Alleles Associated with Delayed Progression to AIDS Contribute Strongly to the Initial CD8(+) T Cell Response against HIV-1.* PLoS Med, 2006. **3**(10): p. e403.

165. Altfeld, M., et al., *Influence of HLA-B57 on clinical presentation and viral control during acute HIV-1 infection.* AIDS, 2003. **17**(18): p. 2581-91.

166. Evans, D.T., et al., *Rapid and slow progressors differ by a single MHC class I haplotype in a family of MHC-defined rhesus macaques infected with SIV.* Immunol Lett, 1999. **66**(1-3): p. 53-9.

167. Loffredo, J.T., et al., *Mamu-B*08-positive macaques control simian immunodeficiency virus replication.* J Virol, 2007. **81**(16): p. 8827-32.

168. Peris-Pertusa, A., et al., *Evolution of the functional profile of HIV-specific CD8+ T cells in patients with different progression of HIV infection over 4 years.* J Acquir Immune Defic Syndr, 2010. **55**(1): p. 29-38.

169. Betts, M.R., et al., *HIV nonprogressors preferentially maintain highly functional HIV-specific CD8+ T cells.* Blood, 2006. **107**(12): p. 4781-9.

170. Cartwright, E.K., et al., *CD8(+) Lymphocytes Are Required for Maintaining Viral Suppression in SIV-Infected Macaques Treated with Short-Term Antiretroviral Therapy.* Immunity, 2016. **45**(3): p. 656-68.

171. Virgin, H.W., E.J. Wherry, and R. Ahmed, *Redefining chronic viral infection.* Cell, 2009. **138**(1): p. 30-50.

172. Zajac, A.J., et al., *Viral immune evasion due to persistence of activated T cells without effector function.* J Exp Med, 1998. **188**(12): p. 2205-13.

173. Wherry, E.J., et al., *Viral persistence alters CD8 T-cell immunodominance and tissue distribution and results in distinct stages of functional impairment.* J Virol, 2003. **77**(8): p. 4911-27.

174. Freeman, G.J., et al., *Reinvigorating exhausted HIV-specific T cells via PD-1-PD-1 ligand blockade.* J Exp Med, 2006. **203**(10): p. 2223-7.

175. Crawford, A. and E.J. Wherry, *The diversity of costimulatory and inhibitory receptor pathways and the regulation of antiviral T cell responses.* Curr Opin Immunol, 2009. **21**(2): p. 179-86.

176. Trautmann, L., et al., *Upregulation of PD-1 expression on HIV-specific CD8+ T cells leads to reversible immune dysfunction.* Nat Med, 2006. **12**(10): p. 1198-202.

177. Petrovas, C., et al., *SIV-specific CD8+ T cells express high levels of PD1 and cytokines but have impaired proliferative capacity in acute and chronic SIVmac251 infection.* Blood, 2007. **110**(3): p. 928-36.

178. Jones, R.B., et al., *Tim-3 expression defines a novel population of dysfunctional T cells with highly elevated frequencies in progressive HIV-1 infection.* J Exp Med, 2008. **205**(12): p. 2763-79.

179. Blackburn, S.D., et al., *Coregulation of CD8+ T cell exhaustion by multiple inhibitory receptors during chronic viral infection.* Nat Immunol, 2009. **10**(1): p. 29-37.

180. Day, C.L., et al., *PD-1 expression on HIV-specific T cells is associated with T-cell exhaustion and disease progression.* Nature, 2006. **443**(7109): p. 350-4.

181. Kaufmann, D.E. and B.D. Walker, *PD-1 and CTLA-4 inhibitory cosignaling pathways in HIV infection and the potential for therapeutic intervention.* J Immunol, 2009. **182**(10): p. 5891-7.

182. Velu, V., et al., *Enhancing SIV-specific immunity in vivo by PD-1 blockade.* Nature, 2009. **458**(7235): p. 206-10.

183. Amancha, P.K., et al., *In vivo blockade of the programmed cell death-1 pathway using soluble recombinant PD-1-Fc enhances CD4+ and CD8+ T cell responses but has limited clinical benefit.* J Immunol, 2013. **191**(12): p. 6060-70.

184. Buchbinder, E.I. and A. Desai, *CTLA-4 and PD-1 Pathways: Similarities, Differences, and Implications of Their Inhibition.* Am J Clin Oncol, 2016. **39**(1): p. 98-106.

185. Allers, K., et al., *Evidence for the cure of HIV infection by CCR5Delta32/Delta32 stem cell transplantation.* Blood, 2011. **117**(10): p. 2791-9.

186. Samson, M., et al., *Resistance to HIV-1 infection in caucasian individuals bearing mutant alleles of the CCR-5 chemokine receptor gene.* Nature, 1996. **382**(6593): p. 722-5.

187. Hutter, G., et al., *Long-term control of HIV by CCR5 Delta32/Delta32 stem-cell transplantation.* N Engl J Med, 2009. **360**(7): p. 692-8.

188.   Henrich, T.J., et al., *Antiretroviral-free HIV-1 remission and viral rebound after allogeneic stem cell transplantation: report of 2 cases.* Ann Intern Med, 2014. **161**(5): p. 319-27.

189.   Manjunath, N., et al., *Newer gene editing technologies toward HIV gene therapy.* Viruses, 2013. **5**(11): p. 2748-66.

190.   Tebas, P., et al., *Gene editing of CCR5 in autologous CD4 T cells of persons infected with HIV.* N Engl J Med, 2014. **370**(10): p. 901-10.

191.   Hou, P., et al., *Genome editing of CXCR4 by CRISPR/cas9 confers cells resistant to HIV-1 infection.* Sci Rep, 2015. **5**: p. 15577.

192.   Kaminski, R., et al., *Elimination of HIV-1 Genomes from Human T-lymphoid Cells by CRISPR/Cas9 Gene Editing.* Sci Rep, 2016. **6**: p. 22555.

193.   Hale, M., et al., *Engineering HIV-Resistant, Anti-HIV Chimeric Antigen Receptor T Cells.* Mol Ther, 2017. **25**(3): p. 570-579.

194.   Darcis, G., B. Van Driessche, and C. Van Lint, *HIV Latency: Should We Shock or Lock?* Trends Immunol, 2017. **38**(3): p. 217-228.

195.   Mousseau, G., et al., *An analog of the natural steroidal alkaloid cortistatin A potently suppresses Tat-dependent HIV transcription.* Cell Host Microbe, 2012. **12**(1): p. 97-108.

196.   Boden, D., et al., *Enhanced gene silencing of HIV-1 specific siRNA using microRNA designed hairpins.* Nucleic Acids Res, 2004. **32**(3): p. 1154-8.

197.   Tsai, A., et al., *Toll-Like Receptor 7 Agonist GS-9620 Induces HIV Expression and HIV-Specific Immunity in Cells from HIV-Infected Individuals on Suppressive Antiretroviral Therapy.* J Virol, 2017. **91**(8).

198.   Li, P., et al., *Stimulating the RIG-I pathway to kill cells in the latent HIV reservoir following viral reactivation.* Nat Med, 2016. **22**(7): p. 807-11.

199.   Van Lint, C., S. Bouchat, and A. Marcello, *HIV-1 transcription and latency: an update.* Retrovirology, 2013. **10**: p. 67.

200.   Wightman, F., et al., *Effect of ipilimumab on the HIV reservoir in an HIV-infected individual with metastatic melanoma.* AIDS, 2015. **29**(4): p. 504-6.

201.   Spivak, A.M., et al., *A pilot study assessing the safety and latency-reversing activity of disulfiram in HIV-1-infected adults on antiretroviral therapy.* Clin Infect Dis, 2014. **58**(6): p. 883-90.

202.   Sogaard, O.S., et al., *The Depsipeptide Romidepsin Reverses HIV-1 Latency In Vivo.* PLoS Pathog, 2015. **11**(9): p. e1005142.

203.   Rasmussen, T.A., et al., *Panobinostat, a histone deacetylase inhibitor, for latent-virus reactivation in HIV-infected patients on suppressive antiretroviral therapy: a phase 1/2, single group, clinical trial.* Lancet HIV, 2014. **1**(1): p. e13-21.

204.   Archin, N.M., et al., *HIV-1 expression within resting CD4+ T cells after multiple doses of vorinostat.* J Infect Dis, 2014. **210**(5): p. 728-35.

205.   Elliott, J.H., et al., *Activation of HIV transcription with short-course vorinostat in HIV-infected patients on suppressive antiretroviral therapy.* PLoS Pathog, 2014. **10**(10): p. e1004473.

206. Archin, N.M., et al., *Administration of vorinostat disrupts HIV-1 latency in patients on antiretroviral therapy.* Nature, 2012. **487**(7408): p. 482-5.

207. Dyavar Shetty, R., et al., *PD-1 blockade during chronic SIV infection reduces hyperimmune activation and microbial translocation in rhesus macaques.* J Clin Invest, 2012. **122**(5): p. 1712-6.

208. Porichis, F. and D.E. Kaufmann, *Role of PD-1 in HIV pathogenesis and as target for therapy.* Curr HIV/AIDS Rep, 2012. **9**(1): p. 81-90.

209. Vali, B., et al., *HCV-specific T cells in HCV/HIV co-infection show elevated frequencies of dual Tim-3/PD-1 expression that correlate with liver disease progression.* Eur J Immunol, 2010. **40**(9): p. 2493-505.

210. Vigano, S., et al., *CD160-associated CD8 T-cell functional impairment is independent of PD-1 expression.* PLoS Pathog, 2014. **10**(9): p. e1004380.

211. Tian, X., et al., *The Upregulation of LAG-3 on T Cells Defines a Subpopulation with Functional Exhaustion and Correlates with Disease Progression in HIV-Infected Subjects.* J Immunol, 2015. **194**(8): p. 3873-82.

212. Gardiner, D., et al., *A randomized, double-blind, placebo-controlled assessment of BMS-936558, a fully human monoclonal antibody to programmed death-1 (PD-1), in patients with chronic hepatitis C virus infection.* PLoS One, 2013. **8**(5): p. e63818.

213. Yadav, M., et al., *Predicting immunogenic tumour mutations by combining mass spectrometry and exome sequencing.* Nature, 2014. **515**(7528): p. 572-6.

214. Powles, T., et al., *MPDL3280A (anti-PD-L1) treatment leads to clinical activity in metastatic bladder cancer.* Nature, 2014. **515**(7528): p. 558-62.

215. Hamid, O., et al., *Safety and tumor responses with lambrolizumab (anti-PD-1) in melanoma.* N Engl J Med, 2013. **369**(2): p. 134-44.

216. Chen, D.S. and I. Mellman, *Oncology meets immunology: the cancer-immunity cycle.* Immunity, 2013. **39**(1): p. 1-10.

217. Johnston, R.J., et al., *The immunoreceptor TIGIT regulates antitumor and antiviral CD8(+) T cell effector function.* Cancer Cell, 2014. **26**(6): p. 923-37.

218. Chauvin, J.M., et al., *TIGIT and PD-1 impair tumor antigen-specific CD8+ T cells in melanoma patients.* J Clin Invest, 2015.

219. Yamamoto, T., et al., *Surface expression patterns of negative regulatory molecules identify determinants of virus-specific CD8+ T-cell exhaustion in HIV infection.* Blood, 2011. **117**(18): p. 4805-15.

220. Duraiswamy, J., et al., *Dual blockade of PD-1 and CTLA-4 combined with tumor vaccine effectively restores T-cell rejection function in tumors.* Cancer Res, 2013. **73**(12): p. 3591-603.

221. Yu, X., et al., *The surface protein TIGIT suppresses T cell activation by promoting the generation of mature immunoregulatory dendritic cells.* Nat Immunol, 2009. **10**(1): p. 48-57.

222. Stengel, K.F., et al., *Structure of TIGIT immunoreceptor bound to poliovirus receptor reveals a cell-cell adhesion and signaling mechanism that requires cis-*

trans receptor clustering. Proc Natl Acad Sci U S A, 2012. **109**(14): p. 5399-404.

223. Joller, N., et al., *Cutting edge: TIGIT has T cell-intrinsic inhibitory functions.* J Immunol, 2011. **186**(3): p. 1338-42.

224. Stanietsky, N., et al., *The interaction of TIGIT with PVR and PVRL2 inhibits human NK cell cytotoxicity.* Proc Natl Acad Sci U S A, 2009. **106**(42): p. 17858-63.

225. Boles, K.S., et al., *A novel molecular interaction for the adhesion of follicular CD4 T cells to follicular DC.* Eur J Immunol, 2009. **39**(3): p. 695-703.

226. Martinet, L. and M.J. Smyth, *Balancing natural killer cell activation through paired receptors.* Nat Rev Immunol, 2015. **15**(4): p. 243-54.

227. Foks, A.C., et al., *Agonistic anti-TIGIT treatment inhibits T cell responses in LDLr deficient mice without affecting atherosclerotic lesion development.* PLoS One, 2013. **8**(12): p. e83134.

228. Joller, N., et al., *Treg cells expressing the coinhibitory molecule TIGIT selectively inhibit proinflammatory Th1 and Th17 cell responses.* Immunity, 2014. **40**(4): p. 569-81.

229. Lozano, E., et al., *The TIGIT/CD226 axis regulates human T cell function.* J Immunol, 2012. **188**(8): p. 3869-75.

230. Chauvin, J.M., et al., *TIGIT and PD-1 impair tumor antigen-specific CD8(+) T cells in melanoma patients.* J Clin Invest, 2015. **125**(5): p. 2046-58.

231. Appay, V., et al., *Memory CD8+ T cells vary in differentiation phenotype in different persistent virus infections.* Nat Med, 2002. **8**(4): p. 379-85.

232. Papagno, L., et al., *Immune activation and CD8+ T-cell differentiation towards senescence in HIV-1 infection.* PLoS Biol, 2004. **2**(2): p. E20.

233. Barbour, J.D., et al., *High CD8+ T cell activation marks a less differentiated HIV-1 specific CD8+ T cell response that is not altered by suppression of viral replication.* PLoS One, 2009. **4**(2): p. e4408.

234. Mujib, S., et al., *Antigen-independent induction of Tim-3 expression on human T cells by the common gamma-chain cytokines IL-2, IL-7, IL-15, and IL-21 is associated with proliferation and is dependent on the phosphoinositide 3-kinase pathway.* J Immunol, 2012. **188**(8): p. 3745-56.

235. Sun, Y., et al., *Dysfunction of simian immunodeficiency virus/simian human immunodeficiency virus-induced IL-2 expression by central memory CD4+ T lymphocytes.* J Immunol, 2005. **174**(8): p. 4753-60.

236. Younes, S.A., et al., *HIV-1 viremia prevents the establishment of interleukin 2-producing HIV-specific memory CD4+ T cells endowed with proliferative capacity.* J Exp Med, 2003. **198**(12): p. 1909-22.

237. Fujita, T., et al., *Expansion of dysfunctional Tim-3-expressing effector memory CD8+ T cells during simian immunodeficiency virus infection in rhesus macaques.* J Immunol, 2014. **193**(11): p. 5576-83.

238. Hosking, M.P., et al., *CD8+ memory T cells appear exhausted within hours of acute virus infection.* J Immunol, 2013. **191**(8): p. 4211-22.

239. Rekik, R., et al., *PD-1 induction through TCR activation is partially regulated by endogenous TGF-beta.* Cell Mol Immunol, 2014.

240. Kinter, A.L., et al., *The common gamma-chain cytokines IL-2, IL-7, IL-15, and IL-21 induce the expression of programmed death-1 and its ligands.* J Immunol, 2008. **181**(10): p. 6738-46.

241. Lambotte, O., et al., *HIV controllers: a homogeneous group of HIV-1-infected patients with spontaneous control of viral replication.* Clin Infect Dis, 2005. **41**(7): p. 1053-6.

242. Krishnan, S., et al., *Evidence for innate immune system activation in HIV type 1-infected elite controllers.* J Infect Dis, 2014. **209**(6): p. 931-9.

243. Okulicz, J.F. and O. Lambotte, *Epidemiology and clinical characteristics of elite controllers.* Curr Opin HIV AIDS, 2011. **6**(3): p. 163-8.

244. Lopez, M., et al., *Elite controllers display higher activation on central memory CD8 T cells than HIV patients successfully on HAART.* AIDS Res Hum Retroviruses, 2011. **27**(2): p. 157-65.

245. Pereyra, F., et al., *Persistent low-level viremia in HIV-1 elite controllers and relationship to immunologic parameters.* J Infect Dis, 2009. **200**(6): p. 984-90.

246. Hatano, H., et al., *Evidence for persistent low-level viremia in individuals who control human immunodeficiency virus in the absence of antiretroviral therapy.* J Virol, 2009. **83**(1): p. 329-35.

247. Crowell, T.A., et al., *Hospitalization Rates and Reasons among HIV Elite Controllers and Persons With Medically Controlled HIV Infection.* J Infect Dis, 2014.

248. Topalian, S.L., et al., *Safety, activity, and immune correlates of anti-PD-1 antibody in cancer.* N Engl J Med, 2012. **366**(26): p. 2443-54.

249. Pasternak, A.O., V.V. Lukashov, and B. Berkhout, *Cell-associated HIV RNA: a dynamic biomarker of viral persistence.* Retrovirology, 2013. **10**: p. 41.

250. Wei, D.G., et al., *Histone deacetylase inhibitor romidepsin induces HIV expression in CD4 T cells from patients on suppressive antiretroviral therapy at concentrations achieved by clinical dosing.* PLoS Pathog, 2014. **10**(4): p. e1004071.

251. Rasmussen, T.A., et al., *Comparison of HDAC inhibitors in clinical development: effect on HIV production in latently infected cells and T-cell activation.* Hum Vaccin Immunother, 2013. **9**(5): p. 993-1001.

252. Shan, L., et al., *Stimulation of HIV-1-specific cytolytic T lymphocytes facilitates elimination of latent viral reservoir after virus reactivation.* Immunity, 2012. **36**(3): p. 491-501.

253. Deng, K., et al., *Broad CTL response is required to clear latent HIV-1 due to dominance of escape mutations.* Nature, 2015. **517**(7534): p. 381-5.

254. Clayton, K.L., et al., *Soluble T Cell Immunoglobulin Mucin Domain 3 Is Shed from CD8+ T Cells by the Sheddase ADAM10, Is Increased in Plasma during Untreated HIV Infection, and Correlates with HIV Disease Progression.* J Virol, 2015. **89**(7): p. 3723-36.

255. Watters, M.R., et al., *Symptomatic distal sensory polyneuropathy in HIV after age 50.* Neurology, 2004. **62**(8): p. 1378-83.

256. Kumar, A.M., et al., *Human immunodeficiency virus type 1 RNA Levels in different regions of human brain: quantification using real-time reverse transcriptase-polymerase chain reaction.* J Neurovirol, 2007. **13**(3): p. 210-24.

257. Lonberg, N., et al., *Antigen-specific human antibodies from mice comprising four distinct genetic modifications.* Nature, 1994. **368**(6474): p. 856-9.

258. Fishwild, D.M., et al., *High-avidity human IgG kappa monoclonal antibodies from a novel strain of minilocus transgenic mice.* Nat Biotechnol, 1996. **14**(7): p. 845-51.

259. Gross, J.A., et al., *TACI-Ig neutralizes molecules critical for B cell development and autoimmune disease. impaired B cell maturation in mice lacking BLyS.* Immunity, 2001. **15**(2): p. 289-302.

260. Mothe, B.R., et al., *Dominance of CD8 responses specific for epitopes bound by a single major histocompatibility complex class I molecule during the acute phase of viral infection.* J Virol, 2002. **76**(2): p. 875-84.

261. Vogel, T.U., et al., *Escape in one of two cytotoxic T-lymphocyte epitopes bound by a high-frequency major histocompatibility complex class I molecule, Mamu-A*02: a paradigm for virus evolution and persistence?* J Virol, 2002. **76**(22): p. 11623-36.

262. Chew, G.M., et al., *TIGIT Marks Exhausted T Cells, Correlates with Disease Progression, and Serves as a Target for Immune Restoration in HIV and SIV Infection.* PLoS Pathog, 2016. **12**(1): p. e1005349.

263. Bangham, C.R., *CTL quality and the control of human retroviral infections.* Eur J Immunol, 2009. **39**(7): p. 1700-12.

264. Koup, R.A., *Virus escape from CTL recognition.* J Exp Med, 1994. **180**(3): p. 779-82.

265. Borrow, P., et al., *Virus-specific CD8+ cytotoxic T-lymphocyte activity associated with control of viremia in primary human immunodeficiency virus type 1 infection.* J Virol, 1994. **68**(9): p. 6103-10.

266. Denton, P.W., et al., *IL-2 receptor gamma-chain molecule is critical for intestinal T-cell reconstitution in humanized mice.* Mucosal Immunol, 2012. **5**(5): p. 555-66.

267. Flies, D.B., et al., *Blockade of the B7-H1/PD-1 pathway for cancer immunotherapy.* Yale J Biol Med, 2011. **84**(4): p. 409-21.

268. Lipson, E.J., et al., *Durable cancer regression off-treatment and effective reinduction therapy with an anti-PD-1 antibody.* Clin Cancer Res, 2013. **19**(2): p. 462-8.

269. Hirano, F., et al., *Blockade of B7-H1 and PD-1 by monoclonal antibodies potentiates cancer therapeutic immunity.* Cancer Res, 2005. **65**(3): p. 1089-96.

270. Dulos, J., et al., *PD-1 blockade augments Th1 and Th17 and suppresses Th2 responses in peripheral blood from patients with prostate and advanced melanoma cancer.* J Immunother, 2012. **35**(2): p. 169-78.

271. Larkin, J., et al., *Combined Nivolumab and Ipilimumab or Monotherapy in Untreated Melanoma.* N Engl J Med, 2015. **373**(1): p. 23-34.

272. Robert, C., et al., *Nivolumab in previously untreated melanoma without BRAF mutation.* N Engl J Med, 2015. **372**(4): p. 320-30.

273. Brahmer, J., et al., *Nivolumab versus Docetaxel in Advanced Squamous-Cell Non-Small-Cell Lung Cancer.* N Engl J Med, 2015. **373**(2): p. 123-35.

274. Garon, E.B., et al., *Pembrolizumab for the treatment of non-small-cell lung cancer.* N Engl J Med, 2015. **372**(21): p. 2018-28.

275. Motzer, R.J., et al., *Nivolumab for Metastatic Renal Cell Carcinoma: Results of a Randomized Phase II Trial.* J Clin Oncol, 2015. **33**(13): p. 1430-7.

276. Callahan, M.K. and J.D. Wolchok, *At the bedside: CTLA-4- and PD-1-blocking antibodies in cancer immunotherapy.* J Leukoc Biol, 2013. **94**(1): p. 41-53.

277. Dolan, D.E. and S. Gupta, *PD-1 pathway inhibitors: changing the landscape of cancer immunotherapy.* Cancer Control, 2014. **21**(3): p. 231-7.

278. Westermann, J. and R. Pabst, *Distribution of lymphocyte subsets and natural killer cells in the human body.* Clin Investig, 1992. **70**(7): p. 539-44.

279. Lorenzo-Redondo, R., et al., *Persistent HIV-1 replication maintains the tissue reservoir during therapy.* Nature, 2016. **530**(7588): p. 51-6.

280. Yukl, S.A., et al., *Effect of raltegravir-containing intensification on HIV burden and T-cell activation in multiple gut sites of HIV-positive adults on suppressive antiretroviral therapy.* AIDS, 2010. **24**(16): p. 2451-60.

281. Anton, P.A., et al., *Enhanced levels of functional HIV-1 co-receptors on human mucosal T cells demonstrated using intestinal biopsy tissue.* AIDS, 2000. **14**(12): p. 1761-5.

282. Lapenta, C., et al., *Human intestinal lamina propria lymphocytes are naturally permissive to HIV-1 infection.* Eur J Immunol, 1999. **29**(4): p. 1202-8.

283. Poles, M.A., et al., *Lack of decay of HIV-1 in gut-associated lymphoid tissue reservoirs in maximally suppressed individuals.* J Acquir Immune Defic Syndr, 2006. **43**(1): p. 65-8.

284. Bekiaris, V., E.K. Persson, and W.W. Agace, *Intestinal dendritic cells in the regulation of mucosal immunity.* Immunol Rev, 2014. **260**(1): p. 86-101.

285. Rescigno, M., *Intestinal dendritic cells.* Adv Immunol, 2010. **107**: p. 109-38.

286. Cheng, X., et al., *Structure and interactions of the human programmed cell death 1 receptor.* J Biol Chem, 2013. **288**(17): p. 11771-85.

287. Coombes, J.L. and F. Powrie, *Dendritic cells in intestinal immune regulation.* Nat Rev Immunol, 2008. **8**(6): p. 435-46.

288. Vetizou, M., et al., *Anticancer immunotherapy by CTLA-4 blockade relies on the gut microbiota.* Science, 2015. **350**(6264): p. 1079-84.

289. Sivan, A., et al., *Commensal Bifidobacterium promotes antitumor immunity and facilitates anti-PD-L1 efficacy.* Science, 2015. **350**(6264): p. 1084-9.

290. Gur, C., et al., *Binding of the Fap2 protein of Fusobacterium nucleatum to human inhibitory receptor TIGIT protects tumors from immune cell attack.* Immunity, 2015. **42**(2): p. 344-55.

291. Abed, J., et al., *Fap2 Mediates Fusobacterium nucleatum Colorectal Adenocarcinoma Enrichment by Binding to Tumor-Expressed Gal-GalNAc.* Cell Host Microbe, 2016. **20**(2): p. 215-25.

292. DeSantis, T.Z., Jr., et al., *NAST: a multiple sequence alignment server for comparative analysis of 16S rRNA genes.* Nucleic Acids Res, 2006. **34**(Web Server issue): p. W394-9.

293. DeSantis, T.Z., et al., *Greengenes, a chimera-checked 16S rRNA gene database and workbench compatible with ARB.* Appl Environ Microbiol, 2006. **72**(7): p. 5069-72.

294. Shortman, K. and Y.J. Liu, *Mouse and human dendritic cell subtypes.* Nat Rev Immunol, 2002. **2**(3): p. 151-61.

295. Byrareddy, S.N., et al., *Sustained virologic control in SIV+ macaques after antiretroviral and alpha4beta7 antibody therapy.* Science, 2016. **354**(6309): p. 197-202.

296. Ansari, A.A., et al., *Blocking of alpha4beta7 gut-homing integrin during acute infection leads to decreased plasma and gastrointestinal tissue viral loads in simian immunodeficiency virus-infected rhesus macaques.* J Immunol, 2011. **186**(2): p. 1044-59.

297. Reynoso, E.D., et al., *Intestinal tolerance is converted to autoimmune enteritis upon PD-1 ligand blockade.* J Immunol, 2009. **182**(4): p. 2102-12.

298. Kenway-Lynch, C.S., et al., *Dynamics of cytokine/chemokine responses in intestinal CD4+ and CD8+ T Cells during Acute Simian Immunodeficiency Virus Infection.* J Virol, 2013. **87**(21): p. 11916-23.

299. Bin Dhuban, K., et al., *Coexpression of TIGIT and FCRL3 identifies Helios+ human memory regulatory T cells.* J Immunol, 2015. **194**(8): p. 3687-96.

300. Zhang, Y., et al., *Genome-wide DNA methylation analysis identifies hypomethylated genes regulated by FOXP3 in human regulatory T cells.* Blood, 2013. **122**(16): p. 2823-36.

301. Sage, P.T., et al., *The receptor PD-1 controls follicular regulatory T cells in the lymph nodes and blood.* Nat Immunol, 2013. **14**(2): p. 152-61.

302. Raimondi, G., et al., *Regulated compartmentalization of programmed cell death-1 discriminates CD4+CD25+ resting regulatory T cells from activated T cells.* J Immunol, 2006. **176**(5): p. 2808-16.

303. Fromentin, R., et al., *CD4+ T Cells Expressing PD-1, TIGIT and LAG-3 Contribute to HIV Persistence during ART.* PLoS Pathog, 2016. **12**(7): p. e1005761.

304. Riley, J.L., *PD-1 signaling in primary T cells.* Immunol Rev, 2009. **229**(1): p. 114-25.

305. Xu, J., et al., *Expression of Programmed Cell Death 1 Ligands (PD-L1 and PD-L2) in Histiocytic and Dendritic Cell Disorders.* Am J Surg Pathol, 2016. **40**(4): p. 443-53.

306. Meier, A., et al., *Upregulation of PD-L1 on monocytes and dendritic cells by HIV-1 derived TLR ligands.* AIDS, 2008. **22**(5): p. 655-8.

307. Trabattoni, D., et al., *B7-H1 is up-regulated in HIV infection and is a novel surrogate marker of disease progression.* Blood, 2003. **101**(7): p. 2514-20.

308. Bui, F.Q., et al., *Fusobacterium nucleatum infection of gingival epithelial cells leads to NLRP3 inflammasome-dependent secretion of IL-1beta and the danger signals ASC and HMGB1.* Cell Microbiol, 2016. **18**(7): p. 970-81.

309. Goncalves, L.S., B.M. Goncalves, and T.V. Fontes, *Periodontal disease in HIV-infected adults in the HAART era: Clinical, immunological, and microbiological aspects.* Arch Oral Biol, 2013. **58**(10): p. 1385-96.

310. Ashare, A., et al., *Chronic liver disease impairs bacterial clearance in a human model of induced bacteremia.* Clin Transl Sci, 2009. **2**(3): p. 199-205.

311. McKaig, R.G., et al., *Factors associated with periodontitis in an HIV-infected southeast USA study.* Oral Dis, 2000. **6**(3): p. 158-65.

312. Hofer, D., et al., *Long-term results of supportive periodontal therapy (SPT) in HIV-seropositive and HIV-seronegative patients.* J Clin Periodontol, 2002. **29**(7): p. 630-7.

313. Sankaran, S., et al., *Rapid onset of intestinal epithelial barrier dysfunction in primary human immunodeficiency virus infection is driven by an imbalance between immune response and mucosal repair and regeneration.* J Virol, 2008. **82**(1): p. 538-45.

314. Sandler, N.G. and D.C. Douek, *Microbial translocation in HIV infection: causes, consequences and treatment opportunities.* Nat Rev Microbiol, 2012. **10**(9): p. 655-66.

315. Jiang, W., et al., *Plasma levels of bacterial DNA correlate with immune activation and the magnitude of immune restoration in persons with antiretroviral-treated HIV infection.* J Infect Dis, 2009. **199**(8): p. 1177-85.

316. Chao, T., H. Wang, and P.C. Ho, *Mitochondrial Control and Guidance of Cellular Activities of T Cells.* Front Immunol, 2017. **8**: p. 473.

317. Bengsch, B., et al., *Bioenergetic Insufficiencies Due to Metabolic Alterations Regulated by the Inhibitory Receptor PD-1 Are an Early Driver of CD8(+) T Cell Exhaustion.* Immunity, 2016. **45**(2): p. 358-73.

318. Ferraris, R.P., et al., *Luminal glucose concentrations in the gut under normal conditions.* Am J Physiol, 1990. **259**(5 Pt 1): p. G822-37.

319. Emerging Risk Factors, C., et al., *Diabetes mellitus, fasting blood glucose concentration, and risk of vascular disease: a collaborative meta-analysis of 102 prospective studies.* Lancet, 2010. **375**(9733): p. 2215-22.

320. Cahill, R.N., et al., *Two distinct pools of recirculating T lymphocytes: migratory characteristics of nodal and intestinal T lymphocytes.* J Exp Med, 1977. **145**(2): p. 420-8.

321. Agace, W.W., *Tissue-tropic effector T cells: generation and targeting opportunities.* Nat Rev Immunol, 2006. **6**(9): p. 682-92.

322. Harrison, O.J. and F.M. Powrie, *Regulatory T cells and immune tolerance in the intestine.* Cold Spring Harb Perspect Biol, 2013. **5**(7).

323. Chatterjee, A., H. Bhattacharya, and A. Kandwal, *Probiotics in periodontal health and disease.* J Indian Soc Periodontol, 2011. **15**(1): p. 23-8.

324. Seekatz, A.M., et al., *Recovery of the gut microbiome following fecal microbiota transplantation.* MBio, 2014. **5**(3): p. e00893-14.

325. Saison, J., et al., *Fatal cumulative toxicities of HAART in a stable, AIDS-free, HIV-infected patient.* BMJ Case Rep, 2012. **2012**.

326. Warriner, A.H., G.A. Burkholder, and E.T. Overton, *HIV-related metabolic comorbidities in the current ART era.* Infect Dis Clin North Am, 2014. **28**(3): p. 457-76.

327. Barrett, L., K.R. Fowke, and M.D. Grant, *Cytomegalovirus, aging, and HIV: a perfect storm.* AIDS Rev, 2012. **14**(3): p. 159-67.

328. Persaud, D., et al., *A stable latent reservoir for HIV-1 in resting CD4(+) T lymphocytes in infected children.* J Clin Invest, 2000. **105**(7): p. 995-1003.

329. Tumeh, P.C., et al., *PD-1 blockade induces responses by inhibiting adaptive immune resistance.* Nature, 2014. **515**(7528): p. 568-71.

330. Herbst, R.S., et al., *Predictive correlates of response to the anti-PD-L1 antibody MPDL3280A in cancer patients.* Nature, 2014. **515**(7528): p. 563-7.

331. Pearce, E.L. and E.J. Pearce, *Metabolic pathways in immune cell activation and quiescence.* Immunity, 2013. **38**(4): p. 633-43.

332. Patsoukis, N., et al., *PD-1 alters T-cell metabolic reprogramming by inhibiting glycolysis and promoting lipolysis and fatty acid oxidation.* Nat Commun, 2015. **6**: p. 6692.

333. Marwitz, S., et al., *Epigenetic modifications of the immune-checkpoint genes CTLA4 and PDCD1 in non-small cell lung cancer results in increased expression.* Clin Epigenetics, 2017. **9**: p. 51.

334. Bally, A.P., J.W. Austin, and J.M. Boss, *Genetic and Epigenetic Regulation of PD-1 Expression.* J Immunol, 2016. **196**(6): p. 2431-7.

335. Pauken, K.E., et al., *Epigenetic stability of exhausted T cells limits durability of reinvigoration by PD-1 blockade.* Science, 2016. **354**(6316): p. 1160-1165.